2014

Integration of network protector relays on downtown distribution networks with penetration of renewable energy

Nigel Ramon Jordan
Louisiana State University and Agricultural and Mechanical College, nigeljordan13@gmail.com

INTEGRATION OF NETWORK PROTECTOR RELAYS ON DOWNTOWN DISTRIBUTION NETWORKS WITH PENETRATION OF RENEWABLE ENERGY

A Thesis

Submitted to the Graduate Faculty of the
Louisiana State University and
Agricultural and Mechanical College
in partial fulfillment of the
requirements for the degree of
Master of Science in Electrical Engineering

in

The Department of Electrical and Computer Engineering

by
Nigel Jordan
B.S., University of Mississippi, 2007
MBA, University of Alabama—Birmingham, 2011
May 2014

ACKNOWLEDGMENTS

I would like to thank my family and friends for their support during my academic studies at Louisiana State University. Without their support and encouragement, my goal of furthering my education would be nearly impossible.

I would like to thank Entergy for funding and providing the necessary information to make this research possible. I would also like to thank my advisor, Professor Shahab Mehraeen, for guiding me during this stage of my academic career, and sharing his wealth of experience and knowledge.

I also would like to thank the professors at Louisiana State University, particularly Dr. Ernest Mendrela, Dr. Leszek Czarnecki, and Mr. Michael McAnelly for agreeing to serve on my advisory committee, as well as sharing their knowledge in the area of power systems.

TABLE OF CONTENTS

ACKNOWLEDGMENTS……..…….……..….ii

LIST OF TABLES…….…….……...……vi

LIST OF FIGURES…….……...…….viii

ABSTRACT……...……...….xi

CHAPTER 1. INTRODUCTION……..……..…….…….1

CHAPTER 2. LOAD FLOW ANALYSIS……..……..……..…….…..…4

2.1 Per-Unit System…….……4

2.2 Power Flow Studies…….……..5

2.3 Newton-Raphson Method……..6

2.4 Load Flow Program…….……..7

CHAPTER 3. OPERATION OF NETWORK PROTECTOR RELAY……..……10

3.1 Operation…….……10

3.2 Trip Modes……...10

3.3 Reclose Modes……..……...…11

CHAPTER 4. OVERVIEW OF DISTRIBUTION SECONDARY NETWORK SYSTEMS……...…….…..12

CHAPTER 5. MODEL OF DOWNTOWN NETWORK……....15

5.1 Model Parameters……...…….15

CHAPTER 6. VOLTAGE ANALYSIS……..……..……17

6.1 PV Penetration Only in Grid Mesh Network……..……17

6.1.1 Voltage Profiles under Different PV Arrangements……17

6.1.2 Renewable Sources with Peak Loading……...20

6.1.3 Renewable Sources with Minimum Loading……...22

6.2 PV Penetration in Grid Mesh & Spot Networks…….…23

6.2.1 Renewable Sources with Peak Loading……...23
6.2.2 Renewable Sources with Minimum Loading……...24

CHAPTER 7. EFFECTS OF NETWORK PROTECTOR OPERATION…..…..…….26
7.1 PV Penetration in Grid Network…….…26
7.1.1 Reverse Power Flows in Distribution Lines (PV Penetration in Grid Network)……..……..……..……..……..…….27
7.1.2 PV Penetration and Transformer Loading…….……..29
7.2 PV Penetration in Grid & Spot Networks……...29
7.2.1 Reverse power flows in distribution lines (PV penetration in grid & spot networks)……..……...……....29

CHAPTER 8. CLOUD EFFECTS…….……..……..……...…31
8.1 Clouds with 5% PV Penetration……..31
8.2 Clouds with 15% PV Penetration……32
8.3 Clouds with 30% PV Penetration……33

CHAPTER 9. CASE STUDIES…….……..…..……...……35
9.1 Simulations with Faults on Feeder Networks……...…..35
9.2 Simulations with No PV Penetration Present…….…..…35
9.3 Simulations with 2% PV Penetration Present…….….38
9.4 Simulations with 5% PV Penetration Present……..…40
9.5 Simulations with 8% PV Penetration Present……..……41

CHAPTER 10. RECLOSE VOLTAGE ANALYSIS…..……..…….44
10.1 Closing Characteristic of Network Protector Relay……..…….44
10.2 Reclose Settings Analysis……..……45

CHAPTER 11. PV PENETRATION LIMITS……....…..……47
11.1 Simulations with 8% PV Penetration……..……..47

CHAPTER 12. PROPOSED SOLUTION.…….…….…….48
12.1 Feeder 1 Simulations with 5% PV Penetration……..……49
12.1.1 5% PV Penetration without Fault…….……...……50
12.1.2 5% PV Penetration with Fault…….……51

12.1.3 30% PV Penetration without Fault…….……...……..54
12.1.4 30% PV Penetration with Fault……...……56

CHAPTER 13. CONCLUSION……..……..……..…...……..….61

APPENDIX A- CASE STUDIES FOR 60% AND 90% PV PENETRATION…..…..….62

APPENDIX B – CASE STUDIES FOR FEEDERS 2-7: 30% PV PENETRATION.....68

APPENDIX C – VOLTAGE LIMITS…….……...…….…….....86

REFERENCES…….……...……..87

VITA…….…….…….……..89

LIST OF TABLES

Table 1—Base Values……..……8

Table 2—per unit grid voltages with 0% PV penetration…….……17

Table 3—per unit grid voltages with 5% PV penetration…….……18

Table 4—per unit grid voltages with 15% PV penetration……19

Table 5—per unit grid voltages with 30% PV penetration……..……..19

Table 6—per unit grid voltages with clouds in Areas A, B, & C (5% PV Penetration)....31

Table 7—per unit grid voltages with clouds in Area A, B, & C (15% PV Penetration)...32

Table 8—per unit grid voltages with clouds in Area A, B, & C (30% PV Penetration)...33

Table 9—Arrangement 1 with 2% PV penetration……..…..…39

Table 10—Arrangement 2 with 2% PV penetration…….…39

Table 11—Arrangement 3 with 2% PV penetration……..40

Table 12—Arrangement 1 with 5% PV penetration…….….40

Table 13—Arrangement 2 with 5% PV penetration…….….41

Table 14—Arrangement 3 with 5% PV penetration…….….41

Table 15—Arrangement 1 with 8% PV penetration…….….42

Table 16—Arrangement 2 with 8% PV penetration…….….42

Table 17—Arrangement 3 with 8% PV penetration…….….43

Table 18—Current calculations for simulation with 5% PV penetration……..……53

Table 19—Power flows for simulation with 5% PV penetration……..……54

Table 20—Current calculations for simulation with 30% PV penetration……58

Table 21—Power flows for simulation with 30% PV penetration……59

Table A.1—Current calculations for simulation with 60% PV penetration……..……63

Table A.2—Power flows for simulation with 60% PV penetration……..…64

Table A.3—Current calculations for simulation with 90% PV penetration……..……66

Table A.4—Power flows for simulation with 90% PV penetration……..……67

Table B.1—Current calculations for Feeder network 2 simulation (30% PV) ……..…69

Table B.2—Power flows for Feeder network 2 simulation (30% PV) ……..……70

Table B.3—Current calculations for Feeder network 3 simulation (30% PV) ……..…72

Table B.4—Power flows for Feeder network 3 simulation (30% PV) ……..……73

Table B.5—Current calculations for Feeder network 4 simulation (30% PV) ……..…75

Table B.6—Power flows for Feeder network 4 simulation (30% PV) ……..……76

Table B.7—Current calculations for Feeder network 5 simulation (30% PV) ……..…78

Table B.8—Power flows for Feeder network 5 simulation (30% PV) ……..……79

Table B.9—Current calculations for Feeder network 6 simulation (30% PV) ……..…81

Table B.10—Power flows for Feeder network 6 simulation (30% PV) ……...……82

Table B.11—Current calculations for Feeder network 7 simulation (30% PV) ……...…84

Table B.12—Power flows for Feeder network 7 simulation (30% PV) ……...……85

Table C.1—ANSI C84.1 Voltage Limits (Service Voltage)……..……...…86

Table C.2—ANSI C84.1 Voltage Limits (Utilization Voltage)……...…..……86

LIST OF FIGURES

Figure 2.1— Power flow diagram……...……5

Figure 2.2— Power injected into secondary grid due to PV penetration……9

Figure 3.1—Sensitive Trip Characteristic…….……10

Figure 3.2—Reclose Characteristic……...……11

Figure 4.1—Network Unit Components……12

Figure 4.2— Example of spot network configuration……...……13

Figure 4.3— Example of grid network configuration……...……14

Figure 5.1— Feeder network breakers……...……15

Figure 5.2— Feeder 1 Network…….……16

Figure 6.1— Grid Voltages for all arrangements with 5% PV penetration……...……18

Figure 6.2— Grid Voltages for all arrangements with 15% PV penetration…….……18

Figure 6.3— Grid Voltages for all arrangements with 30% PV penetration…….……19

Figure 6.4— Network protector operations in grid network…….……20

Figure 6.5— Voltage profile for Arrangement 1 under peak loads……...……20

Figure 6.6— Voltage profile for Arrangement 2 under peak loads……...……21

Figure 6.7— Voltage profile for Arrangement 3 under peak loads……...……21

Figure 6.8— Voltage profile for Arrangement 1 under minimum loads……...……22

Figure 6.9— Voltage profile for Arrangement 2 under minimum loads……...22

Figure 6.10— Voltage profile for Arrangement 3 under minimum loads…….……23

Figure 6.11— Voltage profile with PV penetration in grid mesh & spot network (peak loads) ……24

Figure 6.12— Voltage profile with PV penetration in grid mesh & spot network (min. loads) ……24

Figure 6.13— Grid_154 voltages under minimum loads……..……25

Figure 6.14— Grid_357 voltages under minimum loads……..……25

Figure 7.1— Transformers disconnected under peak and minimum loading……26

Figure 7.2— Reverse power flows with PV penetration in Grid Mesh Network (peak loads) ……..……27

Figure 7.3— Reverse power flows with PV penetration in Grid Mesh Network (min. loads) ……..…28

Figure 7.4— Power flows for SV_27 with no PV Penetration……..……28

Figure 7.5— Transformers disconnected under peak loading conditions…….……29

Figure 7.6— Reverse power flows with PV penetration in Grid & Spot Networks (peak loads) ……..……30

Figure 7.7— Reverse power flows with PV penetration in Grid & Spot Networks (min. loads) ……..…30

Figure 8.1— Grid Network Voltage with clouds in Areas A, B, & C (5% PV Penetration)……32

Figure 8.2— Grid Network Voltage with clouds in Areas A, B, & C (15% PV Penetration) ……...……33

Figure 8.3— Grid Network Voltage with clouds in Areas A, B, & C (30% PV Penetration) ……...……34

Figure 9.1— Simulation results for a fault on feeder network 1 (No PV Penetration) ……35

Figure 9.2— Simulation results for a fault on feeder network 2 (No PV Penetration) ……36

Figure 9.3— Simulation results for a fault on feeder network 3 (No PV Penetration) ……36

Figure 9.4— Simulation results for a fault on feeder network 4 (No PV Penetration) ……37

Figure 9.5— Simulation results for a fault on feeder network 5 (No PV Penetration) ……37

Figure 9.6— Simulation results for a fault on feeder network 6 (No PV Penetration) ……38

Figure 9.7—Simulation results for a fault on feeder network 7 (No PV Penetration).……...……38

Figure 10.1— Closing characteristic of the network protector relay……..……...……44

Figure 10.2— V_D before a fault has cleared on feeder 5……..…….……45

Figure 10.3— V_D before a fault has cleared on feeder 5…….…….……..…46

Figure 10.4— V_D after a fault has cleared on feeder 5…….……..…46

Figure 12.1— Logic diagram of fault detection system……49

Figure 12.2— Feeder network 1 without fault (5% PV penetration) ……...……50

Figure 12.3— Feeder network 1 with fault (5% PV penetration) ……..…52

Figure 12.4— Feeder network 1 without fault (30% PV) ……55

Figure 12.5— Feeder network 1 with fault (30% PV) ……..……57

Figure B.1— Feeder network 2 with fault (30% PV) ……...……68

Figure B.2— Feeder network 3 with fault (30% PV) ……...……71

Figure B.3— Feeder network 4 with fault (30% PV) ……...……74

Figure B.4— Feeder network 5 with fault (30% PV) ……...……77

Figure B.5— Feeder network 6 with fault (30% PV) ……...…80

Figure B.6— Feeder network 7 with fault (30% PV) ……...……83

ABSTRACT

The demand and use of renewable energy sources such as solar panels is steadily increasing in today's world. Renewable energy sources in distribution networks effectively reduce the amount of load consumed by customers. Renewable energy sources are also a solution to many environmental concerns. However, when these sources of energy are added to downtown networks they interfere with the normal operation of the protective relays and impose challenges such as unexpected tripping of network protector relays. In this paper, the effects of network protector relay operation is studied as a function of increasing photovoltaic (PV) penetration within the secondary grid network. Additionally, network protector operation under faulted conditions within the primary feeder network or network transformer is investigated. Finally, a solution is proposed to detect abnormal or faulted conditions in the upstream network, and trip the associated network protector relay only for these conditions. The proposed method, when applied in the downtown distribution network, prevents the network protector relays from erroneously tripping during minimum loading conditions and during high levels of PV penetration within the secondary grid network.

CHAPTER 1. INTRODUCTION

The number of photovoltaic (PV) systems present in downtown distribution networks has been steadily increasing over the years. These sources of renewable energy effectively reduce the apparent load and excess energy flows towards the consumers [11]. These renewable energy sources also assist in the reduction of greenhouse gas emissions, a major environmental concern [3]. Due to their proximity to the point of use, PV systems can reduce or eliminate line losses [26]. This ultimately eliminates the need to build new transmission lines and large power plants where there is increasing public opposition [3]. PV systems also provide a viable solution to improved power quality and reliability, with the potential to reduce total outage times during power outages. Developers are installing PV systems that are able to operate autonomously when storms, fires, or other disturbances disrupt the electrical utilities [9] [15]. Additionally, during minimum loading conditions such as early in the morning these sources may export energy back to the utility grid in a transaction known as net metering. However, these loading conditions along with increased levels of PV penetration in downtown distribution networks may interfere with the normal operations of the protective devices and impose challenges such as unexpected tripping in the network protectors. One example of this issue occurs in the Central Business District of New Orleans, where residential, commercial and schools generating their own power receive credit for unused power provided by the utility [9]. These areas, however, are not allowed to interconnect their generation due to safety and reliability concerns [9]. A network protector (NP) relay is a device installed on the low-voltage side of each network transformer. The normal direction of current flow in the downtown network is unidirectional from the utility to the customers on the secondary side of the network transformer. However, the direction of current flow will reverse during short circuits on the primary feeder network, or when the PV generation within the downtown distribution network exceeds the load demand.

In the downtown distribution network, multiple feeders supply power to a number of transformers which are interconnected together on the secondary side to serve multiple loads. When a fault occurs in the upstream network, the network protector disconnects the transformer that sees the fault current to isolate it. Then, the network protector protects the transformer of the disconnected circuit by disconnecting the downstream network and isolating the fault in the primary feeder or network transformer. A three-phase power directional relay called master relay provides this tripping mechanism. The relay monitors the magnitude and direction of the current flowing through the network protector when the network protector is closed for the tripping mechanism. This relay trips the protector when it senses reverse power flow from the secondary grid towards the fault located within the primary feeder network. The network protector automatically closes when the voltage on the transformer side of the open network protector is higher in magnitude, and is in phase with or leading the voltage on the secondary side of the protector after the faulted circuit is repaired and re-energized.

The network protector is an important protective device in the downtown distribution network because it ensures reliable and continuous operation even if one or more feeders are lost due to a fault or other abnormal conditions. The presence of renewable sources in the downtown distribution network presents a few challenges. One of the major issues that we are facing today is the problem of distinguishing an abnormal or fault condition from excess power flow coming

from the secondary grid network. The network protector senses power flow towards the utility in both cases, and trips to prevent the backflow to the primary feeder network. The network protector is designed to reclose for power flow from the utility to the downtown network. However, without synchronizing capabilities, it is possible that the network protector may try to reclose out of sync on a downtown network that has been islanded [5]. Due to these challenges, many utilities that have networks have not been allowing their customers that have PV systems (or any generating system) to connect to the grid. The National Renewable Energy Laboratory (NREL) has outlined six cases of utilities successfully implementing PV systems onto their system. These utilities usually implement the interconnection so that the energy produced in the downtown network is not fed back towards the grid. This is accomplished by several methods outline below [1]:

1. Size the PV system lower than the minimum daytime load at the customer meter. If the total demand data for the secondary network can be gathered for a considerable amount of time, the amount of PV penetration in the downtown distribution network can be limited such that it will always produce less energy than the secondary network consumes at all times. This ensures that the utility is always transmitting power towards the load in the secondary network.
2. Install a minimum import relay (MIR) or a reverse power relay. The MIR disconnects the PV system if the powers flow from the utility drops below a set value. The reverse power relay will disconnect the PV system in the secondary network from the utility if the power flow from the utility drops to zero or reverses direction.
3. Install a dynamically controlled inverter (DCI) to monitor the amount of power coming in to the customer location and decrease PV penetration if the load decreases below a specific level. The energy flow is monitored at the main feeder and a control signal is sent to the inverter which initiates a reduction in generated power, if required.
4. Allow smaller PV systems to connect to the network which decrease the chances of sending power back to the utility.

All of the methods above, however, limit the amount of energy produced by solar panels in the downtown network. Method 4 places limits on the size of PV systems installed at the customer's site, while methods 2 and 3 control the output as a function of the power flow in the network. The minimum load identification (Method 1) method can fail to work if the load becomes lower than previously evaluated.

The methods mentioned above allow customers to interconnect their PV systems onto the grid, at the expense of limiting the available energy in the secondary network. Other solutions to reverse power flow as a result of high PV penetration revolve around implementing changes within the downtown network on the customer's side [4]. Some of these alternatives are listed below:

1. Decrease the network's series impedance so that it has low voltage drop along its length. This essentially increases the voltage in the primary feeder network, but can become costly.

2. Require customer loads to operate at improved power factor, reducing the need for a higher voltage in the primary feeder network.
3. Require customers with large loads to shed their loads when the voltage in the downtown network drops below a certain threshold.
4. Discretionary loads can be used when the downtown network voltage is high to provide additional load for excess power to flow.
5. Provide a means of energy storage to use up the extra power provided by PV.

Since the existing solutions impose limitations on the amount of solar generation present in secondary networks, a new method is proposed to prevent the undesired tripping of the network protector relay. A solution is proposed to be able to detect reverse power flow caused by a fault condition, and trip the network protector to isolate the fault. This solution improves the efficiency of the PV systems installed in the downtown network by allowing the transformers to remain in service for higher levels of PV penetration, and allowing the downtown network to provide more power to the local network and the utility system.

We begin by looking at theory used in load flow studies, including a brief overview of the per-unit calculations used throughout the study, as well as a review of the Newton-Raphson iterative method used to run load flow simulations. Next, we examine the operation of the network protector relay by looking at the trip and reclose characteristics. We also provide a background on secondary distribution networks, including spot and secondary grid mesh networks. This study will examine different arrangements of distributed generation (DG) located within the downtown network to determine if the location of DGs have a major effect on the operation of the network protectors and the voltage profile within the network. We also study the downtown distribution network under peak load conditions, and look at the worst case scenario of minimum loads with the addition of distributed generation in the downtown distribution network. Reverse power flows in the entire downtown network will be studied as a result of increased PV penetration. The effect of clouds on the operation of network protectors is then studied, as this case also has an effect on the voltage stability and available power from the PV systems. Finally this study examines various case studies with different levels of PV penetration present in the secondary network, with the occurrence of fault conditions in the feeder network. We are then able to demonstrate the proposed solution that will distinguish a fault from excess PV penetration in the downtown distribution network.

CHAPTER 2. LOAD FLOW ANALYSIS

2.1 Per-Unit System

Performing circuit analysis with transformers can become tedious due to the different voltage levels in systems. The per-unit method is a system that eliminates the need to transform the voltages at every transformer in the system. In the per unit system the currents, voltages, impedances, powers, and other electrical quantities are not measured in their usual SI units (amperes, volts, watts, etc.). Instead, each quantity is measured as some decimal fraction of a base level. Quantities can be expressed in the per unit system by the following equations [13]:

$$\text{P.U. volts} = \frac{actual}{base} volts \tag{1}$$

$$\text{P.U. amps} = \frac{actual}{base} amps \tag{2}$$

$$\text{P.U. ohms} = \frac{actual}{base} ohms \tag{3}$$

The first step in the per-unit calculation process involves selecting the system kVA which is usually chosen based on one of the predominant pieces of equipment or a round number such as 10,000 [13]. Next, a voltage base (V_{LL}) is selected which is usually the nominal line voltage at that level. The other base voltages can be determined by the turn-to-turn ratios of the transformers in the network. The base impedance can be calculated for each voltage level, and the per-unit values can be determined. The following equations show the relationships between the electrical quantities used in per-unit calculations:

$$I_{base} = \frac{kVA_{base}}{\sqrt{3} \times kV_{base}} \tag{4}$$

$$Z_{base} = \frac{kV^2_{base}}{kVA_{base}} \times 1000 \tag{5}$$

$$kVA_{base} = \sqrt{3} \times kV_{base} \times I_{base} \tag{6}$$

The main advantage of the per-unit system is the fact that the transformers can be removed from the calculations since transformer turns ratios are now 1:1. Once the per-unit values have been calculated for an entire system, the actual values can then be determined by multiplying each per-unit value by the associated base value.

2.2 Power Flow Studies

Power flow studies attempt to determine the voltage magnitude and angle as well as the real and reactive power flows for each bus in the electrical system under balanced three-phase steady state conditions [14]. Typically, the load power consumption at all of the buses and the power produced at each generator are provided to run these studies. These studies determine if the system voltages remain within their limits under different loading scenarios, and whether equipment such as transformers and lines are overloaded [13]. Figure 2.1 shows the conventions used during the power flow studies.

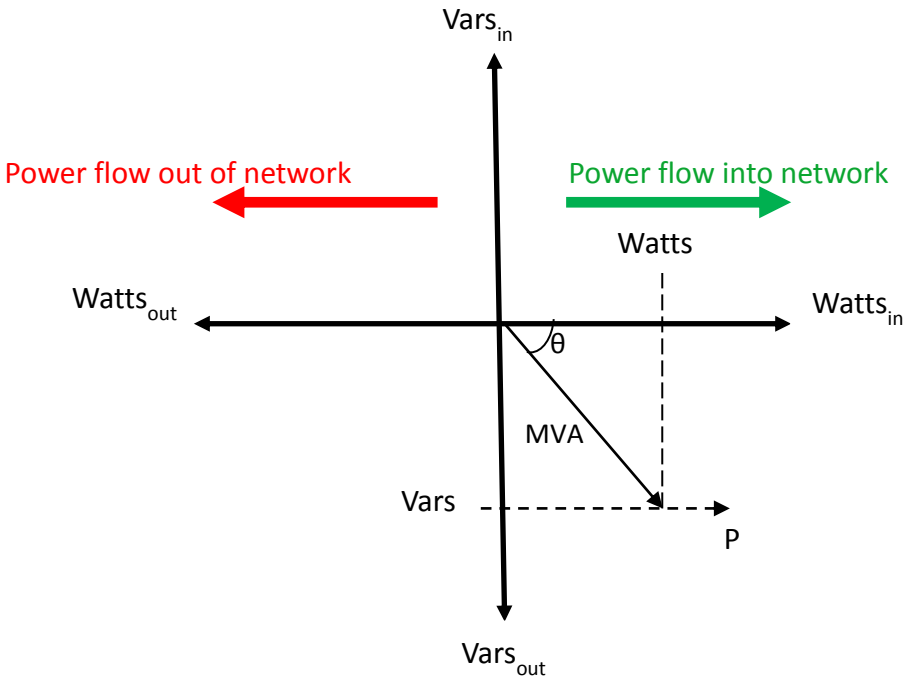

Figure 2.1— Power flow diagram

The basic calculation process is to solve a non-linear equation that contains:

- P – the active power into the network
- Q – the reactive power into the network
- V_{mag} – the magnitude of the bus voltage
- θ – the angle of the bus voltage referred to a common reference

The definition of the load flow problem involves two of the four parameters listed above at each bus, while the other parameters are solved. For generators (PV buses), P and V_{mag} are usually chosen because the power and voltages are usually controlled via the governor and excitation control systems, respectively. The slack bus is a special generator bus that serves as the reference bus for the power system. The slack bus maintains a fixed voltage, while supplying whatever real or reactive power needed to make the power flows in the system balance.

The magnitude of the voltage is kept constant by adjusting the synchronous generator connected to the bus. Due to the physical characteristics of generation and load, the terminal parameters at each load bus is usually described in terms of its active and reactive powers (PQ buses) [13].

2.3 Newton-Raphson Method

The Newton-Raphson power flow method was used to determine the voltage magnitudes and angles at each bus in the downtown network. To execute the Newton-Raphson method, all data (including line impedances and bus loads) of the equipment within the network must be converted to their per unit values on common bases as outlined in section 2.1. Next, the admittance matrix (Y_{bus}) is formed using the following guidelines for admittances connected between nodes i and j:

- Add the admittance to the (i,i) position of the the Y_{bus} matrix
- Add the admittance to the (j,j) position of the the Y_{bus} matrix
- Add the negative of the admittance to the (i,j) position of the the Y_{bus} matrix
- Add the negative of the admittance to the (j,i) position of the the Y_{bus} matrix

With this information, the power balance equations are ready to be solved:

$$0 = P_i = P_{G,i} - P_{L,i} - \sum_{j=1}^{N} V_i V_j y_{ij} cos(\delta_i - \delta_j - \gamma_{ij}) \quad (7)$$

$$0 = Q_i = Q_{G,i} - Q_{L,i} - \sum_{j=1}^{N} V_i V_j y_{ij} sin(\delta_i - \delta_j - \gamma_{ij}) \quad (8)$$

where:

- v_i – Voltage at node i
- v_j – Voltage at node j
- δ_i – Angle of voltage at node i
- δ_j – Angle of voltage at node j
- γ_{ij} – Angle between bus i and bus j
- y_{ij} – i,j component of the Ybus matrix
- $P_{G,i}$ – Real power generated
- $P_{L,i}$ – Load real power
- $P_{T,i}$ –Real power transmitted
- $Q_{G,i}$– Reactive power generated
- $Q_{L,i}$ – Load reactive power
- $Q_{T,i}$ –Reactive power transmitted

The power balance equations are solved using the following iterative process until the power balance equation converges to zero.

1. Estimate the values of δ_i and |vi| for the state variables
2. Use the estimates to calculate $P_{i,calc}$ & $Q_{i,calc}$, mismatches, ΔP_i , ΔQ_i, and the Jacobian.
3. Solve the matrix equations for $\Delta\delta_i$ and $\frac{\Delta|vi|}{|vi|}$ correction.
4. Add the solved corrections in the initial estimates
   a. $\delta_i = \delta_i + \Delta\delta_i$
   b. $|vi| = |vi| + \Delta|vi| = |vi|\ (1+\frac{\Delta|vi|}{|vi|})$
5. Use the new values δ_i and |vi| as starting values for the next iteration.

2.4 Load Flow Program

The Newton-Raphson iterative method was utilized via MATLAB to obtain load flow solutions throughout this study. To run the load flow simulations, the actual values provided from Entergy had to be converted into per unit values. We selected an apparent power base of 1000 KVA and calculated the voltage and impedance bases below:

$$\text{Vbase1} = 13.2\text{KV} \tag{10}$$

$$\text{Vbase2} = \text{Vbase1} \times \text{N} = 13200 \times \frac{208}{13200} = 208V \tag{11}$$

$$\text{Vbase3} = \text{Vbase2} \times \text{N} = 13200 \times \frac{480}{13200} = 480V \tag{12}$$

$$\text{Zbase1} = \frac{Vbase1^2}{Sbase} = \frac{13200^2}{1000000} = 174.24 \tag{13}$$

$$\text{Zbase2} = \frac{Vbase2^2}{Sbase} = \frac{208^2}{1000000} = 0.043264 \tag{14}$$

$$\text{Zbase3} = \frac{Vbase3^2}{Sbase} = \frac{480^2}{1000000} = 0.2304 \tag{15}$$

$$\text{Ibase1} = \frac{Sbase}{Vbase1 \times \sqrt{3}} = \frac{1000000}{13200 \times \sqrt{3}} = 43.7367 \tag{16}$$

$$\text{Ibase2} = \frac{Sbase}{Vbase2 \times \sqrt{3}} = \frac{1000000}{208 \times \sqrt{3}} = 2775.72 \tag{17}$$

$$\text{Ibase3} = \frac{Sbase}{Vbase3 \times \sqrt{3}} = \frac{1000000}{480 \times \sqrt{3}} = 1202.81 \tag{18}$$

Table 1 below shows the values that were used for the base values throughout the study.

Table 1—Base Values

	13.2KV Network	408V Network	208 Network
APPARENT POWER (S)	1000KVA	1000KVA	1000KVA
VBASE	13.2KV	408V	208V
ZBASE	174.24	0.043264	0.2304

The modeling data provided from Entergy was converted into bus and line matrixes as input for the load flow program. The bus data consisted of 1,209 nodes/loads with each node containing information on:

- Bus voltage
- Bus voltage angle
- Real power generated/consumed at bus
- Reactive power generated/consumed at bus

There were 433 secondary grid nodes, 408 feeder network nodes, 215 nodes within the grid vaults, 7 nodes for the origination points of each network at the substation, and 152 spot vault nodes.

The line matrix consisted of 1, 412 lines with each line containing information on:

- Series resistance in each line
- Series reactance in each line
- Susceptance in each line
- Impedance of each transformer

PV systems that are connected to the electric grid are designed to inject all of the real power produced by PV modules into the secondary grid [16]. They control the amount of power regardless of the voltage level, so we represented locations of PV penetration as negative constant power loads in the simulation [26]. Additionally, standards such as IEEE 1547 and UL1741 state that the inverter "shall not actively regulate the voltage at the PCC (Point of Common Coupling)" [16] [12]. Therefore, PV systems are designed to operate at unity power factor because this condition will produce the most real power and energy.

Essentially, the PV penetration reduces the amount of real power consumed at the connected bus. When more PV penetration is added the bus node can actually generate real power onto the grid.

It is known that high levels of PV penetration which results in replacing generating units with distributed PV systems can limit the amount of available reactive power [12]. The task of supplying the reactive power is usually undertaken by the electric utility [11]. This is shown

graphically in Figure 2.2 where the grid-connected inverter supplies the real power to the load and grid, leaving the utility the task of supplying the required reactive power for the loads.

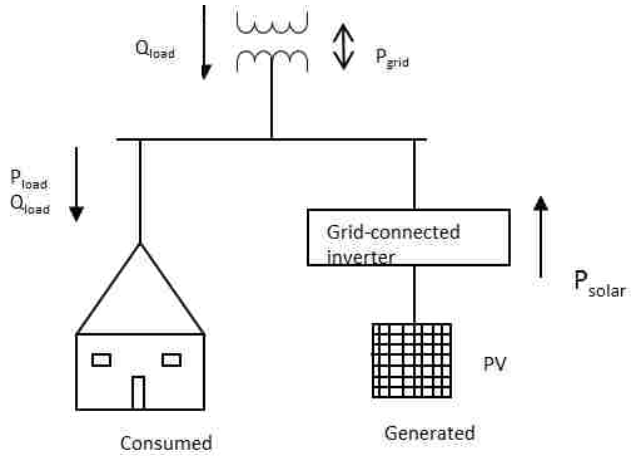

Figure 2.2— Power injected into secondary grid due to PV penetration

When high levels of PV penetration are present, the dynamic performance of the system can be affected when reactive power supply is interrupted during a system disturbance, such as a fault, within the electric utility [12]. These issues will be examined further in Chapter 9.

CHAPTER 3. OPERATION OF NETWORK PROTECTOR RELAY

3.1 Operation

Currently, Entergy uses network protectors manufactured by Richards manufacturing. The Richards 313NP Network Protector that is widely used in the Entergy grids consists of a circuit breaker, a motor operated mechanism, and an Electronic Technology Inc. (ETI) microprocessor-based network protector relay. The network protector relay responds to power flowing to and from the secondary distribution network. If a fault occurs in the primary feeder network or in a connected transformer, or if the substation feeder breaker is de-energized by opening the circuit breaker, the network protector (in sensitive trip mode) will energize the network protector's trip coil to open the network protector. After the fault clears in the primary network, and if the transformer voltage is greater than the secondary voltage, and if the transformer voltage angle leads the angle of the network voltage, then the network protector relay will energize the reclose output contact and close the protector [2].

3.2 Trip Modes

- Sensitive Trip – The network protector relay will trip the protector when the net reverse power flow exceeds the set point. Range: -1.0 to -1000.0 mA.
- Sensitive Trip Delay – The sensitive trip criteria must be met for the duration of the time delay period before the network protector will open. Range: 1 to 255 cycles.
- Insensitive Trip – The protector will not open during normal system conditions. It will open when the "Insensitive Current" set point is exceeded on one of the phases (during a fault condition). Range: 0 to 15 amps
- Watt-Var – The network protector relay will rotate the trip region to ensure that the network protector will open under certain conditions. Range: 0 to 15 amps

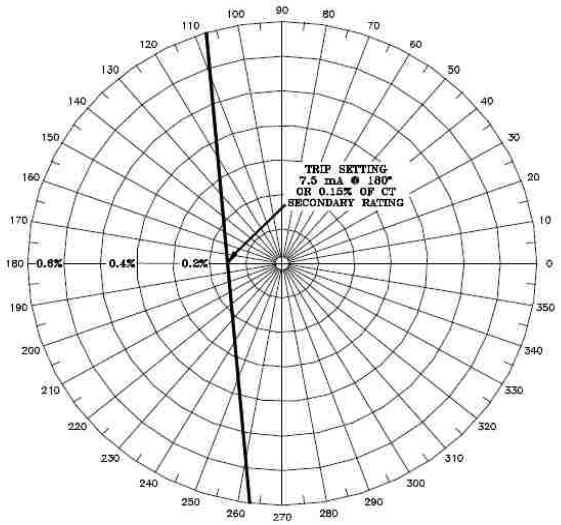

Figure 3.1—Sensitive Trip Characteristic [2]

3.3 Reclose Modes

- Reclose Voltage – Minimum three phase average differential voltage required to close the protector. Range: 0.0 to 15.0 volts
- Reclose Angle – The phase angle between the transformer voltage and the secondary network voltage must be greater or equal to this setting. Range: -60 to +30 degrees
- Reclose Time Delay - Large regenerative loads such as elevators or feeder voltage fluctuations can cause momentary reversal of power. In such cases, an erroneous tripping may occur and hence time delay is used to delay the reverse power trip function to avoid this faulty operation. Time delayed trip restrains the relay from tripping for a user-defined time on low levels of reverse power. Range: 1 to 255 cycles

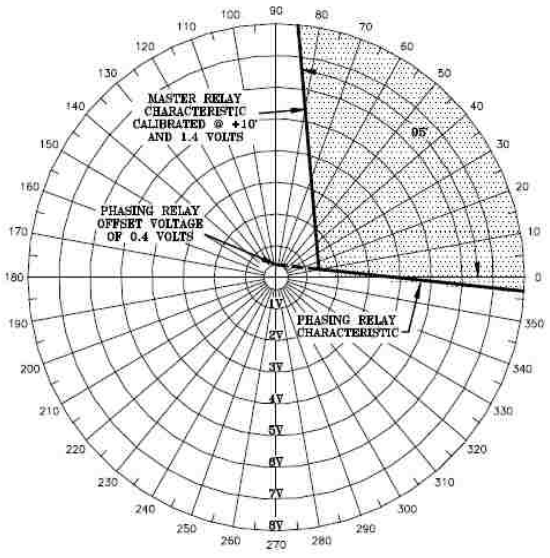

Figure 3.2—Reclose Characteristic [2]

CHAPTER 4. OVERVIEW OF DISTRIBUTION SECONDARY NETWORK SYSTEMS

Secondary networks consisting of spot and network vaults were first developed in the 1920s to serve several customers located primarily in downtown areas of major cities [6] [7]. Most spot and grid vaults are fed by two to four transformers, each from a different feeder, but a few grid vaults are fed from single transformers. This redundancy increases the reliability of the network, allowing loads to remain in service with the loss of one of its sources. For example, a faulted primary feeder or transformer connection to the secondary network is isolated within a few cycles and service is continually provided to the load without any interruption [6].

Network transformers and protectors may be located in vaults below the street or sidewalk, above the street on pole-supported structures, or throughout high-rise buildings [6]. Figure 4.1 shows the components of a network unit is located inside the vaults.

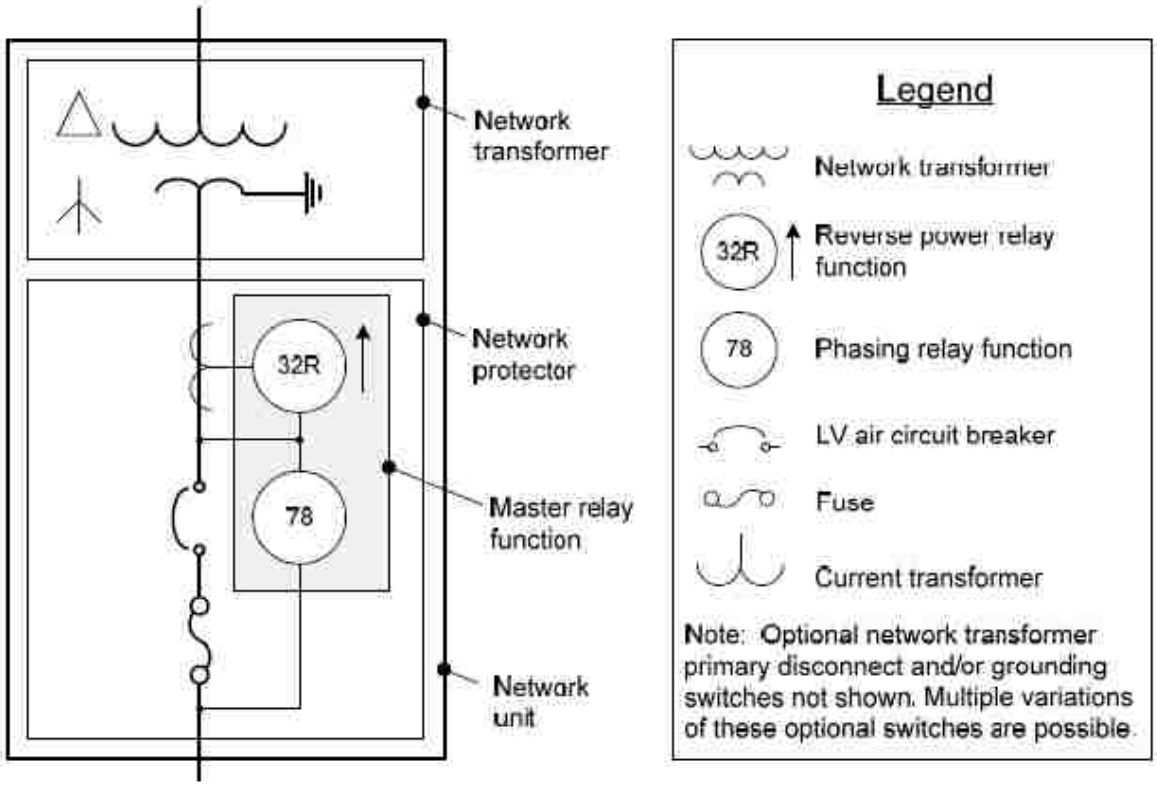

Figure 4.1—Network Unit Components [6]

As shown in Figure 4.1, the primary side of the network transformer is typically delta connected, with the secondary connected grounded wye to supply voltage to the grid and spot network customers. The cable limiters (fuses) operate for arcing faults within the vault, and help protect the insulation of the secondary cables from excessive heating.

A spot network is a type of secondary network distribution system that is usually used to serve a single customer or multiple customers in a single building such as apartment buildings, high-rise office buildings, and hospitals [5]. Figure 4.2 shows an example of a typical spot network configuration.

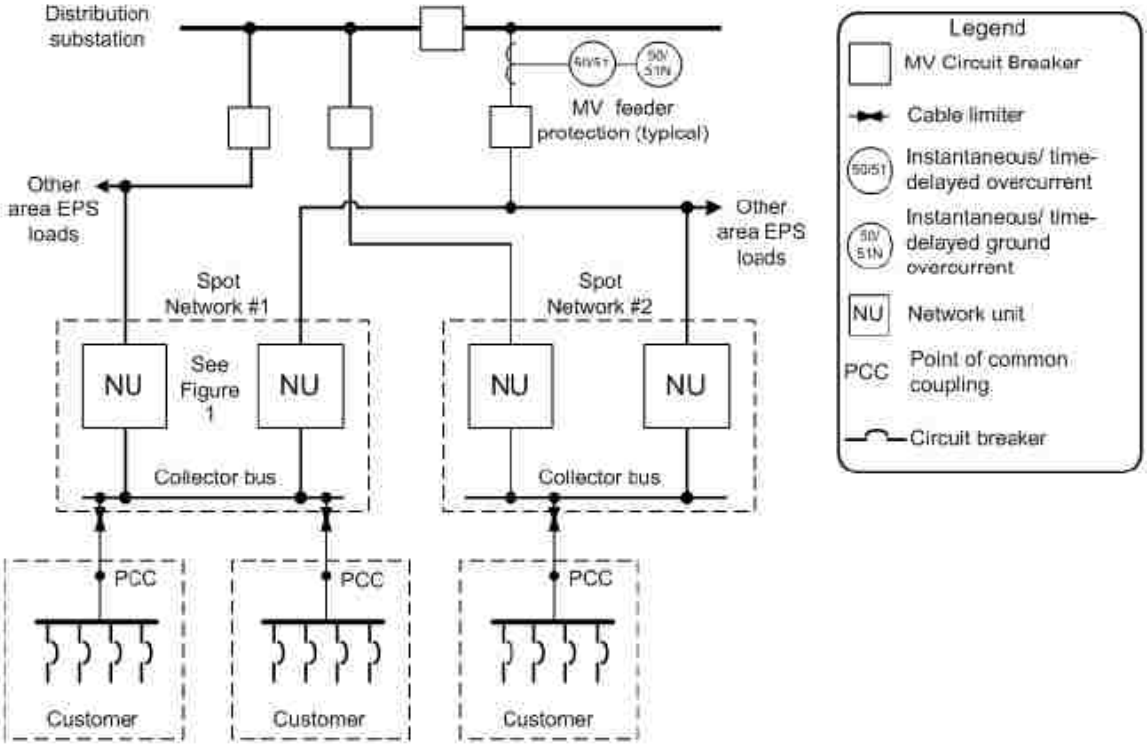

Figure 4.2—Example of spot network configuration [6]

Grid networks are designed to serve all network customer loads during peak hours, with an N-1 or N-2 contingency (1 or 2 network feeders out of service). The low voltage circuits of the grid networks are highly meshed and served by several network units. This arrangement ensures that the secondary load will not be interrupted in case of an issue with the transformer or within the primary feeder network. Grid networks are also referred to as an area network or street network. Figure 4.3 shows an example of a typical grid network configuration. Instantaneous and time-delayed relays is typically utilized on each feeder within the primary network for overcurrent protection.

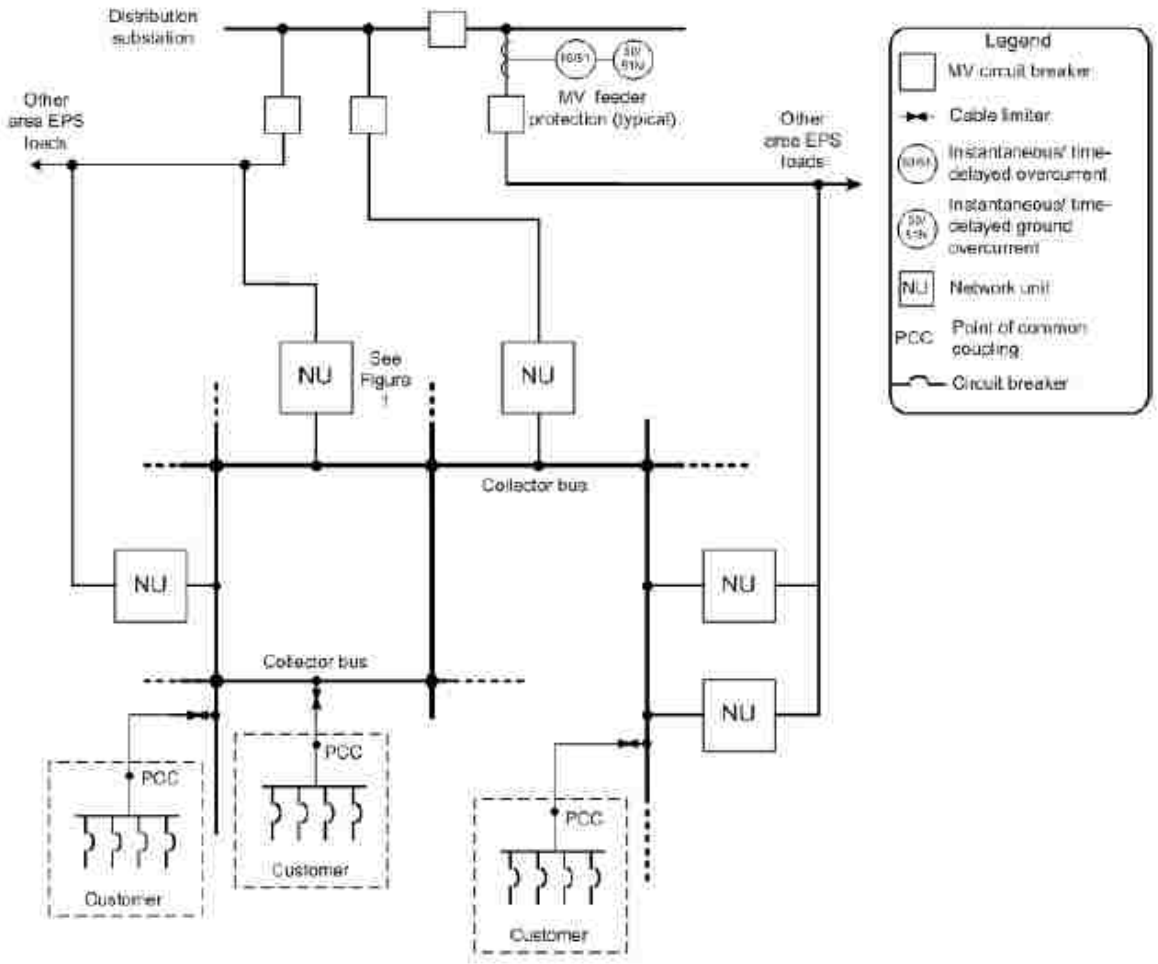

Figure 4.3— Example of grid network configuration [6]

CHAPTER 5. MODEL OF DOWNTOWN NETWORK

5.1 Model Parameters

The network model provided from Entergy consisted of seven 13.2 kV underground feeders (referred to as Feeder 1 through Feeder 7), each feeding spot network vaults (277/480V or 120/208V) and secondary grid vaults (120/208V). Entergy also provided an excel workbook of the modeling data that included both primary and secondary nodes along with impedances and lengths of line sections. Information for transformers located in the spot and grid vaults included: impedance ratings, primary and secondary connections, and voltage ratios. A list of node locations along with peak levels of all spot and grid network loads was provided. The peak load demand for the entire downtown network in this study is 33.6MW. All seven feeders originated from the same substation transformer. Figure 5.1 below shows all seven feeder breakers originating from the main substation.

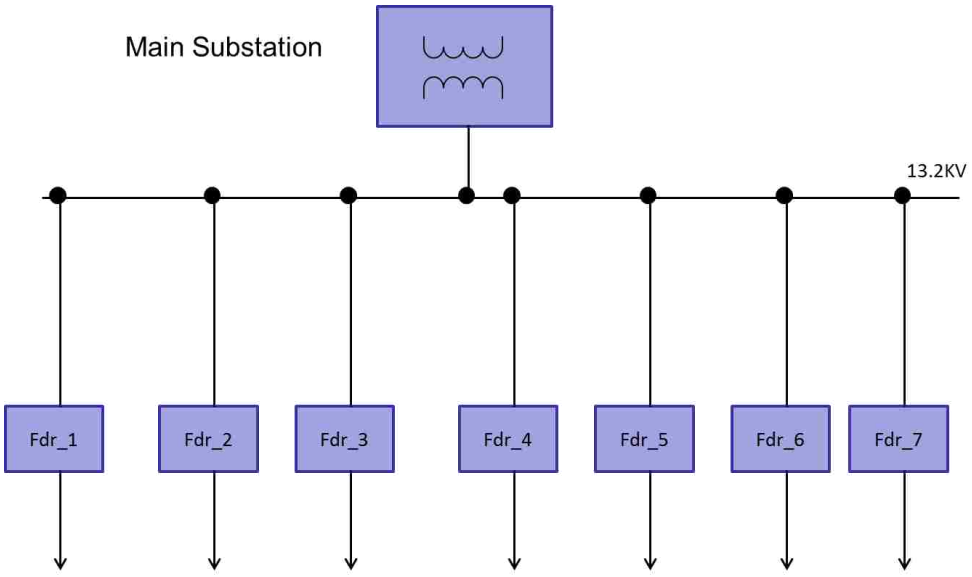

Figure 5.1—Feeder network breakers

Each feeder breaker feeds a feeder network, where the spot and grid vaults are located. Figure 5.2 shows a one line diagram of feeder network 1 with relative locations of spot and grid vaults. Feeder networks 2 through 7 have similar arrangements.

The following node nomenclature was used throughout the study:

- F1_Node005 = Node 5 on Feeder 1 (13.2kV)
- Grid_005 = Node 5 on secondary network grid (120/208V)

- GV03_Load, GV03_Fdr7, or GV03_Node1 = a node located inside grid vault GV_03
- SV04_Load, SV04_Fdr1, or SV04_Node5 = a node located inside spot vault SV_04
- Sub_Fdr3 = Origination point of Feeder 3 at the substation

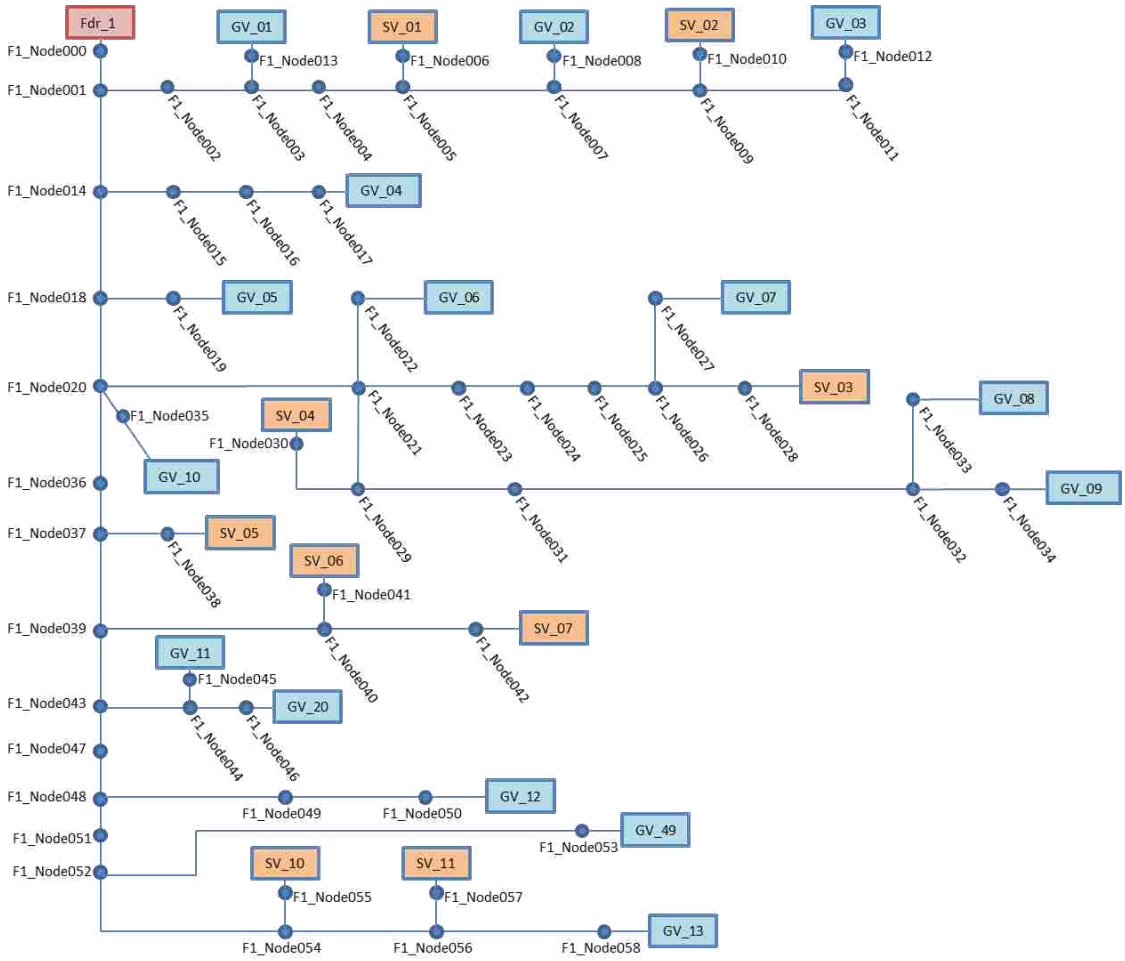

Figure 5.2—Feeder 1 Network

CHAPTER 6. VOLTAGE ANALYSIS

6.1 PV Penetration Only in Grid Mesh Network

This section is devoted the analysis of the downtown network under peak and minimum loading conditions. We evenly distributed the renewable sources at 24 load nodes throughout the grid network. For the simulations the total peak load was distributed equally among all 24 PV sources within the secondary grid. At this level, the total PV generation within the grid network was equal to the total peak load demand (Total PV penetration = 33.6MW). During the simulations, we increased the PV penetration from 5%, to 15%, up to 150% of total peak demand to observe the effect of network protector operation and stability with increasing PV penetration. The penetration levels are defined as the ratio of the real power output of the PV module to the peak load at the node. For example, if the peak real power consumed at a particular node is 10kw, 1.5kw of power would be generated at this location with 15% PV penetration present.

$$\text{PV Penetration} = \frac{Real\ power\ output\ of\ PV\ module\ (Watts)}{Real\ power\ consumed\ at\ node\ (Watts)} \tag{19}$$

6.1.1 Voltage Profiles under Different PV Arrangements

After the model of the downtown network was completed, the renewable sources were inserted into the grid network. These renewable sources essentially reduced the amount of real power that was consumed at the loads. At high levels of generation, these renewable sources transmit real power to nearby nodes and other loads. For our analysis, we studied three different arrangements of renewable sources in the grid network. Next, a comparison was made among all three PV arrangements to determine if the location of the PV penetration would have a significant effect on our simulations. Tables 2-5 show the per unit voltages in the grid network for 0%, 5%, 15%, and 30% PV penetration using different arrangements. The voltage profiles of all the arrangements at 5%, 15%, and 30% of PV penetration are shown in Figures 6.1-6.3.

Table 2—per unit grid voltages with no PV Penetration in network

0% PV Penetration	Base Case
Minimum Voltage (pu)	0.916248
Maximum Voltage (pu)	0.99728
Mean Voltage (pu)	0.9758183

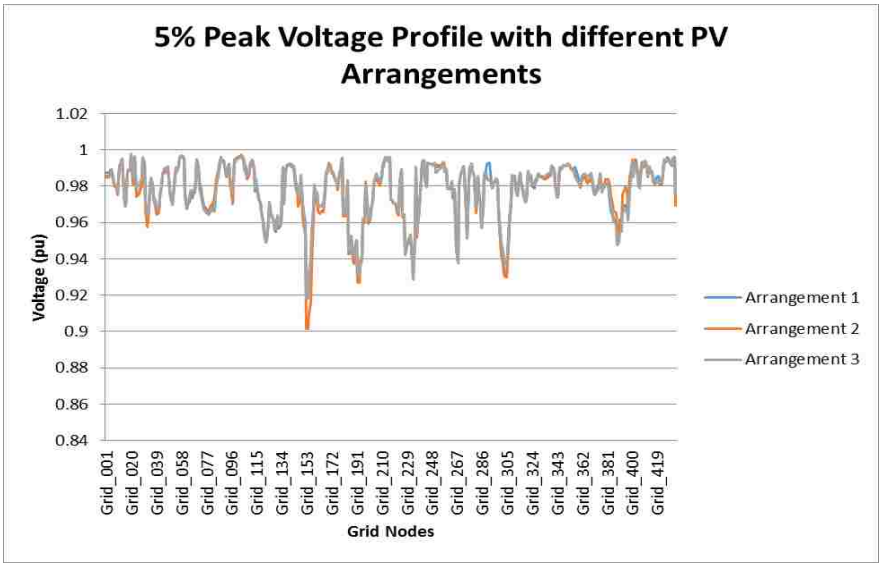

Figure 6.1—Grid Voltages for all arrangements with 5% PV penetration

Table 3—per unit grid voltages with 5% PV penetration

5% PV Penetration	Arrangement 1	Arrangement 2	Arrangement 3
Minimum Voltage (pu)	0.918112	0.901363	0.918585
Maximum Voltage (pu)	0.997398	0.99801	0.99774
Mean Voltage (pu)	0.977865	0.977427	0.977885

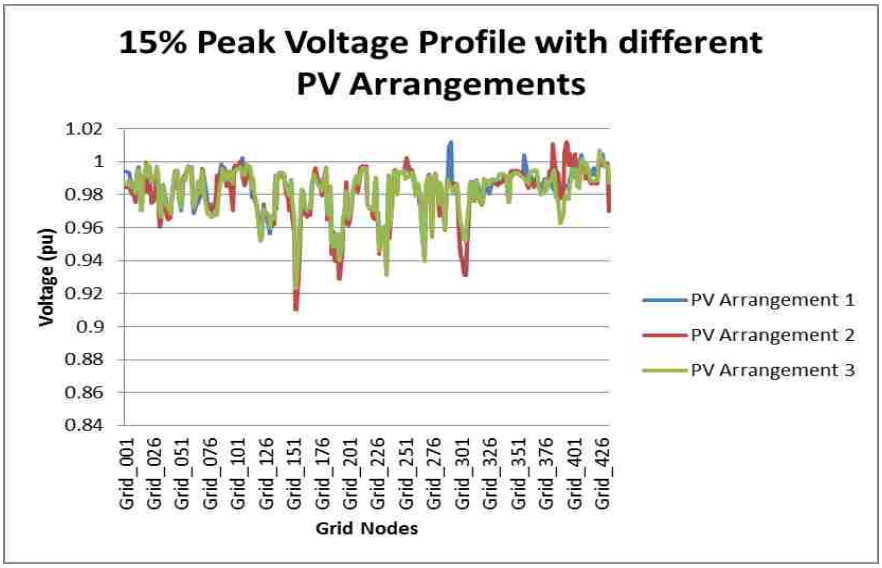

Figure 6.2—Grid Voltages for all arrangements with 15% PV penetration

Table 4—per unit grid voltages with 15% PV penetration

15% PV Penetration	Arrangement 1	Arrangement 2	Arrangement 3
Minimum Voltage (pu)	0.921712	0.910074	0.923127
Maximum Voltage (pu)	1.012061	1.011921	1.007138
Mean Voltage (pu)	0.981671	0.981145	0.981743

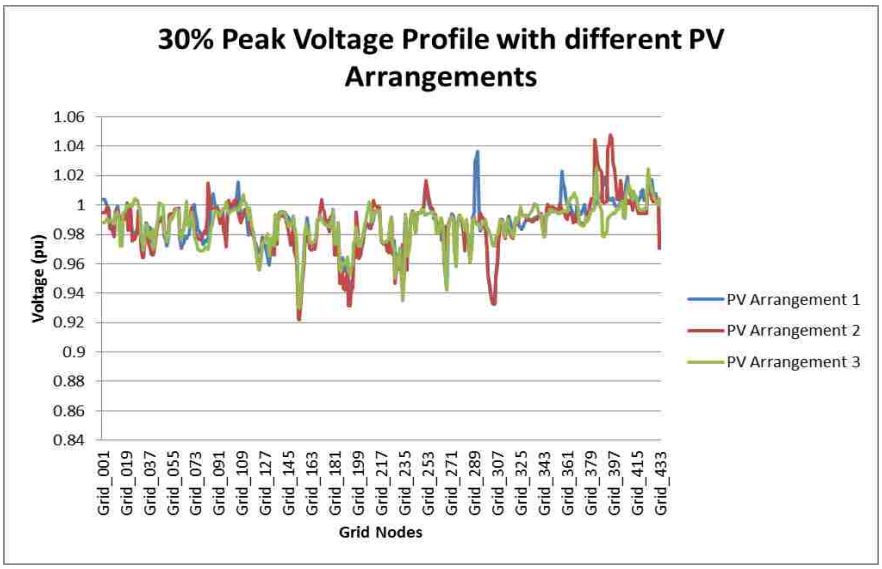

Figure 6.3—Grid Voltages for all arrangements with 30% PV penetration

Table 5—per unit grid voltages with 30% PV penetration

30% PV Penetration	Arrangement 1	Arrangement 2	Arrangement 3
Minimum Voltage (pu)	0.9268	0.921752	0.929644
Maximum Voltage (pu)	1.036362	1.04793	1.024666
Mean Voltage (pu)	0.986753	0.986083	0.986922

No major differences were observed with the voltage profiles among the different topologies at low levels of PV penetration. However, at high levels of penetration we observed differences with the stability of each arrangement. For example, under peak loading conditions both arrangements 1 and 3 became unstable after 135% PV penetration. Arrangement 2, however, was determined to be less stable at high levels of PV penetration, becoming unstable when PV penetration exceeded 90%. These results are shown in Figure 6.4. This result provides a

framework for ongoing research to examine the optimal placement of PV modules within distribution networks.

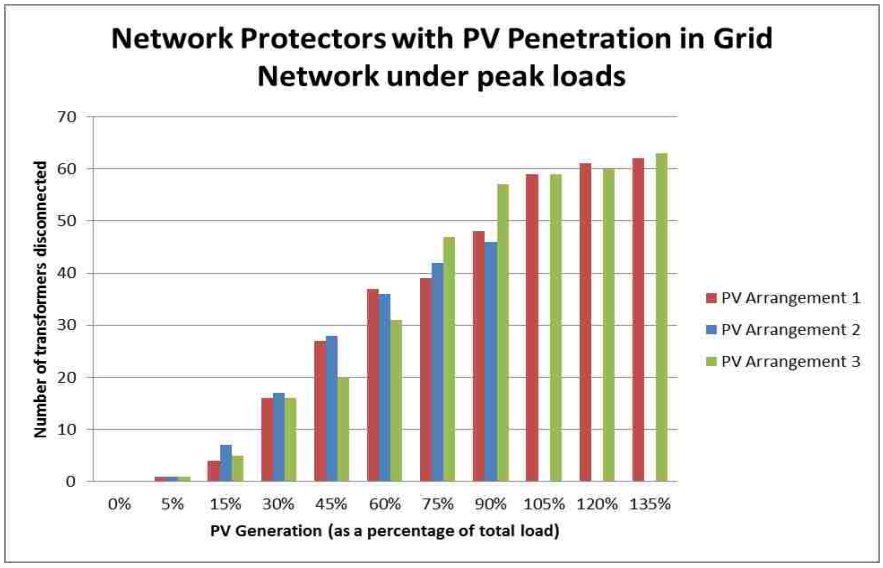

Figure 6.4—Network protector operations in grid network

6.1.2 Renewable Sources with Peak Loading

In this section, the voltage profile of the feeder networks and the grid networks are studied under peak loading conditions. The peak loading information at each bus was provided from Entergy. The PV penetration was increased from 5%, to 15%, to 150% of the total peak load in increments of 15%. This allowed us to study the effect of the renewable sources under peak loads throughout the feeder and grid networks. Figures 6.6 and 6.7 show similar results for arrangements 2 and 3 under peak loading conditions.

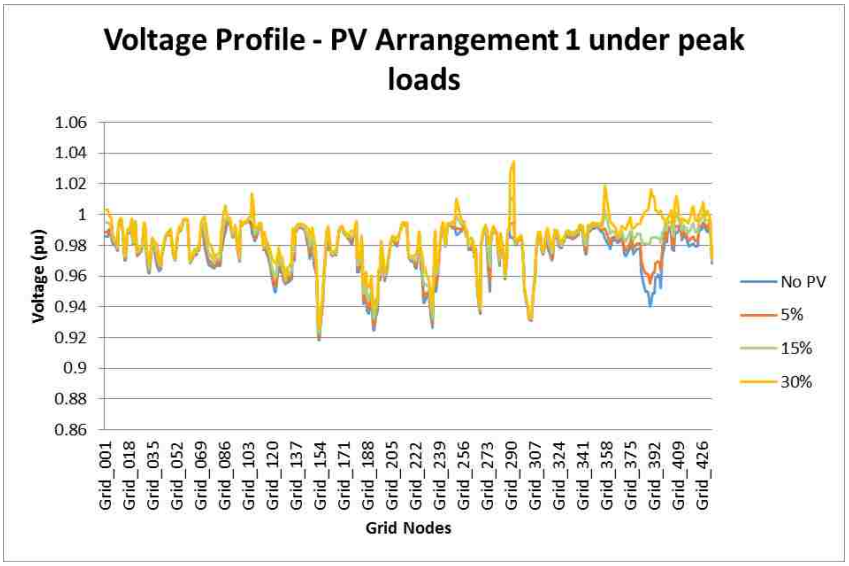

Figure 6.5—Voltage profile for Arrangement 1 under peak loads

Figure 6.5 shows that the voltage within the grid network for arrangement 1 increases as a result of more PV penetration within the grid network. Cases where PV penetration equals 5%, 15%, and 30% of the peak loads were simulated.

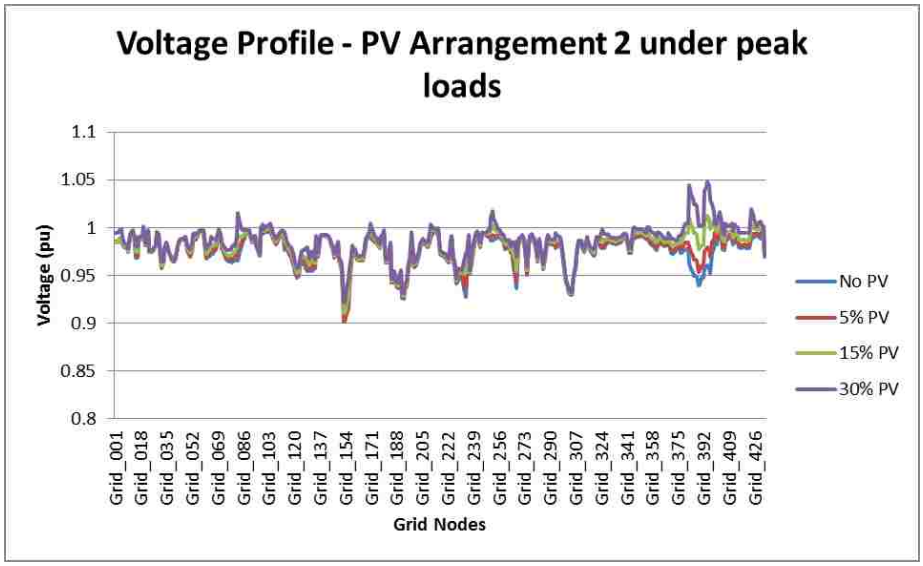

Figure 6.6—Voltage profile for Arrangement 2 under peak loads

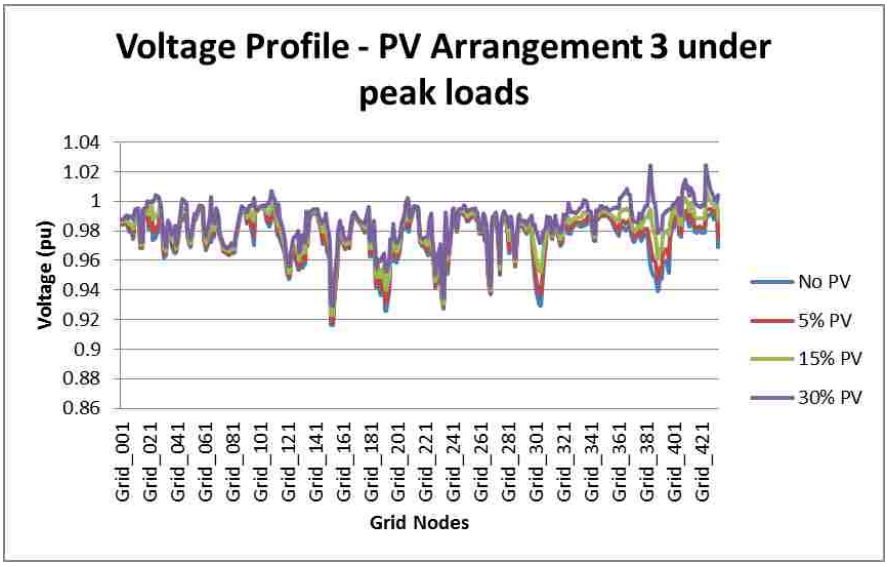

Figure 6.7—Voltage profile for Arrangement 3 under peak loads

6.1.3 Renewable Sources with Minimum Loading

In this section, the voltage profile of the grid network is studied under minimum loading conditions. In this case, the minimum loads were calculated as 16% of the peak loads. The PV penetration was increased from 5%, to 15%, to 150% of the load in increments of 15%. This allowed us to study the effect of the renewable sources under minimum loads throughout the feeder and grid networks. Figure 6.8 shows that the voltage within the grid network for arrangement 1 increases as a result of more PV penetration within the grid network. Cases where PV penetration equals 5%, 15%, and 30% of the peak loads were simulated. Figures 6.9 and 6.10 show similar results for arrangements 2 and 3 under peak loading conditions.

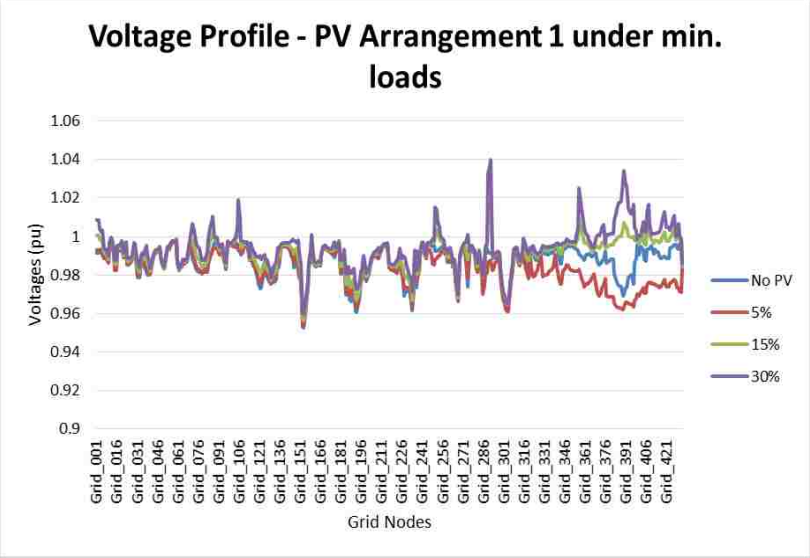

Figure 6.8— Voltage profile for Arrangement 1 under minimum loads

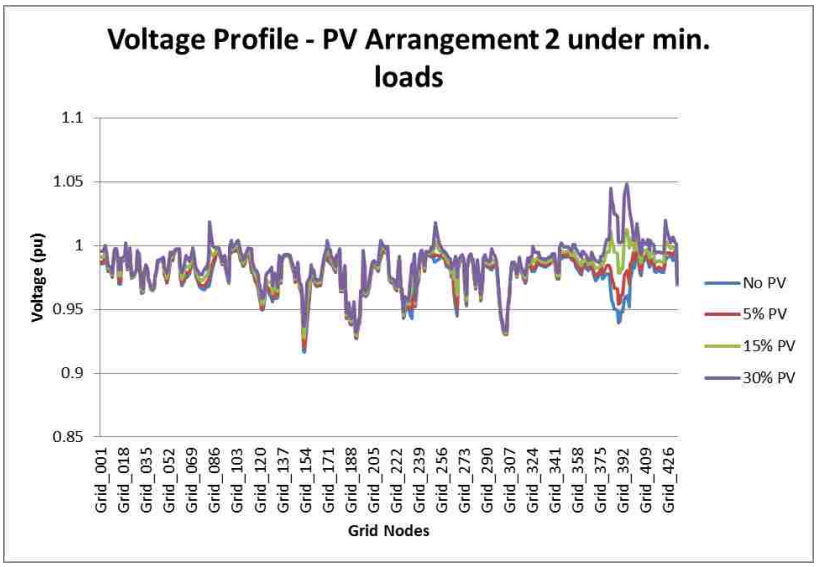

Figure 6.9— Voltage profile for Arrangement 2 under minimum loads

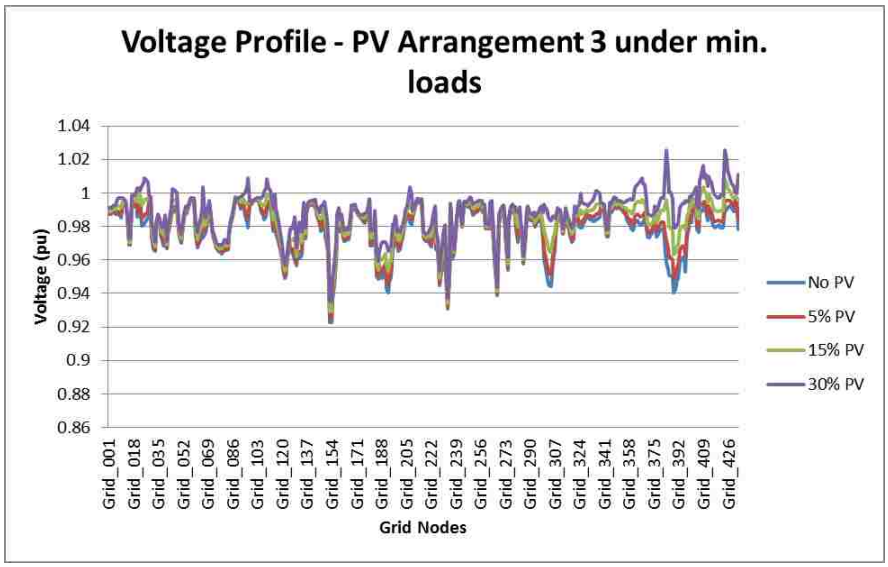

Figure 6.10— Voltage profile for Arrangement 3 under minimum loads

We see an improvement in the voltage profile for all arrangements at low levels of PV penetration. Unless explicitly stated, the remainder of the simulations in this study are performed using arrangement 1.

6.2 PV Penetration in Grid Mesh & Spot Networks

Until this point, all distributed generation has been present only within the grid mesh network. In this section, the effect of PV penetration within both the grid mesh and spot networks are observed. For our simulations, we inserted PV penetration at 6 locations within the spot networks. At peak load conditions, these locations consumed 3.66MW (10.89% of total peak demand). These loads, however, now generate 5%, 15%, up to 150% (of peak load) of their loads. The remaining PV penetration at each level is distributed equally among the original 24 grid nodes. As an example, at 100% PV penetration 3.66MW is generated within the spot network. Within the grid network 29.94MW (33.6MW – 3.66MW = 29.94MW) is generated among the 24 grid loads. This essentially decreases the PV penetration within the grid mesh network, with the addition of renewables within the spot networks.

6.2.1 Renewable Sources with Peak Loading

Figure 6.11 shows the voltage profile of the grid mesh network with PV penetration in the grid and spot networks. At low penetration levels, the distributed generation provides voltage support for multiple grid mesh nodes. However, we begin to see grid voltages above 5% nominal rating when the PV penetration exceeds 60%. Additionally, we begin to see a decline in bus voltages when the PV penetration levels exceed 120% of the peak loads.

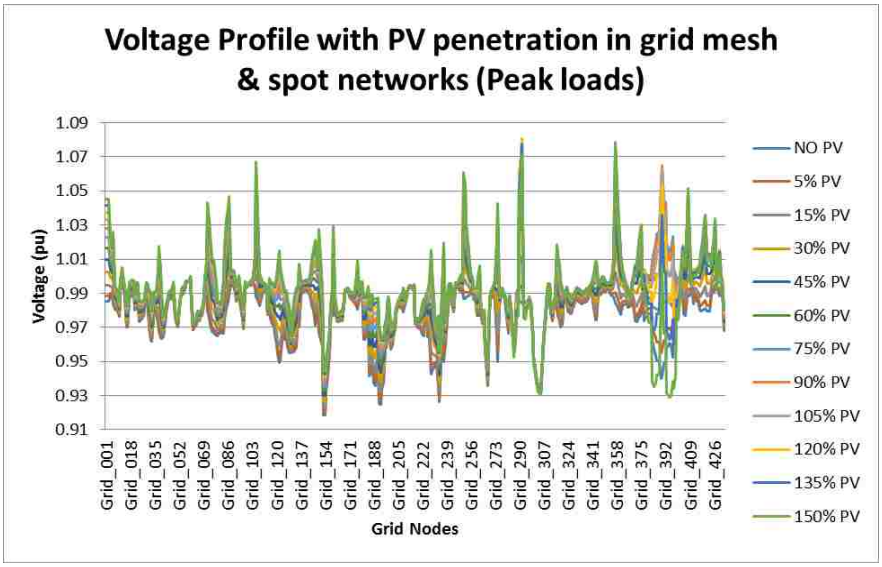

Figure 6.11— Voltage profile with PV penetration in grid mesh & spot network (peak loads)

6.2.2 Renewable Sources with Minimum Loading

Figure 6.12 shows the voltage profile of the grid mesh network with PV penetration in the grid and spot networks. We see more severe voltage problems in the case of minimum loads. At 45% PV penetration, there are locations where voltage levels increased a 5% above of its nominal rating. Additionally, we begin to see a decline in bus voltages when the PV penetration levels exceed 105% of the peak loads. This issue can be attributed to the loss of reactive power due to the increased PV penetration, which only provides real power.

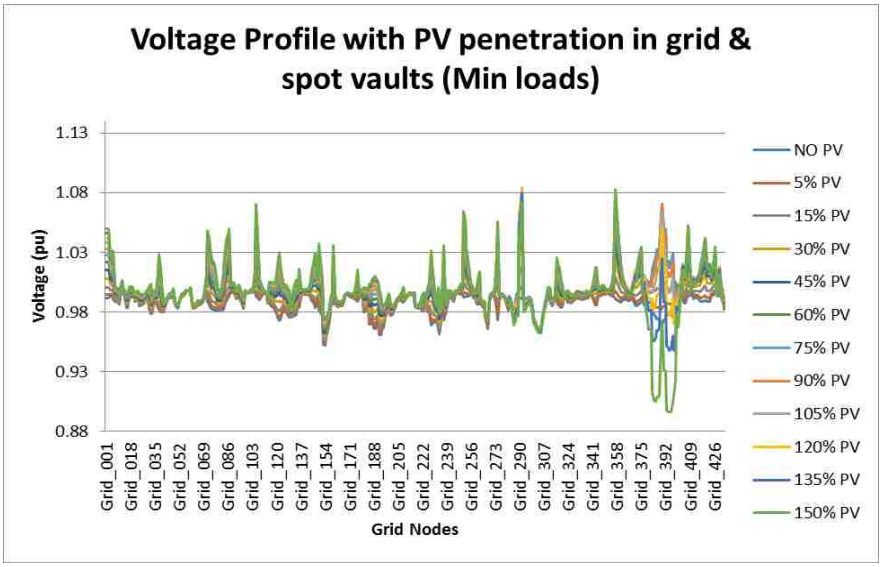

Figure 6.12— Voltage profile with PV penetration in grid mesh & spot network (min. loads)

We can take a closer look at some of the grid nodes by observing Figure 6.13. Figure 6.13 displays the effect of increased PV penetration on both the voltage and phase at the Grid_154 node. The voltage at this node is increased from 0.952 p.u. at 0% PV to 0.974 p.u. at 150% PV. In this case, the renewable source provides voltage support for this large load (422.9 kVA).

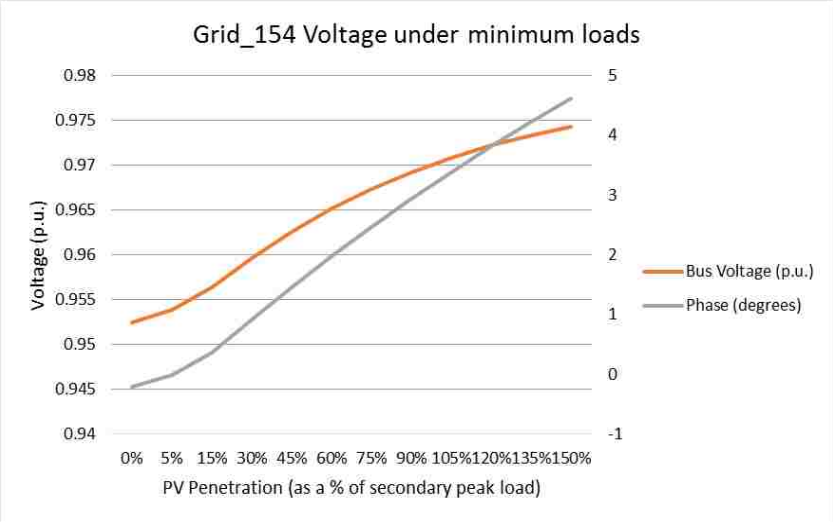

Figure 6.13— Grid_154 voltages under minimum loads

However, there are cases where the addition of renewable sources impacts the network negatively. For a load located at Grid_357, a PV source is also installed, similar to the previous case at Grid_154. In this case, however, we experience high voltages that can cause issues within the network. For example, the PV source causes the bus voltage to increase from 0.99 p.u. at 0% PV to 1.08 p.u. at 150% PV penetration. This high level is above the ANSI C84.1 voltage level (5%).

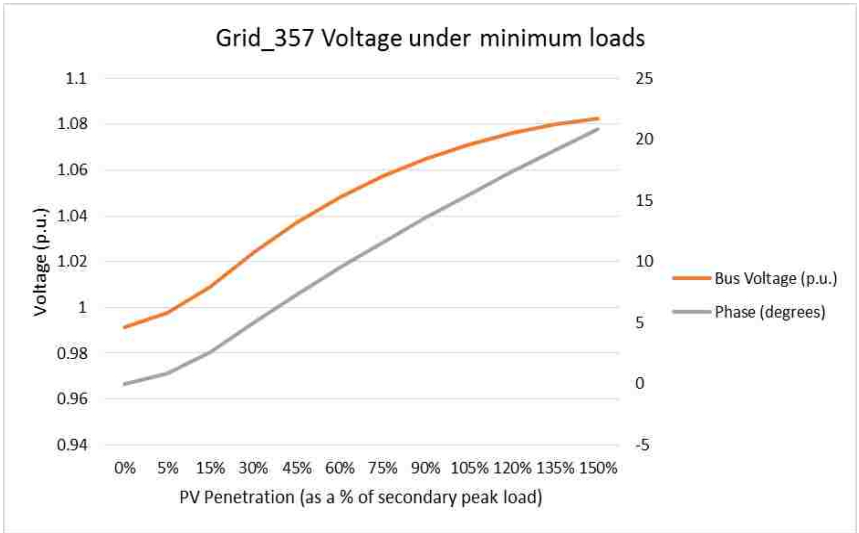

Figure 6.14— Grid_357 voltages under minimum loads

CHAPTER 7. EFFECTS OF NETWORK PROTECTOR OPERATION

7.1 PV Penetration in Grid Network

In this section we will look at the effects of network protector operation on the grid network when PV penetration is initially added only to the grid network in our simulations. We can visualize a scenario during the day where the PV modules are initially off, and then all turned on at the same time. The penetration levels will vary as a function of the available sunlight throughout the day. For these simulations, there are no communications present between the network protectors within the grid network. The sensitive trip setting is set to trip when 1.5% of rated transformer current flows from the grid network towards the utility. Also, reclose operations of the network protectors were disabled; so, once the network protector relays trip, the transformer will remain open throughout the remainder of the simulation. In addition to the network protector, the transformer protection will disconnect overloaded transformers when the loading exceeds 100% of the rated load of the transformer. Figure 6.1 below shows the amount of transformers that will be disconnected when we connect the network protectors in the downtown network. We observed that the simulation did not converge to a solution when the penetration levels exceeded 120% and 135% (of the peak loads) for the cases of minimum and peak loads respectively. This indicates that the network becomes unstable at these levels of PV penetration due to a loss of reactive power from the utility. The peak loads used were calculated at 100% of the loading information provided from Entergy. The minimum load was calculated as 16% of the peak loads.

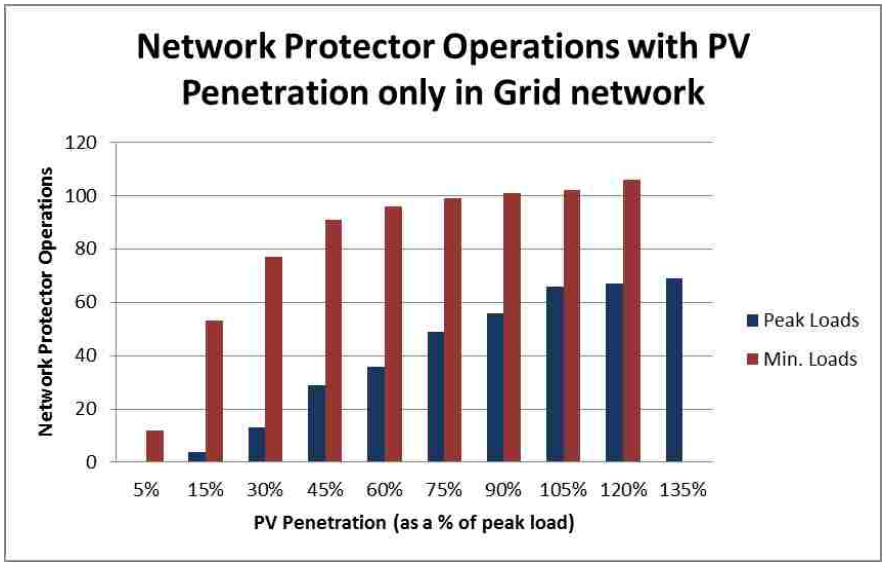

Figure 7.1— Transformers disconnected under peak and minimum loading

As expected, we see that with increased PV penetration within the grid network, we will experience more reverse power flows. We see even more reverse power flows in the case of minimum loads. This is consistent with the fact that power will flow towards the feeder network

once the load requirement is met at each grid load. Minimum loads require less power, and will therefore cause more power to flow towards the feeder networks than the case of peak loads.

7.1.1 Reverse Power Flows in Distribution Lines (PV Penetration in Grid Network)

Next, we examine the reverse power flows in the distribution lines as PV penetration is increased. The downtown network consists of 1,412 lines/transformer connections including:

- 169 network protector relays (for each network transformer)
- 717 line connections in the grid mesh network
- 118 line connections in the spot network
- 408 line connections in the primary feeder networks

Figures 7.2 and 7.3 examine the power flows for the lines within the distribution network when PV penetration is increased. Generally, we can expect to see an increase in reverse power flows as PV penetration is increased. It is interesting to note that although the spot networks are not generating any real power in this case, line sections within the spot networks experience reverse power flows. Increased penetration within the grid network has an effect on the power flows in the spot networks. In general, PV penetration in the grid network affects the power flow in the primary feeder networks, which will alter the power flows within the spot networks as well.

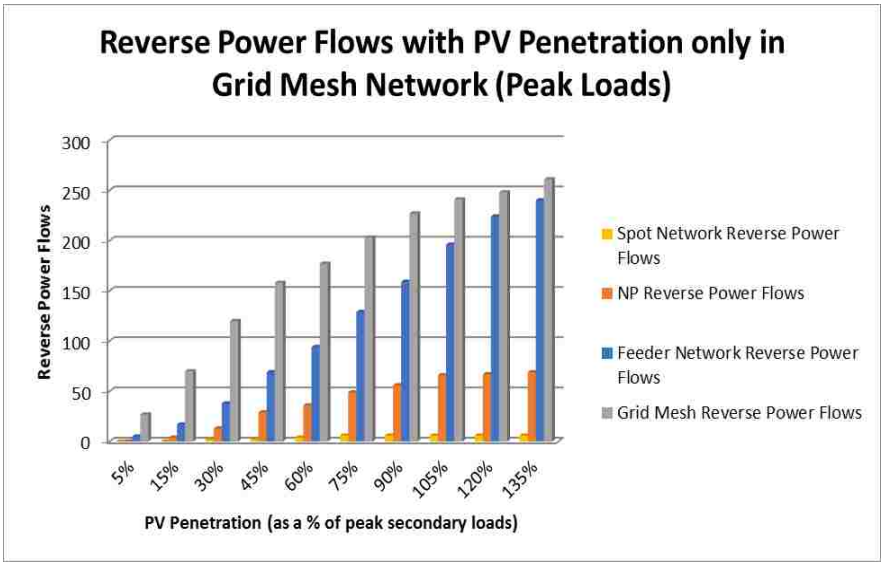

Figure 7.2— Reverse power flows with PV penetration in Grid Mesh Network (peak loads)

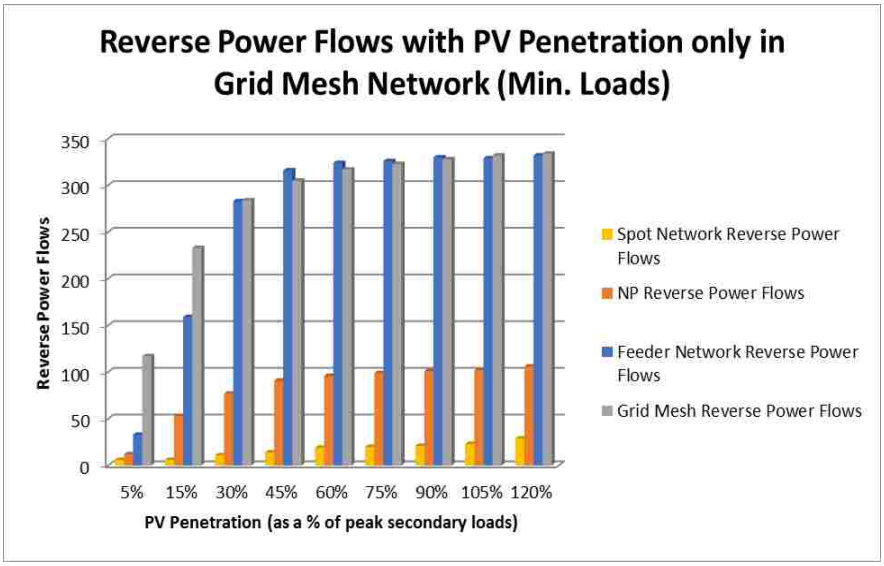

Figure 7.3— Reverse power flows with PV penetration in Grid Mesh Network (min. loads)

It is interesting to note that although no PV penetration is present within the spot networks for these simulations, we still experience reverse power flows in the spot networks. Although the secondary grid mesh and spot networks are not connected at the loads, their primary networks are tied together as shown in Figure 7.4. In this case, both transformers provide the power to the SV27_Load without PV penetration present in the network. The sources for the feeds originate from feeder networks 3 and 5. However, when PV penetration is added, the direction of power flow is reversed at the transformer coming from feeder network 3. Therefore, we see that PV penetration within the grid mesh network can cause reverse power flows, and even network protector operations in the spot networks.

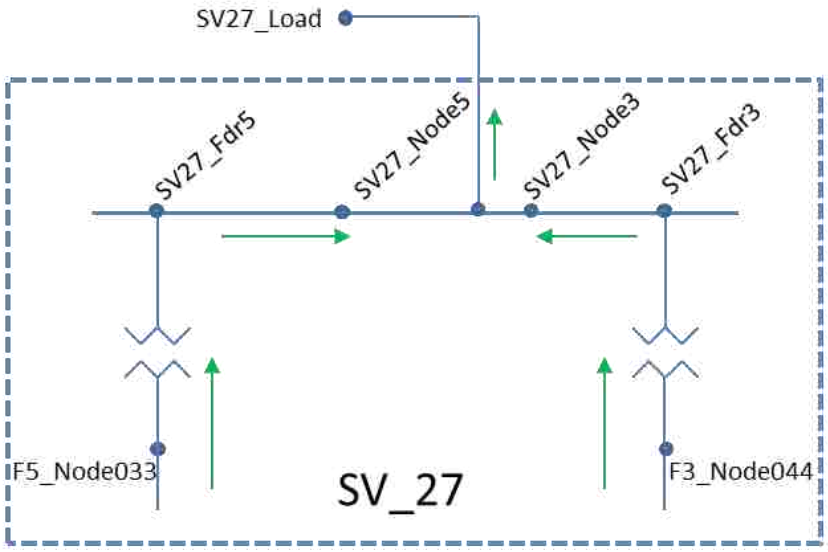

Figure 7.4— Power flows for SV_27 with no PV Penetration

7.1.2 PV Penetration and Transformer Loading

Next, we add the effect of transformer overloads to the simulation. Figure 7.5 shows the number of transformers that will be disconnected due to reverse power flows and transformer overloads under peak loading conditions using arrangement 1. We see that we begin to experience transformer overloads when the PV penetration in the grid network exceeds 45% of the load. As the PV penetration is increased, more network protectors will experience more reverse power flows and trip. With fewer transformers in the downtown network, the power has fewer paths to flow towards the load and can overload the remaining lines and transformers in the network. This process may provoke a cascading event where overcurrent relays operate as a result of the increased power flows. Consequently, the voltage profiles within the secondary grid network can be seriously affected and initiate a voltage collapse situation [3].

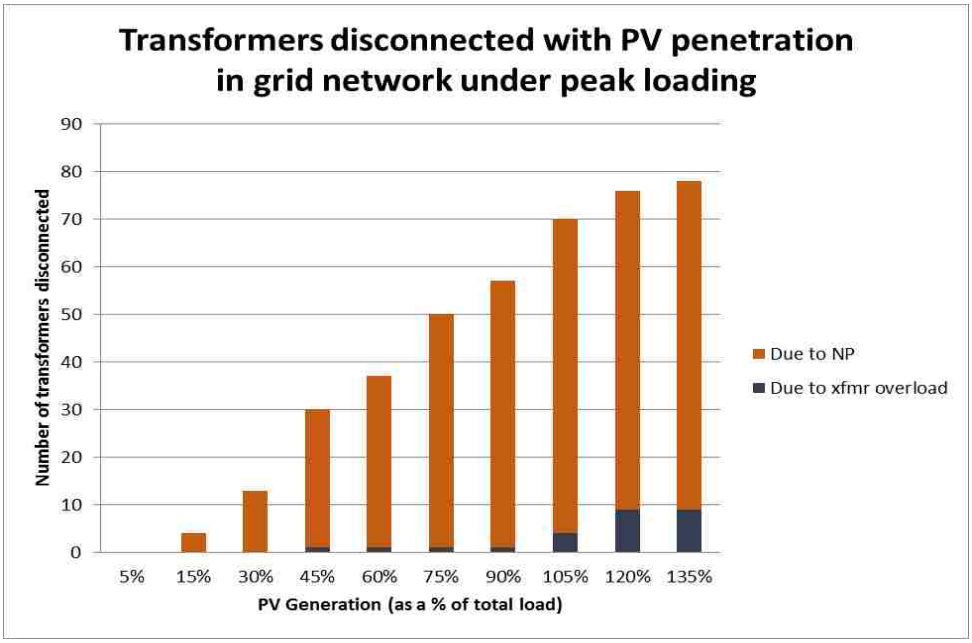

Figure 7.5— Transformers disconnected under peak loading conditions

7.2 PV Penetration in Grid & Spot Networks

7.2.1 Reverse power flows in distribution lines (PV penetration in grid & spot networks)

Figures 7.6 and 7.7 details the reverse power flows in all of the lines in the distribution network for these simulations. For all cases, we see an increase in reverse power flows as PV penetration is increased in both networks. However, the addition of renewables within the spot network provided an increase in voltage stability for the network. We see that under peak and minimum load conditions the downtown network is now stable for all cases (up to 150% PV penetration).

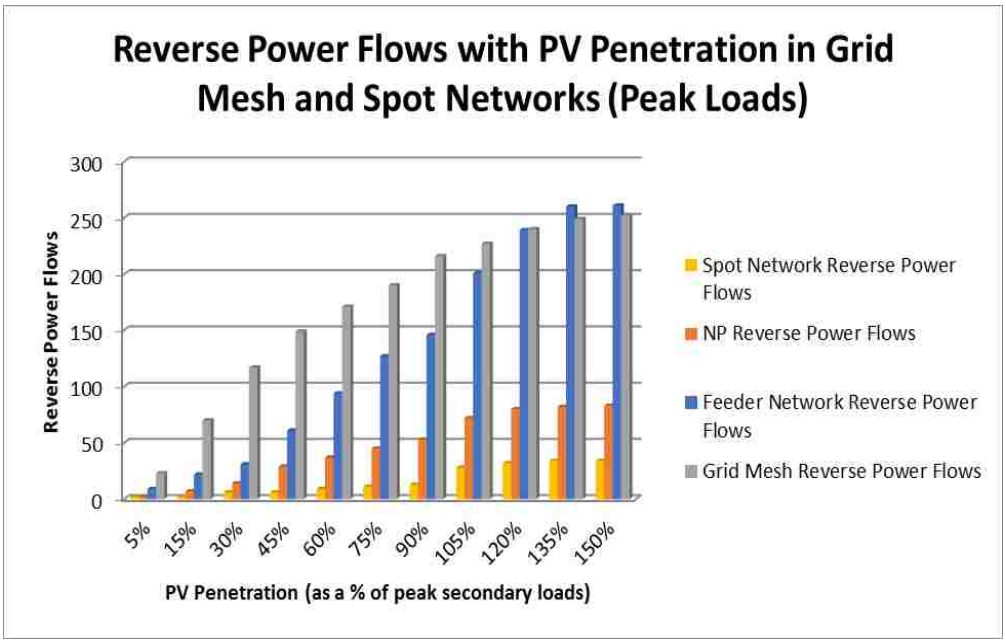

Figure 7.6— Reverse power flows with PV penetration in Grid & Spot Networks (peak loads)

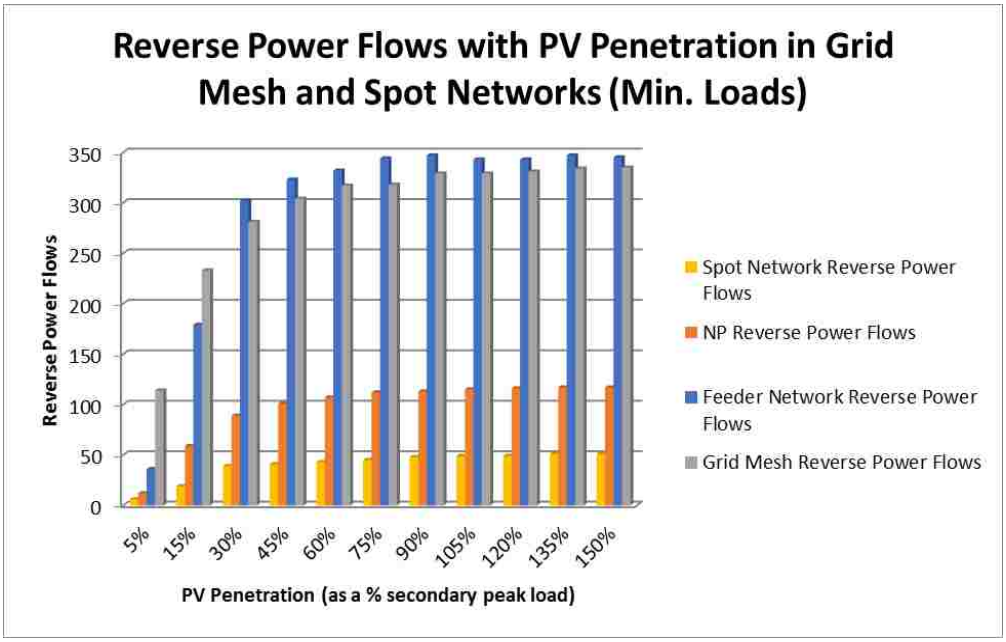

Figure 7.7— Reverse power flows with PV penetration in Grid & Spot Networks (min. loads)

CHAPTER 8. CLOUD EFFECTS

The amount of power that the PV sources deliver is directly proportional to the amount of sunlight it receives. Additionally, the presence of clouds in the downtown network can cause voltage fluctuations in short periods of time when a significant amount of energy is provided via PV penetration. This section is devoted to studying these effects on the downtown network. We will consider the cases when 5%, 15%, and 30% PV penetration is present in the downtown network. We performed these simulations with PV arrangement 1. In all simulations, 6 transformers are out of service in the network, and one additional transformer is disconnected due to the existence of reverse power without PV penetration. For the simulations, we divided the grid network into Areas A, B, and C. The cloud covers 1/3 of the grid network. For each case, this cloud passes over the network from Area A, to Area B, and finally exiting in Area C. With the cloud covering part of the grid network the PV radiation at the renewable sources is reduced 70%. In each case, a "snapshot" of the network is obtained. We use this information to study the voltage profile as a result of the presence of clouds.

8.1 Clouds with 5% PV Penetration

For the first simulation with the clouds in the downtown network peak loading conditions are present with 5% PV penetration. A total of 1.68MW (5% of total load) of PV penetration is added to the grid network. Three additional network protector relays operate as a result of the PV penetration. With 5% PV penetration present in the downtown network a random cloud passes over each area and a "snapshot of the system is obtained. The renewable sources only generate 1.29MW when the cloud is passing through the area.

$$\text{Radiation with cloud present} = \text{PV Penetration} - (\text{PV Penetration} \times 0.7 \times 0.33) \quad (20)$$

$$= 1.68\text{MW} - (1.68\text{MW} \times 0.7 \times 0.33) = 1.29\text{MW} \quad (21)$$

Table 6 shows the per-unit calculations for the voltages as the cloud passes through the network with 5% PV penetration present.

Table 6— per unit grid voltages with clouds in Areas A, B, & C (5% PV Penetration)

	No Clouds	Clouds in A	Clouds in B	Clouds in C
Mean	0.97787198	0.97760624	0.9775441	0.97708528
Minimum	0.91811449	0.91800278	0.91697057	0.91809696
Maximum	0.99739809	0.9973206	0.99739095	0.99739453

Figure 8.1 shows a voltage profile of the grid network with a cloud covering 1/3 of the area.

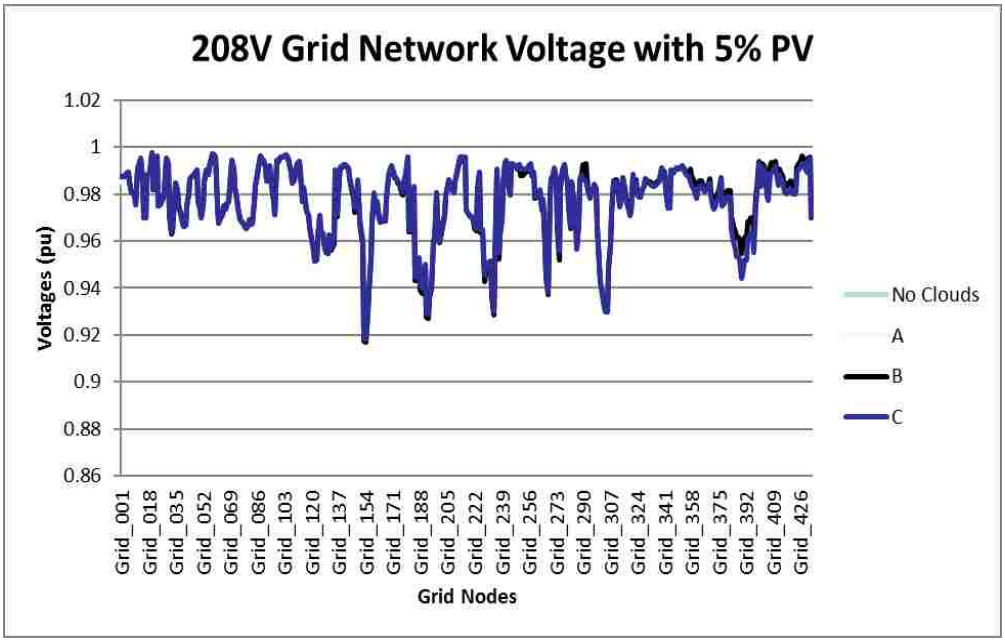

Figure 8.1—Grid Network Voltage with clouds in Areas A, B, & C (5% PV Penetration)

We see that the clouds did not change the voltage profile significantly for the case with 5% PV penetration in the downtown network. Also no additional transformers operated with the presence of clouds in the network.

8.2 Clouds with 15% PV Penetration

The simulation is repeated again for 15% PV penetration. In this case 5.04MW is added to the grid network causing an additional three network protectors to operate. With the presence of the cloud, the total PV penetration reduces to 3.86MW. Table 7 shows the per-unit calculations for the voltages as the cloud passes through the network with 15% PV penetration present.

Table 7— per unit grid voltages with clouds in Areas A, B, & C (15% PV Penetration)

	No Clouds	Clouds in A	Clouds in B	Clouds in C
Mean	0.9805966	0.97982646	0.97959543	0.97459128
Minimum	0.9217445	0.92138914	0.9183868	0.92169502
Maximum	1.0120522	1.01198933	1.01190406	1.00066861

Snapshots of the voltages are provided in Figure 8.2.

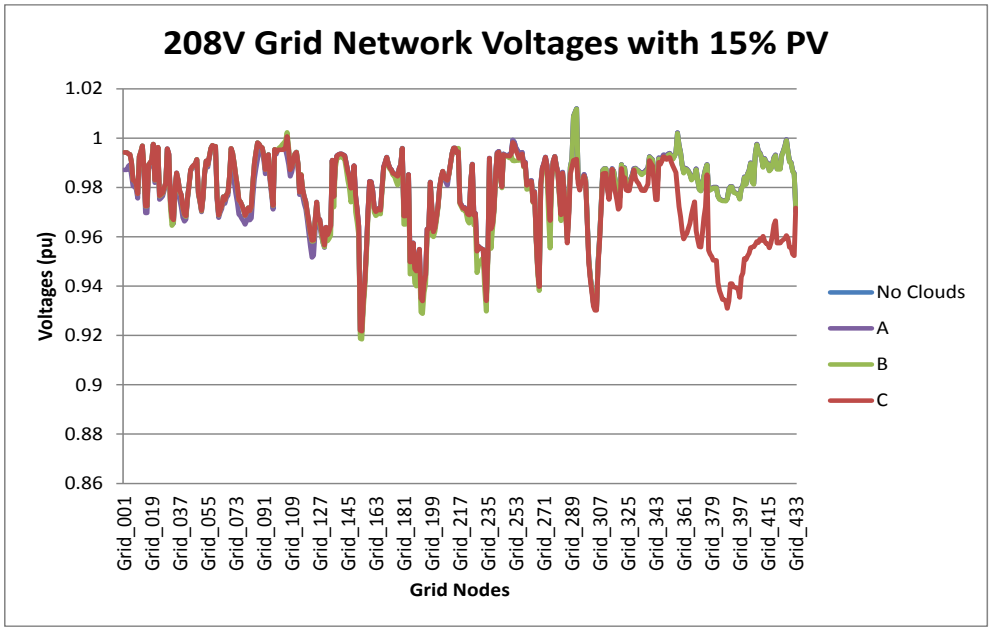

Figure 8.2—Grid Network Voltage with clouds in Areas A, B, & C (15% PV Penetration)

For the case with 15% PV penetration present, we observed a small decrease in the grid network voltages with the clouds present. We also observed one network protector trip with clouds present in both Areas A and B. No transformers became overloaded with the presence of the cloud.

8.3 Clouds with 30% PV Penetration

Next, we observed the passage of a cloud with 30% PV penetration present. With the cloud present, the total PV generated in the downtown network reduces from 10.08MW to 7.73MW. Table 8 shows the per-unit calculations for the voltages as the cloud passes through the network with 30% PV penetration present.

Table 8—per unit grid voltages with clouds in Area A, B, & C (30% PV Penetration)

	No Clouds	Clouds in A	Clouds in B	Clouds in C
Mean	0.9859777	0.98441874	0.98371357	0.97399468
Minimum	0.926892	0.92618371	0.92044291	0.92641014
Maximum	1.0311518	1.0311302	1.02973957	1.01606723

Snapshots of the grid voltages are provided in Figure 8.3.

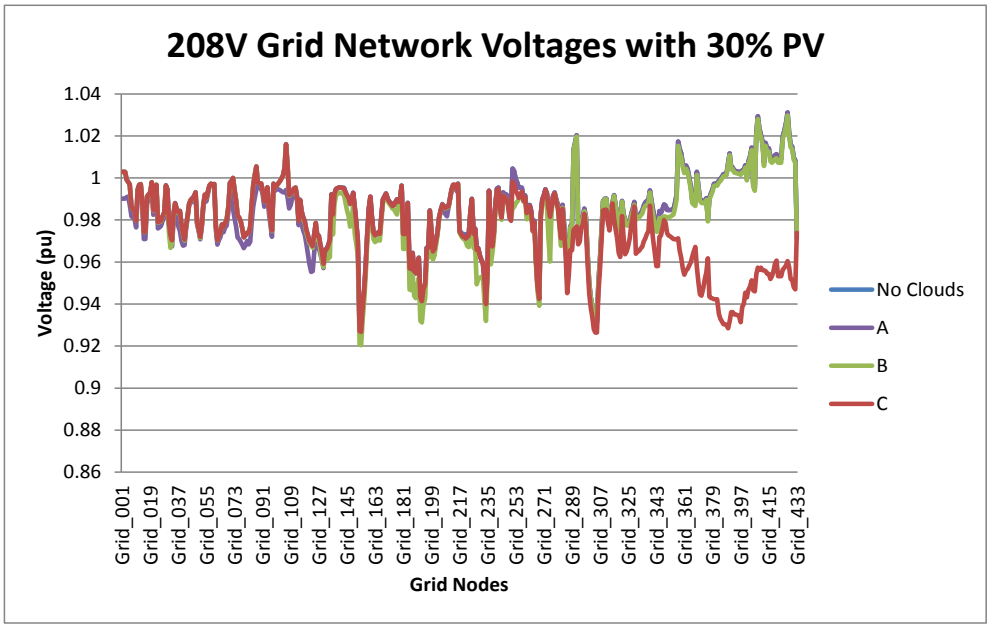

Figure 8.3—Grid Network Voltage with clouds in Areas A, B, & C (30% PV Penetration)

For the case of PV penetration = 30%, the cloud first arrives in Area A, causing 16 additional network protectors to operate. These transformers remain open throughout the remainder of the simulation. The cloud then passes over Area B, causing 3 more network protectors to operate and remain open. The cloud finally passes over Area C, where no additional network protectors operate. However, Figure 8.3 shows that low voltage will be present in the network based on the amount of transformers that are now disconnected at the time.

Through these simulations, we observed that the effect of the presence of clouds is directly proportional to the amount of PV penetration present in the grid network. For example, we see that the voltage of the grid network is impacted as a result of clouds more heavily when the PV penetration is high.

CHAPTER 9. CASE STUDIES

9.1 Simulations with Faults on Feeder Networks

In this section, simulations are performed on the downtown network to investigate network protector operation under faulted conditions, as well as the operation after a fault. These simulations are performed under minimum load conditions where the load is 16% of the peak load conditions. The simulation is summarized below:

1. Load flow solved at 2%, 5%, and 8% PV penetration for all arrangements.
2. Three phase fault established on each primary feeder network
   a. Observe additional network protector trips due to fault
   b. Observe re-close conditions post fault
   c. Observe network protectors in open state post fault (due to reverse power flows and overloads)
   d. Observe changes (open/closed) in network protectors as a result of fault

9.2 Simulations with No PV Penetration Present

The first simulation is performed during the evening with no PV penetration present within the grid network. Initially, there are 6 transformers out of service. An additional transformer is disconnected due to reverse power flow. So at this point we have 162 out of 169 transformers connected to the grid network. Next, a three-phase high resistance (0.05 per unit) fault is introduced in each of the primary feeders. Figure 9.1 shows the location of the fault on feeder side of grid vault 2.

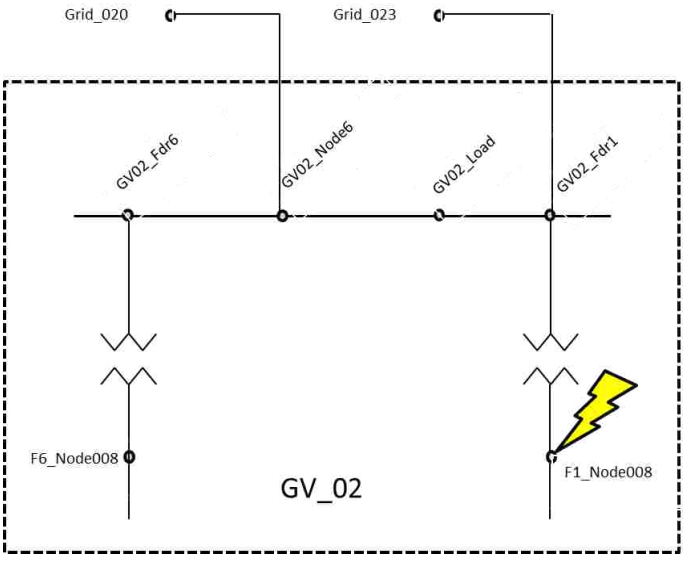

Network Protector Status	Feeder 1
NP out-of-service	6
NP Trips with no PV	1
NP in open state pre-fault	7
Additional NP trips due to fault	6
NP closed after fault	0
NP in open state post fault	13
NP in different state after fault	6

Figure 9.1—Simulation results for a fault on feeder network 1 (No PV Penetration)

After the fault has cleared, the voltages on the primary side of the transformer are slightly higher than the voltage on the secondary side. The primary voltage angle also leads the voltage angle on the secondary side. However, due to the small voltage difference between the primary and secondary networks (V_d=0.39V), no network protectors reclosed after the fault.

This same simulation is repeated for each feeder network below in Figures 9.2 through 9.7.

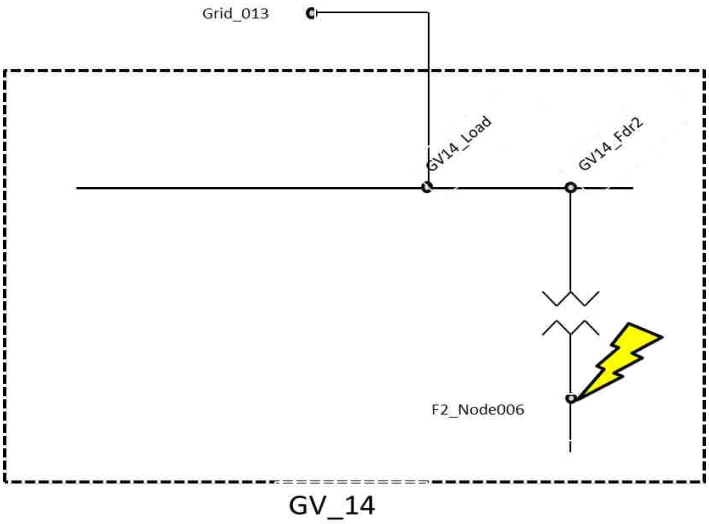

Network Protector Status	Feeder 2
NP out-of-service	6
NP Trips with no PV	1
NP in open state pre-fault	7
Additional NP trips due to fault	6
NP closed after fault	0
NP in open state post fault	13
NP in different state after fault	6

Figure 9.2—Simulation results for a fault on feeder network 2 (No PV Penetration)

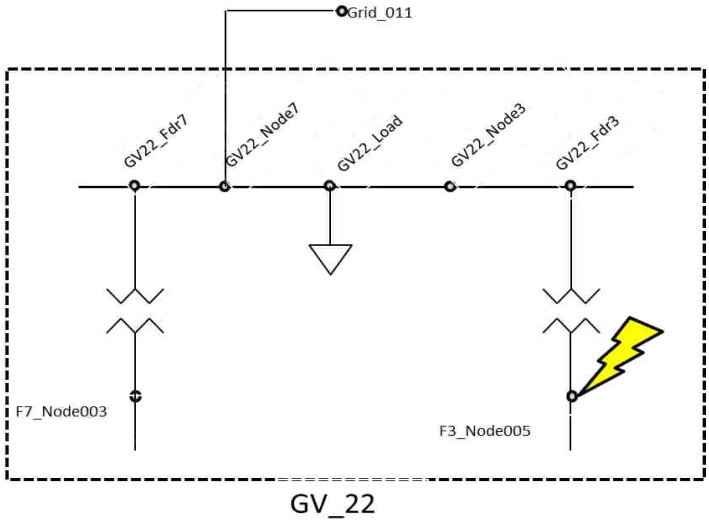

Network Protector Status	Feeder 3
NP out-of-service	6
NP Trips with no PV	1
NP in open state pre-fault	7
Additional NP trips due to fault	4
NP closed after fault	0
NP in open state post fault	11
NP in different state after fault	4

Figure 9.3—Simulation results for a fault on feeder network 3 (No PV Penetration)

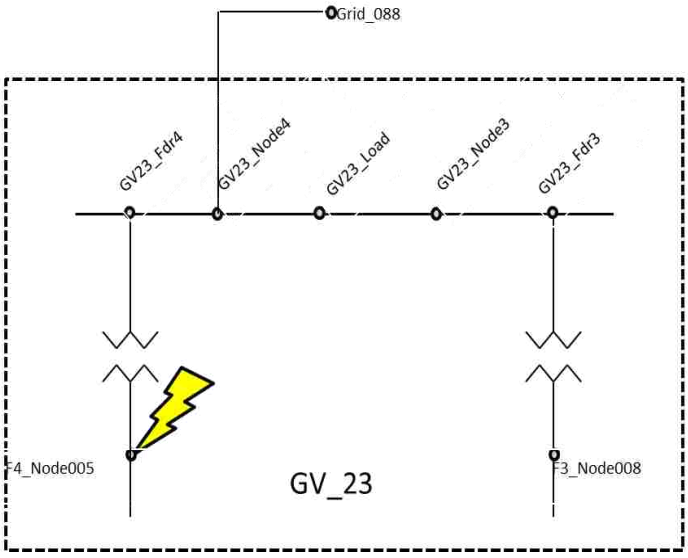

Network Protector Status	Feeder 4
NP out-of-service	6
NP Trips with no PV	1
NP in open state pre-fault	7
Additional NP trips due to fault	4
NP closed after fault	0
NP in open state post fault	11
NP in different state after fault	4

Figure 9.4—Simulation results for a fault on feeder network 4 (No PV Penetration)

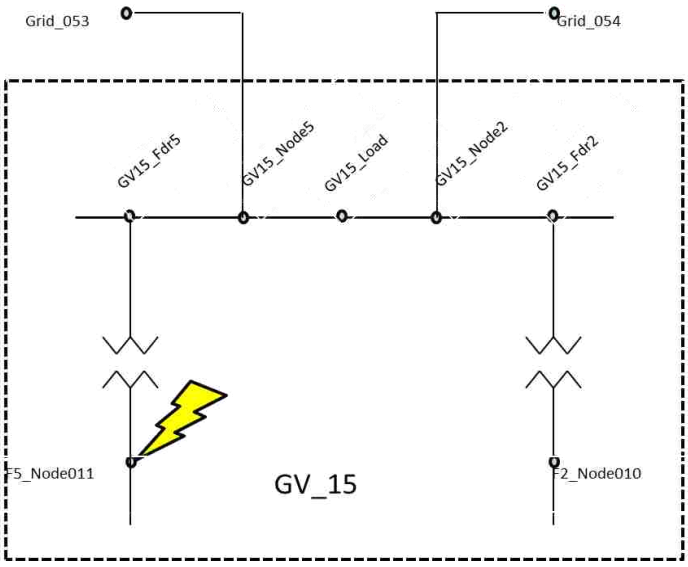

Network Protector Status	Feeder 5
NP out-of-service	6
NP Trips with no PV	1
NP in open state pre-fault	7
Additional NP trips due to fault	20
NP closed after fault	1
NP in open state post fault	26
NP in different state after fault	21

Figure 9.5—Simulation results for a fault on feeder network 5 (No PV Penetration)

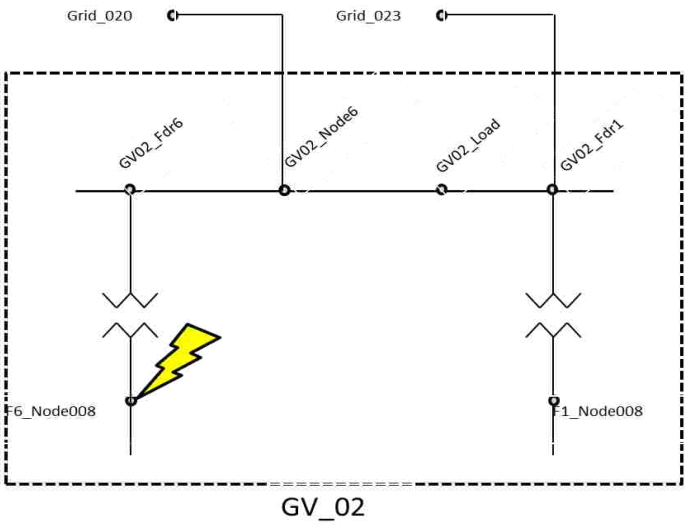

Network Protector Status	Feeder 6
NP out-of-service	6
NP Trips with no PV	1
NP in open state pre-fault	7
Additional NP trips due to fault	13
NP closed after fault	1
NP in open state post fault	19
NP in different state after fault	14

Figure 9.6—Simulation results for a fault on feeder network 6 (No PV Penetration)

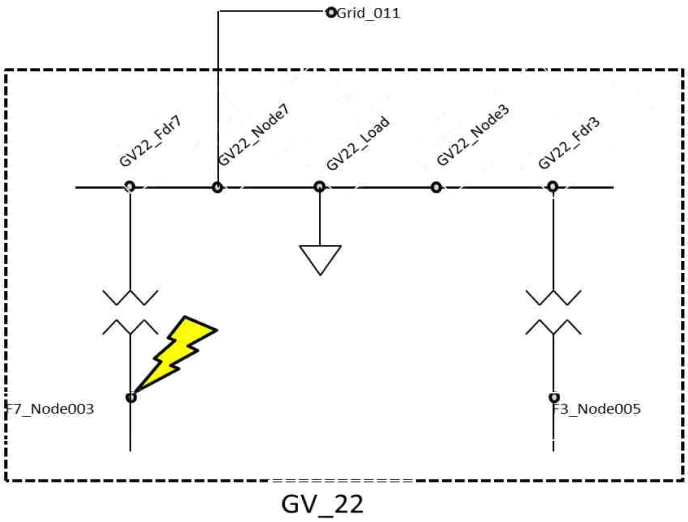

Network Protector Status	Feeder 7
NP out-of-service	6
NP Trips with no PV	1
NP in open state pre-fault	7
Additional NP trips due to fault	1
NP closed after fault	0
NP in open state post fault	8
NP in different state after fault	1

Figure 9.7—Simulation results for a fault on feeder network 7 (No PV Penetration)

9.3 Simulations with 2% PV Penetration Present

In this section, a three phase high impedance fault is introduced into all feeder networks with 2% PV penetration present in the grid. For arrangement 1in Table 9, 5.9% of the transformers in the downtown network are disconnected prior to the fault. We observe that after a fault in feeders 5 and 6 has been cleared, one network protector will reclose in both cases.

Table 9—Arrangement 1 with 2% PV penetration

Simulation	Feeder 1	Feeder 2	Feeder 3	Feeder 4	Feeder 5	Feeder 6	Feeder 7
NP disconnected prior to simulation	6	6	6	6	6	6	6
NP Trips with no PV	1	1	1	1	1	1	1
NP trips with 2% PV	3	3	3	3	3	3	3
NP in open state pre-fault	10	10	10	10	10	10	10
Additional NP trips due to fault	8	6	4	5	20	16	2
NP closed after fault	0	0	0	0	1	1	0
NP in open state post fault	18	16	14	15	29	25	12
NP in different state post fault	8	6	4	5	21	17	2

For arrangement 2, five additional network protectors tripped to remove the reverse power flows caused by the 2% PV penetration. At this stage, 7.1% of the transformers in the downtown network were disconnected prior to the fault. After the fault is cleared, we observe that no network protectors reclose.

Table 10—Arrangement 2 with 2% PV penetration

Simulation	Feeder 1	Feeder 2	Feeder 3	Feeder 4	Feeder 5	Feeder 6	Feeder 7
NP disconnected prior to simulation	6	6	6	6	6	6	6
NP Trips with no PV	1	1	1	1	1	1	1
NP trips with 2% PV	5	5	5	5	5	5	5
NP in open state pre-fault	12	12	12	12	12	12	12
Additional NP trips due to fault	7	6	5	17	19	16	2
NP closed after fault	0	0	0	0	0	0	0
NP in open state post fault	19	18	17	29	31	28	14
NP in different state post fault	7	6	5	17	19	16	2

For arrangement 3, three additional network protectors tripped to remove the reverse power flows caused by the 2% PV penetration. At this stage, 5.9% of the transformers in the downtown network were disconnected prior to the fault. After the fault is cleared, we observe that no network protectors reclose.

Table 11—Arrangement 3 with 2% PV penetration

Simulation	Feeder 1	Feeder 2	Feeder 3	Feeder 4	Feeder 5	Feeder 6	Feeder 7
NP disconnected prior to simulation	6	6	6	6	6	6	6
NP Trips with no PV	1	1	1	1	1	1	1
NP trips with 2% PV	3	3	3	3	3	3	3
NP in open state pre-fault	10	10	10	10	10	10	10
Additional NP trips due to fault	8	6	4	5	20	16	1
NP closed after fault	0	0	0	0	0	0	0
NP in open state post fault	18	16	14	15	30	26	11
NP in different state post fault	8	6	4	5	20	16	1

9.4 Simulations with 5% PV Penetration Present

In this section, a three phase high impedance fault is introduced into all feeder networks with 5% PV penetration present in the grid. For arrangement 1, 19 additional network protectors trip with after 5% PV penetration has been added to the grid network. At this stage, 15.4% of the transformers in the downtown network were disconnected prior to the fault. After the fault is cleared, we see that no network protectors reclose.

Table 12—Arrangement 1 with 5% PV penetration

Simulation	Feeder 1	Feeder 2	Feeder 3	Feeder 4	Feeder 5	Feeder 6	Feeder 7
NP disconnected prior to simulation	6	6	6	6	6	6	6
NP Trips with no PV	1	1	1	1	1	1	1
NP trips with 5% PV	19	19	19	19	19	19	19
NP in open state pre-fault	26	26	26	26	26	26	26
Additional NP trips due to fault	8	6	5	4	18	18	3
NP closed after fault	0	0	0	0	0	0	0
NP in open state post fault	34	32	31	30	44	44	29
NP in different state post fault	8	6	5	4	18	18	3

For arrangement 2, 22 additional network protectors tripped to remove the reverse power flows caused by the 5% PV penetration. At this stage, 17.2% of the transformers in the downtown network were disconnected prior to the fault. After the fault is cleared, we observe that no network protectors reclose.

Table 13—Arrangement 2 with 5% PV penetration

Simulation	Feeder 1	Feeder 2	Feeder 3	Feeder 4	Feeder 5	Feeder 6	Feeder 7
NP disconnected prior to simulation	6	6	6	6	6	6	6
NP Trips with no PV	1	1	1	1	1	1	1
NP trips with 5% PV	22	22	22	22	22	22	22
NP in open state pre-fault	29	29	29	29	29	29	29
Additional NP trips due to fault	9	7	5	5	16	17	5
NP closed after fault	0	0	0	0	0	0	0
NP in open state post fault	38	36	34	34	45	46	34
NP in different state post fault	9	7	5	5	16	17	5

For arrangement 3, 22 additional network protectors tripped to remove the reverse power flows caused by the 5% PV penetration. At this stage, 17.2% of the transformers in the downtown network were disconnected prior to the fault. After the fault is cleared, we observe that no network protectors reclose.

Table 14—Arrangement 3 with 5% PV penetration

Simulation	Feeder 1	Feeder 2	Feeder 3	Feeder 4	Feeder 5	Feeder 6	Feeder 7
NP disconnected prior to simulation	6	6	6	6	6	6	6
NP Trips with no PV	1	1	1	1	1	1	1
NP trips with 5% PV	22	22	22	22	22	22	22
NP in open state pre-fault	29	29	29	29	29	29	29
Additional NP trips due to fault	5	6	5	4	18	16	2
NP closed after fault	0	0	0	0	0	0	0
NP in open state post fault	34	35	34	33	47	45	31
NP in different state post fault	5	6	5	4	18	16	2

9.5 Simulations with 8% PV Penetration Present

In this section, a three phase high impedance fault is introduced into all feeder networks with 8% PV penetration present in the grid. For arrangement 1, 57 additional network protectors trip with after 8% PV penetration has been added to the grid network. At this stage, 37.9% of the transformers in the downtown network were disconnected prior to the fault. After the fault is cleared, we see that no network protectors reclose.

Table 15—Arrangement 1 with 8% PV penetration

Simulation	Feeder 1	Feeder 2	Feeder 3	Feeder 4	Feeder 5	Feeder 6	Feeder 7
NP disconnected prior to simulation	6	6	6	6	6	6	6
NP Trips with no PV	1	1	1	1	1	1	1
NP trips with 8% PV	57	57	57	57	57	57	57
NP in open state pre-fault	64	64	64	64	64	64	64
Additional NP trips due to fault	6	6	2	2	14	6	5
NP closed after fault	0	0	0	0	0	0	0
NP in open state post fault	70	70	66	66	78	70	69
NP in different state post fault	6	6	2	2	14	6	5

For arrangement 2, 56 additional network protectors tripped to remove the reverse power flows caused by the 8% PV penetration. At this stage, 37.3% of the transformers in the downtown network were disconnected prior to the fault. After the fault is cleared, we observe that no network protectors reclose.

Table 16—Arrangement 2 with 8% PV penetration

Simulation	Feeder 1	Feeder 2	Feeder 3	Feeder 4	Feeder 5	Feeder 6	Feeder 7
NP disconnected prior to simulation	6	6	6	6	6	6	6
NP Trips with no PV	1	1	1	1	1	1	1
NP trips with 8% PV	56	56	56	56	56	56	56
NP in open state pre-fault	63	63	63	63	63	63	63
Additional NP trips due to fault	7	5	3	2	13	11	3
NP closed after fault	0	0	0	0	0	0	0
NP in open state post fault	70	68	66	65	76	74	66
NP in different state post fault	7	5	3	2	13	11	3

For arrangement 3, 57 additional network protectors tripped to remove the reverse power flows caused by the 8% PV penetration. At this stage, 37.9% of the transformers in the downtown network were disconnected prior to the fault. After the fault is cleared, we observe that no network protectors reclose.

Table 17—Arrangement 3 with 8% PV penetration

Simulation	Feeder 1	Feeder 2	Feeder 3	Feeder 4	Feeder 5	Feeder 6	Feeder 7
NP disconnected prior to simulation	6	6	6	6	6	6	6
NP Trips with no PV	1	1	1	1	1	1	1
NP trips with 8% PV	57	57	57	57	57	57	57
NP in open state pre-fault	64	64	64	64	64	64	64
Additional NP trips due to fault	3	5	2	4	16	14	5
NP closed after fault	0	0	0	0	0	0	0
NP in open state post fault	67	69	66	68	80	78	69
NP in different state post fault	3	5	2	4	16	14	5

CHAPTER 10. RECLOSE VOLTAGE ANALYSIS

10.1 Closing Characteristic of Network Protector Relay

In this section, the reclosing voltage V_D, which is the voltage difference between the two sides of the network protector (i.e., transformer side voltage and network side voltage,) is observed. The closing characteristic of the network protector relay is shown in Figure 10.1 below.

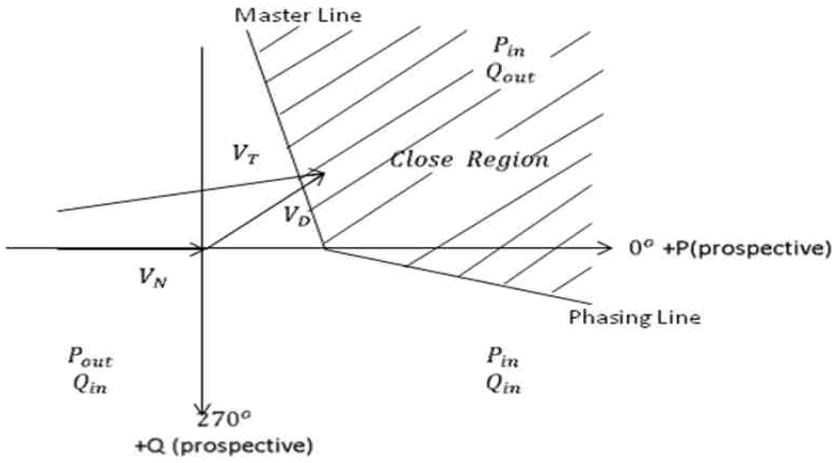

Figure 10.1—Closing characteristic of the network protector relay [10]

The symbols used in Figure 10.1 are summarized below:

$$V_D = V_T - V_N \tag{22}$$

$$V_T = \textit{transformer side voltage} \tag{23}$$

$$V_N = \textit{network side voltage} \tag{24}$$

$$V_D = \textit{difference voltage} \tag{25}$$

Due to the existence of the fault current, the voltage difference in the case of fault is different from when the fault has been cleared. The reclosing action takes place only when the voltage on the transformer side of the open network protector is slightly higher in magnitude and is in phase with or leading the voltage on the network side of the protector. The reclosing action is accomplished primarily with two settings on the Richards network protector provided by Entergy:

- Reclose Volts: Minimum three phase average differential voltage necessary to close the protector.
- Reclose Angle: The protector will not close if the angle between the network voltage and differential voltage is below this setting.

The default setting for the reclose voltage is set at 1.4V with an adjustable range of 0.1 to 10.0 Volts. In other words the protector will not close unless the voltage of the transformer side of the open network protector is at least 1.4V greater than the voltage on the network side of the protector. The default setting for the reclose angle is set at -5 degrees with an adjustable range of -25 to +5 degrees.

10.2 Reclose Settings Analysis

We can look at the reclose analysis of the network protector relay by revisiting the fault analysis covered in Section 8.5 of this paper:

If we look at arrangement 1 with 8% PV penetration present in the grid network we recall that 64 out of the 169 transformers are disconnected prior to the fault. In our simulations, the reclose voltage is set at 2V. However, if we use the default reclose voltage setting of the relay the voltage difference, V_D, before a fault on feeder 5 has cleared will be seen in Figure 10.2.

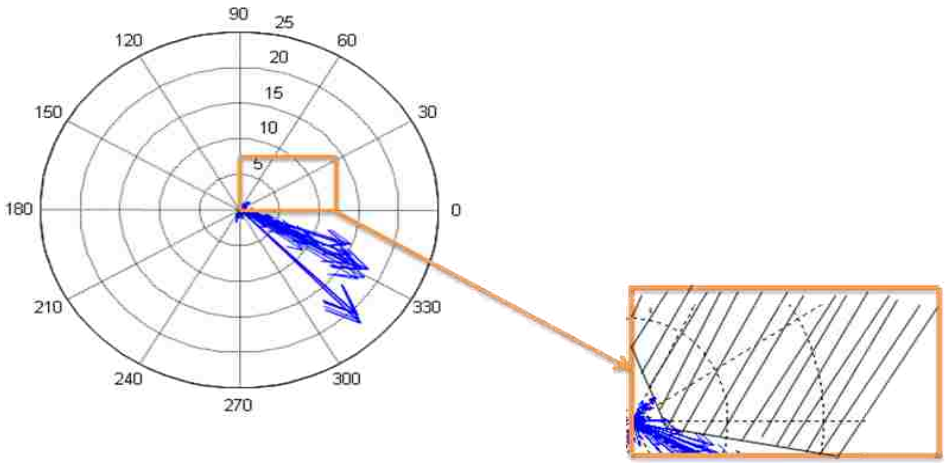

Figure 10.2—V_D before a fault has cleared on feeder 5

With the reclose voltage set at 1.4 Volts, two network protectors will reclose after the fault has cleared. At GV29_Fdr4, the voltage difference, $V_D = 1.87V > 1.4V$; and at GV44_Fdr7, $V_D = 1.62V > 1.4V$. However, after the fault has cleared both transformers will see reverse power and trip again. After a 6 cycle time delay, both transformers will reclose. This process will continue leading to excessive relay operations, known as pumping. The reclose voltage setting establishes the minimum difference voltage magnitude required to issue a close command when the difference voltage and network voltage are in phase [10]. Allowing the network protector to close with a small difference voltage magnitude can lead to pumping. To resolve this issue, minimum reclose voltage was changed to 2V throughout simulations.

To illustrate the reclose analysis with the reclose voltage set at 2V, we will revisit the fault analysis of arrangement 1 with 2% PV penetration. In this simulation 20 network

protectors were disconnected prior to the fault on feeder 5. When a fault occurs on feeder 5 no network protectors reclose, and the voltage difference for the relays resemble Figure 10.3.

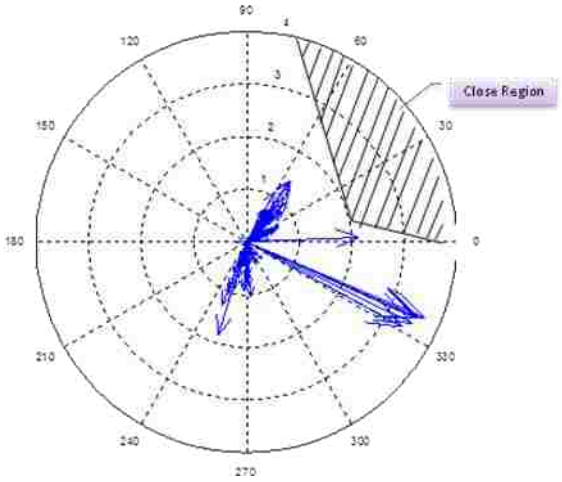

Figure 10.3—V_D before a fault has cleared on feeder 5

After the fault has cleared, we see that one network protector recloses and stays closed. Figure 10.4 shows plots of the voltage difference after the fault has cleared. Increasing the reclose voltage setting to 2V eliminated the excessive breaker operations that were present when this setting was set at the default setting of 1.4V. We only observed this issue of "pumping" in the presence of distributed generation in the secondary grid network.

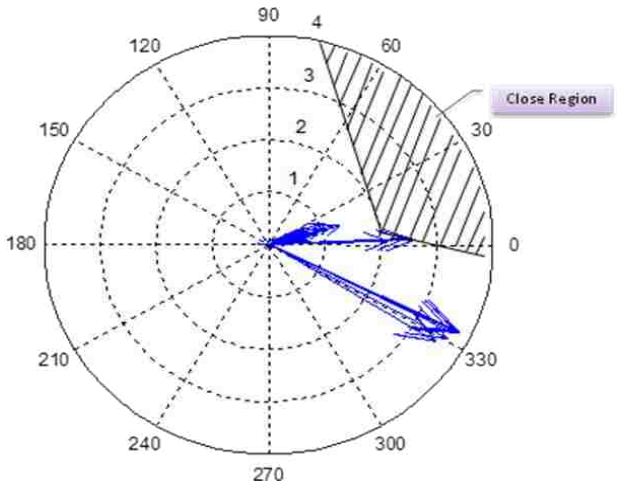

Figure 10.4—V_D after a fault has cleared on feeder 5

CHAPTER 11. PV PENETRATION LIMITS

At this stage, it is very difficult to determine a safe minimum amount of generation on the Downtown Network Electrical Distribution system with our current knowledge of the downtown network. Network protectors operate very rapidly. Under minimum customer electrical usage conditions and when faults occur, network protectors could operate and the local distribution system could become unstable. In addition, tripping the network protectors could cause the secondary cable system to overload. Since reliability of electrical service is paramount, more work and study towards investigation of the downtown network under these incidents are required before allowing customer electrical generation to be connected.

To examine the acceptable PV penetration limits on the grid network, we studied the grid network under minimum loading conditions. This gives us a worst case scenario where the generation within the grid network exceeds the load demand much sooner in simulations. In these simulations the sensitive trip setting is set to trip when 1.5% of rated current flows from the grid network to the feeder network. No communications between network protectors were present during the simulation. The reclose operation of the protector was disabled throughout the simulations. In addition to the network protector protection, the transformer will disconnect overloads at 100% of rated loads.

11.1 Simulations with 8% PV Penetration Present

The effect of the network protectors under minimum loading conditions with 8% PV penetration is outlined below:

- 6 out of 169 transformers out of service prior to simulations
- 1 additional transformer is disconnected due to reverse power flow with no PV penetration
- 8% PV penetration inserted into grid network
    - 33 transformers initially trip due to reverse power flow
    - After 6 cycles, 10 transformers trip due to reverse power flow
    - After another 6 cycles, 6 transformers trip due to reverse power flow
    - After another 6 cycles, 4 transformers trip due to reverse power flow
    - 1 transformer becomes overloaded, and is disconnected from the grid network
    - After another 6 cycles, 1 transformers trip due to reverse power flow
    - 62 out of 169 transformers are disconnected (37% removed)

Since this project only concentrates on the network protector operation, we suggest that another investigation be carried out to observe the downtown network load-flow and transients under different PV penetration levels and when network protectors operate.

CHAPTER 12. PROPOSED SOLUTION

The experimental results obtained above clarifies that the network protector can sense some reverse power flow when distributed solar generation exists in the secondary network even when there is no fault in the primary feeder. This situation can cause the network protectors to falsely trip due to distributed generation from the secondary grid. Hence, this section is dedicated to proposing a solution that could potentially prevent the erroneous tripping of network protectors because of the reverse current produced by the presence of PV penetration within the grid network.

The proposed method requires obtaining all currents, injected and absorbed, by the network protectors and loads on the feeder. This requires a data acquisition system using hard-wire connections or a data transmission infrastructure. The measured currents provide a signal that can override the trip command of all the network protectors inside the feeder. For proper operation, the proposed method must be applied to all the individual feeders, simultaneously.

The following algorithm can be used to detect faults located in the primary feeder network and trip the network protector to isolate the fault. For reverse current flow as a result of excess PV penetration, the network protector will still sense the reverse power; however, a block command will prevent the protector from tripping.

- For each feeder network, N (where N = 1, 2, 3, 4, 5, 6, 7), measure the current flow at the origination point at the substation using current transformers.
    - I_N = current originating from substation in feeder network N
        - When $I_N > 0$ current is flowing from the main substation towards the feeder network.
        - When $I_N < 0$ current is flowing from the feeder network towards the main substation. This happens at high levels of PV penetration within the secondary grid network, where the excess power will flow back to the main transformer. A fault on the main substation transformer can also cause power to flow to the main substation.
- Using current transformers, measure the current associated with feeder network N at each spot and grid vault.
    - I_{grid_n} = current at GV_0n
    - I_{spot_n} = current at SV_0n
- In unfaulted case:
    - $I_N = \sum (I_{grid\_n} + I_{spot\_n})$
- For a fault in feeder network N:
    - $I_N \neq \sum (I_{grid\_n} + I_{spot\_n})$
- This feature will override a trip condition on the network protector

- If the NP senses reverse power flow AND $I_N \neq \sum (I_{grid\_n} + I_{spot\_n})$ the network protector will issue a trip command. Otherwise reverse power flow is due to PV penetration and no trip command is issued.

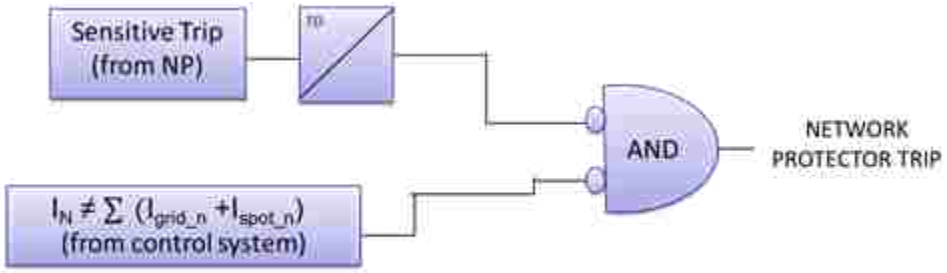

Figure 12.1—Logic diagram of fault detection system

Figure 12.1 is a simple logic diagram for the proposed solution. The network protector will only trip if the network protector relay senses reverse power flow above the sensitive trip setting and if the real power flows originating from the main substation in feeder network N does not equal the real power flows associated with feeder network N at each spot and grid vault. The network protector also has a time delay set at a speed slower than the speed of the central control system. This allows the central control system time to process the algorithm and determine if the power flow in the feeder network N sums to zero. This scheme also requires communication between each network protector and the central control system.

12.1 Feeder 1 Simulations with 5% PV Penetration

To demonstrate the algorithm we will look at the feeder network 1 in Figure 12.2. Current transformers are shown on the 13.2KV primary side of the spot and grid vaults, as well as on the 13.2KV feeder breaker. These currents are combined together to detect faults on the 13.2KV feeder network. In this simulation, 5% PV penetration under minimum loads (16% of peak load) is present. With 5% PV penetration present within the grid network, 12 transformers will sense real power flowing from the secondary network to the feeder network.

After running the load flow simulation with these conditions, we observed that one of the network protectors from feeder network 1 will sense reverse power flow. However, the sum of the currents flowing in feeder network 1 approximates to zero which indicates that there is no fault in the feeder network. Therefore, we do not want any network protectors to trip for this condition. The central control system will calculate the following parameters from the current and voltage transformers connected to each of the vaults. These calculations shown are the per unit values in rectangular form.

- $I_1 = 0.5062262 – j1.7302874$
- $\sum I_{grid\_n} = 0.1911643 – j0.8945817$
- $\sum I_{spot\_n} = 0.3150619 – j0.8357057$
- $\sum I_{grid\_n} + \sum I_{spot\_n} = 0.5062225 – j1.730286$

The power flows within feeder network 1 with 5% PV penetration are also shown below.

- $P_1 = 515.39$ kW
- $\sum P_{grid\_n} = 198.67$ kW
- $\sum P_{spot\_n} = 316.09$ kW
- $\sum P_{grid\_n} + \sum P_{spot\_n} = 514.76$ kW

The positive real part of I_1 indicates that current flows from the main substation towards the feeder 1 network. The summation of the current contributions from the grid and spot vault only differs slightly from the main current, $I_{1,}$ which can be attributed to the line losses in the distribution lines. Based on these calculations, the central control system will send a block signal to the associated network protector relays, preventing these relays from tripping.

12.1.1 5% PV Penetration without Fault

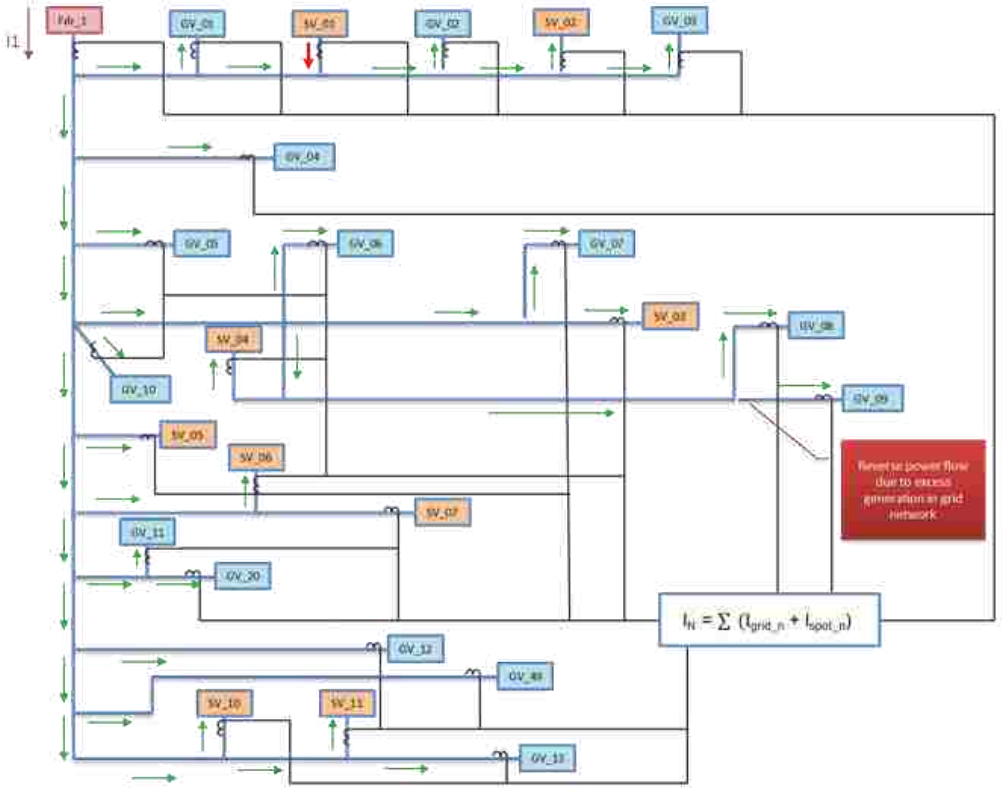

Figure 12.2—Feeder network 1 without fault (5% PV penetration)

12.1.2 5% PV Penetration with Fault

The case for the fault on feeder network 1 is shown in Figure 12.3. A three phase fault occurs on feeder network 1. For this case, 8 network protectors in feeder network 1 will sense the reverse power flowing from the grid network to the feeder network. In this case, we want the network protectors to trip in order to isolate the fault on the feeder network. The central control system detects this as a fault using the calculations below:

- $I_1 = 19.6404299 – j1.4770175$
- $\sum I_{grid\_n} = -0.1810792 – j0.6645902$
- $\sum I_{spot\_n} = -0.0226011 – j0.6298474$
- $\sum I_{grid\_n} + \sum I_{spot\_n} = -0.2036804 – j1.2944375$

The power flows within feeder network 1 with 5% PV penetration and a fault present in the primary feeder network are also shown below.

- $P_1 = 19{,}640$ kW = 19.64 MW
- $\sum P_{grid\_n} = -179.68$ kW
- $\sum P_{spot\_n} = -21.55$ kW
- $\sum P_{grid\_n} + \sum P_{spot\_n} = -201.22$ kW

We see that there is a large mismatch between the current flowing from feeder 1 (I_1) of the main substation and the current flowing through the vaults (I_{grid} and I_{spot}) that are connected to the feeder 1 network. Additionally, the current flowing from the main transformer is of a much higher magnitude than normal which indicates that this is possibly a large source of fault current to the fault on feeder 1. This fault also causes a number of network protectors to sense the reverse current. As a result, all 8 network protectors will trip to isolate this fault on the faulted feeder. Figure 12.3 also shows the network protectors which will trip due to the fault condition within feeder network 1. The arrows indicate the direction of current flow measured at the main substation feeder, as well as at each of the grid and spot vaults in the network using current transformers. In Figure 12.3 current flows from the main substation feeder to the primary feeder. In the case of the grid and spot vaults, the currents flowing towards the primary feeder network will result in network protector relay operations.

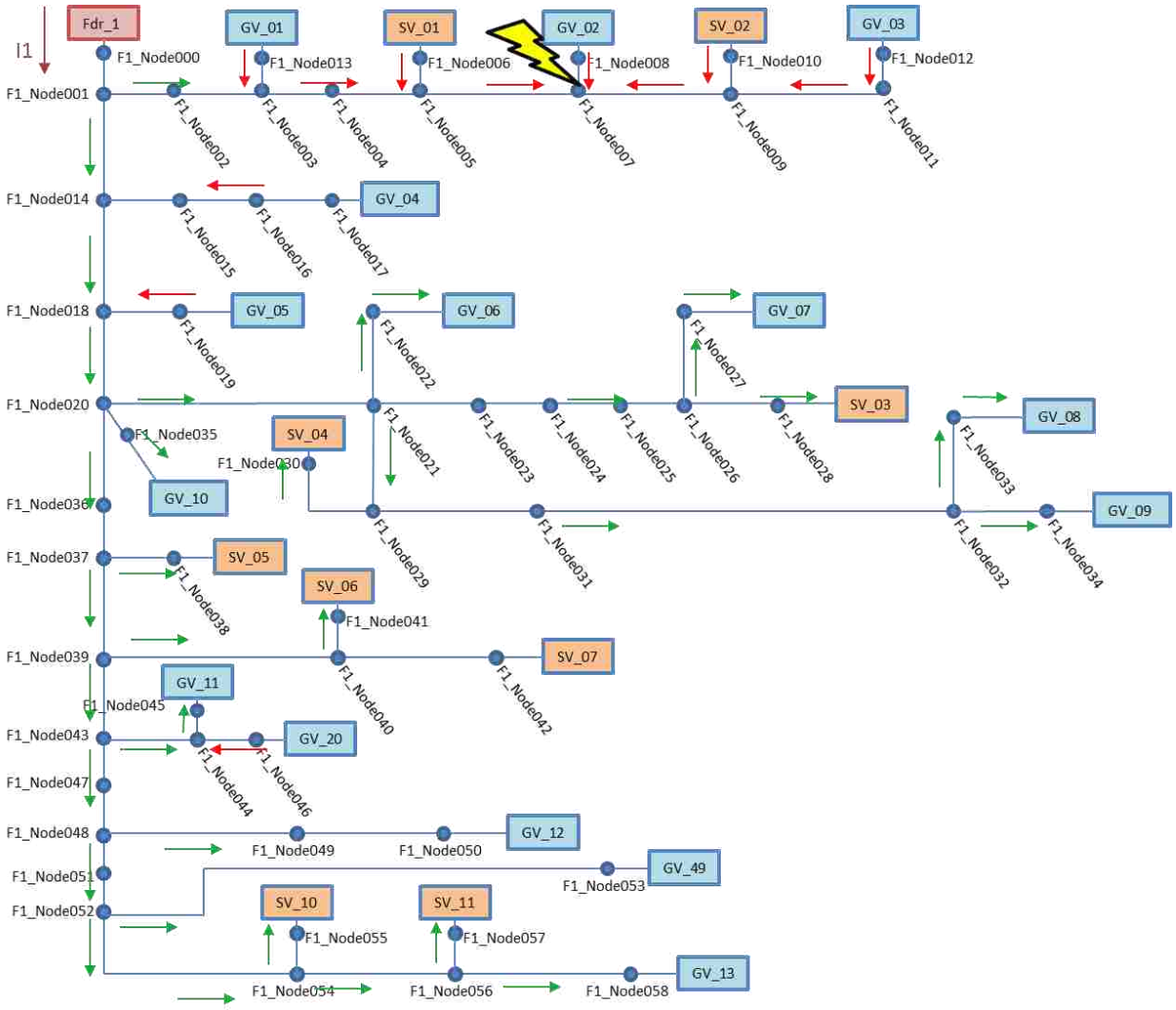

Figure 12.3—Feeder network 1 with fault (5% PV penetration)

Based on Figure 12.3, we see that the network protectors at the following locations will issue a trip:

- GV_01
- SV_01
- GV_02
- SV_02
- GV_03
- GV_04
- GV_05
- GV_20

Table 18 shows the current values (in per unit) which were used to calculate the parameters for the fault detection scheme. Reverse power flows at each network transformer are highlighted.

Table 18—Current calculations for simulation with 5% PV penetration

From Node	To Node	Current (pu) without fault	Current (pu) with fault
Main substation	Fdr_1	0.506-1.73i	19.64-1.477i
F1_Node006	SV01_Fdr1	-0.001-0.005i	-0.089+0.058i
F1_Node008	GV02_Fdr1	0.015-0.046i	-0.126+0.064i
F1_Node010	SV02_Fdr1	0.071-0.185i	-0.116-0.059i
F1_Node012	GV03_Fdr1	0.014-0.07i	-0.089-0.005i
F1_Node013	GV01_Fdr1	0.007-0.101i	-0.048-0.064i
F1_Node017	GV04_Fdr1	0.007-0.129i	-0.006-0.124i
F1_Node019	GV05_Fdr1	0.008-0.032i	-0.005-0.027i
F1_Node022	GV06_Fdr1	0.01-0.034i	-0.03i
F1_Node027	GV07_Fdr1	0.01-0.023i	0.009-0.023i
F1_Node028	SV03_Fdr1	0.02-0.07i	0.015-0.069i
F1_Node030	SV04_Fdr1	0.046-0.112i	0.039-0.11i
F1_Node033	GV08_Fdr1	0	0
F1_Node034	GV09_Fdr1	0	0
F1_Node035	GV10_Fdr1	0.048-0.156i	0.047-0.156i
F1_Node038	SV05_Fdr1	0.028-0.086i	0.015-0.082i
F1_Node041	SV06_Fdr1	0.051-0.106i	0.042-0.103i
F1_Node042	SV07_Fdr1	0.051-0.13i	0.04-0.127i
F1_Node045	GV11_Fdr1	0.008-0.06i	0.006-0.06i
F1_Node046	GV20_Fdr1	-0.011i	-0.004-0.012i
F1_Node050	GV12_Fdr1	0.009-0.02i	0.002-0.018i
F1_Node053	GV49_Fdr1	0.033-0.143i	0.021-0.14i
F1_Node055	SV10_Fdr1	0.024-0.081i	0.016-0.079i
F1_Node057	SV11_Fdr1	0.024-0.061i	0.016-0.059i
F1_Node058	GV13_Fdr1	0.021-0.07i	0.014-0.068i
Current from vaults		0.506-1.73i	-0.204-1.294i

At 5% PV penetration with a fault in feeder network 1, we see that 8 network protector relays will trip to isolate the fault in the primary feeder network. Only1 additional network protector relay sensed reverse power flow from the secondary network for the case without a fault. However the current contribution from the main substation feeder was equal to the sum of currents at the spot and grid vaults, which indicated there was no fault and consequently, no voltage drop in the primary feeder network. Table 19 shows the power flows for the same case.

Table 19—Power flows for simulation with 5% PV penetration

From Node	To Node	Real power flow (kW) without fault	Real power flow (kW) with fault
Main substation	Fdr_1	515.39	19,640.43
F1_Node006	SV01_Fdr1	-1.2600797857	-88.9003490922
F1_Node008	GV02_Fdr1	15.0501748693	-125.8703204335
F1_Node010	SV02_Fdr1	71.2778595240	-115.2393951813
F1_Node012	GV03_Fdr1	14.5700433683	-88.8020109445
F1_Node013	GV01_Fdr1	7.7923436445	-47.9385751271
F1_Node017	GV04_Fdr1	14.6235395479	-5.8822720928
F1_Node019	GV05_Fdr1	10.4061499329	-5.2294614834
F1_Node022	GV06_Fdr1	11.5638748319	0.0375443052
F1_Node027	GV07_Fdr1	9.9435702518	9.0687880765
F1_Node028	SV03_Fdr1	22.3063661387	14.8842323241
F1_Node030	SV04_Fdr1	46.6977834905	39.3862514709
F1_Node033	GV08_Fdr1	-5.4190367188	0.0000000013
F1_Node034	GV09_Fdr1	-2.8531317101	0.0000000052
F1_Node035	GV10_Fdr1	48.5781766184	46.7641366931
F1_Node038	SV05_Fdr1	28.8400223259	14.8059854823
F1_Node041	SV06_Fdr1	50.3437249547	41.8543417745
F1_Node042	SV07_Fdr1	52.8208358439	40.2843884261
F1_Node045	GV11_Fdr1	8.4453844450	5.7119788200
F1_Node046	GV20_Fdr1	1.3000516839	-4.3980195567
F1_Node050	GV12_Fdr1	7.5915989686	2.1156244272
F1_Node053	GV49_Fdr1	35.8412507757	20.7304434839
F1_Node055	SV10_Fdr1	23.8714906139	15.5002465854
F1_Node057	SV11_Fdr1	21.1941836088	15.8780413085
F1_Node058	GV13_Fdr1	21.2316173169	14.0136205886
Power flow from vaults		514.7577945409	-201.2247801387

12.1.3 30% PV Penetration without Fault

Next, we simulate a condition without a fault on feeder network 1 with 30% PV penetration present under minimum loads. Figure 12.4 shows the direction of real power flow in the feeder network under these conditions. At 30% PV penetration we see reverse power flow at the main substation feeder. This is expected as the excess renewable energy is now fed back towards the main substation. This excess energy, however, can provide power for other feeder networks.

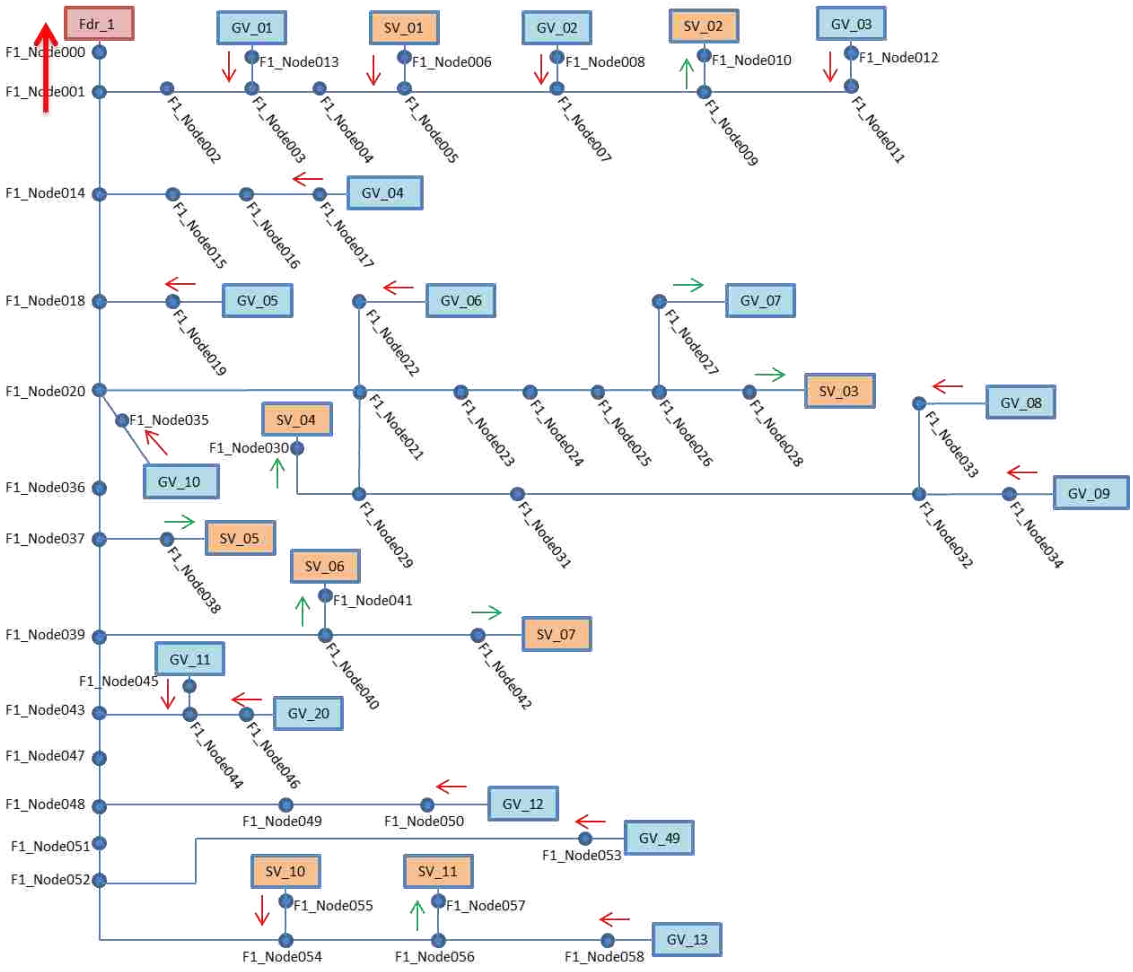

Figure 12.4—Feeder network 1 without fault (30% PV)

The central control system will calculate the following parameters from the current and voltage transformers connected to each of the vaults:

- I_1 = -0.6297444 – j1.7620101
- $\sum I_{grid\_n}$ = -0.8492566 – j0.9672971
- $\sum I_{spot\_n}$ = 0.2195132 – j0.7947125
- $\sum I_{grid\_n} + \sum I_{spot\_n}$ = -0.6297434 – j1.7620096

- P_1 = -629.75 kW
- $\sum$ Pgrid_n = -849.36 kW
- $\sum$ Pspot_n = 218.96 kW
- $\sum$ Pgrid_n + $\sum$ Pspot_n = -630.4 kW

For this calculation, all currents within the network did sum to zero. Therefore, the central control system will issue a block trip to all 16 network protectors associated with the feeder 1 network. This will allow the distributed generation (at 30% of peak load) from the secondary network to safely transmit power to the utility grid.

12.1.4 30% PV Penetration with Fault

The case for the fault on feeder network 1 with 30% PV penetration is shown in Figure 12.5. A three phase fault occurs on feeder network 1 as shown in Figure 12.5. For this case, 18 network protectors in feeder network 1 will sense the reverse power flowing from the grid network to the feeder network. In this case, we want the network protectors to trip in order to isolate the fault on the feeder network. The central control system detects this as a fault using the calculations below:

- I_1 = 18.4853699 – j1.5018959
- $\sum I_{grid\_n}$ = -1.2434276 – j0.7313455
- $\sum I_{spot\_n}$ = -0.1167292 – j0.5898624
- $\sum I_{grid\_n} + \sum I_{spot\_n}$ = -1.3601568 - j1.3212079

- P_1 = 18,485 kW
- $\sum P_{grid\_n}$ = -1,240 kW
- $\sum P_{spot\_n}$ = -115.85 kW
- $\sum P_{grid\_n} + \sum P_{spot\_n}$ = -1,357 kW

For the case with the fault on feeder 1, the sum of currents in feeder 1 network did not sum to zero. Therefore, we know that a true fault exists on the feeder 1 network and the central control system will allow these 18 network protectors to trip to isolate the fault.

Table 20 shows the current values (in per unit) which were used to calculate the parameters for the fault detection scheme. Reverse power flows at each network transformer are highlighted to indicate which network protectors will trip under these conditions.

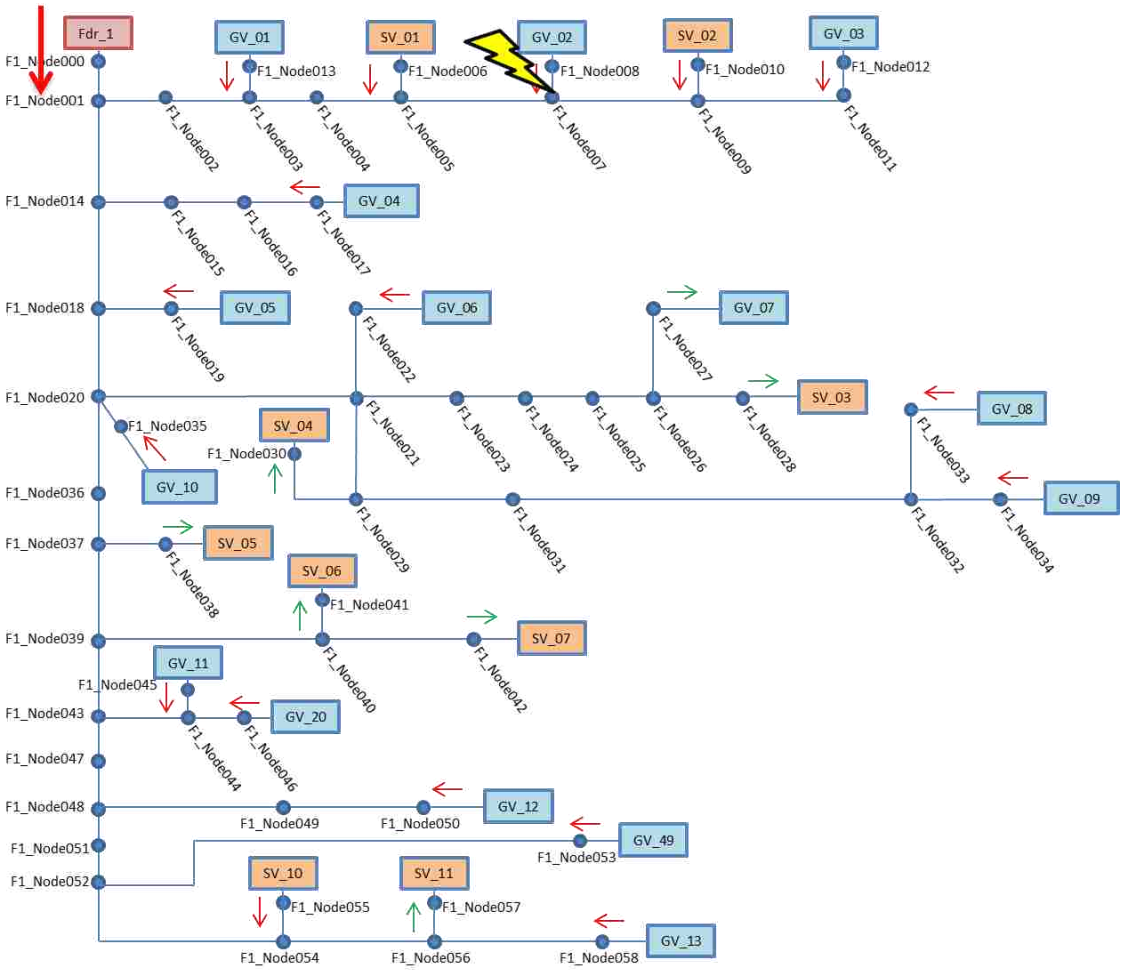

Figure 12.5—Feeder network 1 with fault (30% PV)

We see the 16 network protectors which will sense reverse power from the secondary network. However, for the case without the fault in the primary feeder network 1 the current contribution from the main substation feeder equals the sum of all of the currents in the grid and spot vaults. This indicates that the current that enters the primary feeder network will also exit the primary feeder network, with the exception of line losses. There are no loads located within the primary feeder network, so we would only expect small amounts of voltage drops in the distribution lines. Therefore, for this case the central control system issues a block signal to all 16 network protectors to prevent any operations.

Table 20—Current calculations for simulation with 30% PV penetration

From Node	To Node	Current (pu) without fault	Current (pu) with fault
Main substation	Fdr_1	-0.63-1.762i	18.485-1.502i
F1_Node006	SV01_Fdr1	-0.006-0.003i	-0.095+0.06i
F1_Node008	GV02_Fdr1	-0.021-0.049i	-0.162+0.062i
F1_Node010	SV02_Fdr1	0.058-0.178i	-0.13-0.052i
F1_Node012	GV03_Fdr1	-0.038-0.067i	-0.141-0.001i
F1_Node013	GV01_Fdr1	-0.157-0.092i	-0.213-0.055i
F1_Node017	GV04_Fdr1	-0.107-0.098i	-0.123-0.092i
F1_Node019	GV05_Fdr1	-0.011-0.029i	-0.025-0.024i
F1_Node022	GV06_Fdr1	-0.031-0.037i	-0.041-0.034i
F1_Node027	GV07_Fdr1	0.003-0.023i	0.002-0.023i
F1_Node028	SV03_Fdr1	0.017-0.064i	0.011-0.063i
F1_Node030	SV04_Fdr1	0.04-0.11i	0.033-0.108i
F1_Node033	GV08_Fdr1	-0.098-0.03i	-0.105-0.028i
F1_Node034	GV09_Fdr1	-0.196-0.108i	-0.208-0.105i
F1_Node035	GV10_Fdr1	-0.062-0.159i	-0.064-0.16i
F1_Node038	SV05_Fdr1	0.012-0.08i	-0.001-0.075i
F1_Node041	SV06_Fdr1	0.048-0.108i	0.039-0.105i
F1_Node042	SV07_Fdr1	0.046-0.124i	0.035-0.121i
F1_Node045	GV11_Fdr1	-0.094-0.063i	-0.097-0.063i
F1_Node046	GV20_Fdr1	-0.01-0.009i	-0.014-0.01i
F1_Node050	GV12_Fdr1	-0.009-0.022i	-0.016-0.02i
F1_Node053	GV49_Fdr1	-0.006-0.114i	-0.017-0.111i
F1_Node055	SV10_Fdr1	-0.002-0.074i	-0.01-0.072i
F1_Node057	SV11_Fdr1	0.008-0.054i	-0.053i
F1_Node058	GV13_Fdr1	-0.012-0.068i	-0.019-0.066i
Current from vaults		-0.622-1.76i	-1.361-1.319i

We see a similar amount of network protectors which will sense reverse power flows in the case of a fault in feeder network 1. However, the algorithm developed clearly shows a mismatch between the power flow that enters and exits the primary feeder network. In this case, the central control system will allow all 18 network protectors relays to operate to isolate the fault. Table 21 shows the power flows which can be calculated using current transformers for the current readings, and potential transformers for the voltages.

Table 21—Power flows for simulation with 30% PV penetration

From Node	To Node	Real power flow (kW) without fault	Real power flow (kW) with fault
Main substation	Fdr_1	-629.75	18,485.37
F1_Node006	SV01_Fdr1	-6.23609948	-94.4794342
F1_Node008	GV02_Fdr1	-21.12221481	-161.6464914
F1_Node010	SV02_Fdr1	57.48784276	-128.7126627
F1_Node012	GV03_Fdr1	-38.44512417	-140.7156843
F1_Node013	GV01_Fdr1	-157.2290522	-212.4579764
F1_Node017	GV04_Fdr1	-106.7929891	-122.6756897
F1_Node019	GV05_Fdr1	-11.23322198	-25.19059554
F1_Node022	GV06_Fdr1	-30.97934784	-40.74889626
F1_Node027	GV07_Fdr1	2.867885958	2.066855909
F1_Node028	SV03_Fdr1	16.45468298	11.13455224
F1_Node030	SV04_Fdr1	39.52575411	33.18110094
F1_Node033	GV08_Fdr1	-97.47851483	-104.5261543
F1_Node034	GV09_Fdr1	-196.1349424	-208.2583669
F1_Node035	GV10_Fdr1	-62.45680283	-64.05582001
F1_Node038	SV05_Fdr1	12.35527969	-0.758611033
F1_Node041	SV06_Fdr1	47.48546292	38.5209141
F1_Node042	SV07_Fdr1	45.83909505	34.99907356
F1_Node045	GV11_Fdr1	-93.97877251	-96.56936756
F1_Node046	GV20_Fdr1	-9.694551948	-14.24267043
F1_Node050	GV12_Fdr1	-9.279195074	-15.5579937
F1_Node053	GV49_Fdr1	-5.592892092	-17.39857721
F1_Node055	SV10_Fdr1	-2.090952318	-9.987280658
F1_Node057	SV11_Fdr1	8.137355686	0.250251732
F1_Node058	GV13_Fdr1	-11.81224456	-18.8049518
Power flow from vaults		-630.403559	-1356.634476

Without the fault detection scheme in use with 16% loading and 30% PV penetration, the following scenario would have occurred:

- 6 transformers are out of service on this day.
- An additional network protector trips due to reverse power flow with no PV penetration in grid network.
- 30% PV penetration is inserted in grid network
- 79 network protector relays trip due to reverse power flow.
- After 6 cycles, 24 additional network protectors trip.

- At this point, the voltage collapses due to the amount of transformers disconnected from the downtown network (110/169 disconnected).
- Only 35% of transformers in service.

Therefore, the fault detection scheme solves the problem of distinguishing PV penetration from a faulted condition by tripping the relay for fault conditions and preventing the relays from tripping for the case of PV penetration. This solution also allows a higher amount of PV penetration to be present within the secondary grid network without causing a voltage collapse or unstable condition on the power system. Due to the symmetrical rating of distribution transformers, we also know that the thermal limit of the transformer does not vary depending on the direction of power flow [8]. Appendix A provides calculations for a fault in feeder network 1 with 60% and 90% PV penetration. Additionally, simulation results for faults on the other feeder networks for 30% PV penetration are provided in Appendix B.

CHAPTER 13. CONCLUSION

This project has investigated some of the problems and challenges posed by the potential addition of renewable energy sources present in downtown networks. Actual data was gathered and used to model these renewable energy sources. With these models, we were able to study the effect of higher distributed generation levels in downtown networks under various loading conditions. As expected, we have shown that our load demand in the downtown network decreases with increased PV penetration. We have also studied the effect of network protectors on the downtown network as PV penetration is increased within the grid network. The effect of clouds passing over the downtown network was also studied. It has been shown that the presence of clouds will negatively affect the stability of networks which depend largely on distributed generation for energy. The operation of the network protector relay after a fault condition has cleared was also examined. We were able to eliminate excessive breaker operations by increasing the reclose voltage setting on the network protector relay. Various simulations were conducted to examine the operation of the network protectors when the primary feeder network was subjected to faults. Using the results from these simulations, we were ultimately able to propose a solution that will only trip the network protectors for faults within the primary feeder network. Potential future studies involve investigating the downtown distribution network under more scenarios to determine a safe level of PV penetration. Other future work includes implementing the proposed solution via communication among network protector relays in a test network.

APPENDIX A – CASE STUDIES FOR 60% AND 90% PV PENETRATION

A1. Calculations with 60% PV Penetration

A1.1 60% PV Penetration without Fault

- I_1 = -1.9561132 - j1.9128399
- $\sum I_{grid\_n}$ = -2.0592297-j1.1482305
- $\sum I_{spot\_n}$ = 0.1031161-j0.7646077
- $\sum I_{grid\_n} + \sum I_{spot\_n}$ = -1.9561136-j1.9128382

- P_1 = -1,956.11 kW
- $\sum$ Pgrid_n = -2,059.74 kW
- $\sum$ Pspot_n = 102.31.96 kW
- $\sum$ Pgrid_n + $\sum$ Pspot_n = -1,957.43 kW

A1.2 60% PV Penetration with Fault

- I_1 = 17.1599451 - j1.6498785
- $\sum I_{grid\_n}$ = -2.4538551-j0.9117961
- $\sum I_{spot\_n}$ = -0.2331864-j0.5597579
- $\sum I_{grid\_n} + \sum I_{spot\_n}$ = -2.6870416-j1.4715539

- P_1 = -17,159.95 kW
- $\sum$ Pgrid_n = -2,450.15 kW
- $\sum$ Pspot_n = 232.50 kW
- $\sum$ Pgrid_n + $\sum$ Pspot_n = -1,356.63 kW

Table A.1—Current calculations for simulation with 60% PV penetration

From Node	To Node	Current (pu) without fault	Current (pu) with fault
Main substation	Fdr_1	-1.956-1.913i	17.16-1.65i
F1_Node006	SV01_Fdr1	-0.012-0.001i	-0.101+0.062i
F1_Node008	GV02_Fdr1	-0.064-0.055i	-0.205+0.055i
F1_Node010	SV02_Fdr1	0.041-0.173i	-0.146-0.047i
F1_Node012	GV03_Fdr1	-0.101-0.07i	-0.204-0.005i
F1_Node013	GV01_Fdr1	-0.354-0.093i	-0.41-0.055i
F1_Node017	GV04_Fdr1	-0.25-0.119i	-0.266-0.113i
F1_Node019	GV05_Fdr1	-0.036-0.035i	-0.05-0.03i
F1_Node022	GV06_Fdr1	-0.079-0.049i	-0.089-0.046i
F1_Node027	GV07_Fdr1	-0.005-0.025i	-0.006-0.026i
F1_Node028	SV03_Fdr1	0.01-0.062i	0.004-0.061i
F1_Node030	SV04_Fdr1	0.031-0.109i	0.025-0.107i
F1_Node033	GV08_Fdr1	-0.203-0.044i	-0.211-0.042i
F1_Node034	GV09_Fdr1	-0.406-0.19i	-0.418-0.187i
F1_Node035	GV10_Fdr1	-0.191-0.175i	-0.193-0.176i
F1_Node038	SV05_Fdr1	-0.007-0.075i	-0.02-0.071i
F1_Node041	SV06_Fdr1	0.044-0.108i	0.035-0.105i
F1_Node042	SV07_Fdr1	0.038-0.122i	0.027-0.118i
F1_Node045	GV11_Fdr1	-0.214-0.075i	-0.216-0.076i
F1_Node046	GV20_Fdr1	-0.023-0.01i	-0.027-0.011i
F1_Node050	GV12_Fdr1	-0.029-0.023i	-0.035-0.022i
F1_Node053	GV49_Fdr1	-0.054-0.114i	-0.066-0.112i
F1_Node055	SV10_Fdr1	-0.033-0.07i	-0.041-0.068i
F1_Node057	SV11_Fdr1	-0.008-0.045i	-0.016-0.044i
F1_Node058	GV13_Fdr1	-0.051-0.068i	-0.058-0.067i
Current from vaults		-1.956-1.913i	-2.687-1.472i

Table A.2—Power flows for simulation with 60% PV penetration

From Node	To Node	Real power flow (kW) without fault	Real power flow (kW) with fault
Main substation	Fdr_1	-1956.11	17,159.95
F1_Node006	SV01_Fdr1	-12.2931563	-100.5354233
F1_Node008	GV02_Fdr1	-63.52609367	-203.7262137
F1_Node010	SV02_Fdr1	40.83469625	-145.3485241
F1_Node012	GV03_Fdr1	-100.6597467	-202.6535271
F1_Node013	GV01_Fdr1	-353.5906447	-408.5199946
F1_Node017	GV04_Fdr1	-250.2663023	-266.1251064
F1_Node019	GV05_Fdr1	-36.16357632	-50.11910875
F1_Node022	GV06_Fdr1	-79.3705088	-89.13195008
F1_Node027	GV07_Fdr1	-5.170074807	-5.969628139
F1_Node028	SV03_Fdr1	9.430122019	4.107769699
F1_Node030	SV04_Fdr1	31.1155033	24.77053653
F1_Node033	GV08_Fdr1	-203.4210756	-210.4550981
F1_Node034	GV09_Fdr1	-406.2809647	-418.3581847
F1_Node035	GV10_Fdr1	-191.3193559	-192.8985648
F1_Node038	SV05_Fdr1	-7.369531616	-20.48501954
F1_Node041	SV06_Fdr1	44.15261578	35.18718836
F1_Node042	SV07_Fdr1	37.43325755	26.59135832
F1_Node045	GV11_Fdr1	-213.7724107	-216.3592107
F1_Node046	GV20_Fdr1	-22.50455267	-27.05623718
F1_Node050	GV12_Fdr1	-29.00505017	-35.28450435
F1_Node053	GV49_Fdr1	-54.03014731	-65.83461504
F1_Node055	SV10_Fdr1	-32.95988777	-40.85739931
F1_Node057	SV11_Fdr1	-8.034370768	-15.92610799
F1_Node058	GV13_Fdr1	-50.65982542	-57.65326605
Power flow from vaults (kW)		-1957.431081	-1356.634476

A2. Calculations with 90% PV Penetration

A2.1 90% PV Penetration without Fault

- I_1 = -3.2313851 - j2.2010854
- $\sum I_{grid\_n}$ = -3.2179942-j1.4554658
- $\sum I_{spot\_n}$ = -0.0133911-j0.7456192
- $\sum I_{grid\_n} + \sum I_{spot\_n}$ = -3.2313854-j2.2010851

- P_1 = -3,231.39 kW
- $\sum$ Pgrid_n = -3,219.52 kW
- $\sum$ Pspot_n = 14.49 kW
- $\sum$ Pgrid_n + $\sum$ Pspot_n = -3234.00 kW

A2.2 90% PV Penetration without Fault

- I_1 = 15.8854247 - j1.9354059
- $\sum I_{grid\_n}$ = -3.6130806 - j1.2187094
- $\sum I_{spot\_n}$ = -0.3497503-j0.5407927
- $\sum I_{grid\_n} + \sum I_{spot\_n}$ = -3.9628309-j1.7595021

- P_1 = -1,5885.42 kW
- $\sum$ Pgrid_n = -3,608.79 kW
- $\sum$ Pspot_n = 349.25 kW
- $\sum$ Pgrid_n + $\sum$ Pspot_n = -1,356.63 kW

Table A.3—Current calculations for simulation with 90% PV penetration

From Node	To Node	Current (pu) without fault	Current (pu) with fault
Main substation	Fdr_1	-3.231-2.201i	15.885-1.935i
F1_Node006	SV01_Fdr1	-0.018	-0.107+0.064i
F1_Node008	GV02_Fdr1	-0.105-0.064i	-0.246+0.046i
F1_Node010	SV02_Fdr1	0.024-0.17i	-0.163-0.044i
F1_Node012	GV03_Fdr1	-0.161-0.079i	-0.264-0.013i
F1_Node013	GV01_Fdr1	-0.548-0.1i	-0.605-0.062i
F1_Node017	GV04_Fdr1	-0.391-0.145i	-0.407-0.14i
F1_Node019	GV05_Fdr1	-0.06-0.043i	-0.074-0.039i
F1_Node022	GV06_Fdr1	-0.125-0.067i	-0.135-0.063i
F1_Node027	GV07_Fdr1	-0.013-0.028i	-0.014-0.029i
F1_Node028	SV03_Fdr1	0.003-0.06i	-0.003-0.059i
F1_Node030	SV04_Fdr1	0.023-0.108i	0.017-0.106i
F1_Node033	GV08_Fdr1	-0.305-0.07i	-0.312-0.068i
F1_Node034	GV09_Fdr1	-0.591-0.33i	-0.603-0.327i
F1_Node035	GV10_Fdr1	-0.316-0.202i	-0.317-0.202i
F1_Node038	SV05_Fdr1	-0.027-0.073i	-0.04-0.069i
F1_Node041	SV06_Fdr1	0.041-0.109i	0.032-0.106i
F1_Node042	SV07_Fdr1	0.029-0.12i	0.018-0.117i
F1_Node045	GV11_Fdr1	-0.33-0.096i	-0.333-0.096i
F1_Node046	GV20_Fdr1	-0.035-0.013i	-0.039-0.014i
F1_Node050	GV12_Fdr1	-0.048-0.027i	-0.054-0.025i
F1_Node053	GV49_Fdr1	-0.101-0.12i	-0.113-0.118i
F1_Node055	SV10_Fdr1	-0.063-0.068i	-0.071-0.066i
F1_Node057	SV11_Fdr1	-0.025-0.039i	-0.033-0.038i
F1_Node058	GV13_Fdr1	-0.089-0.072i	-0.096-0.071i
Current from vaults		-3.231-2.201i	-3.963-1.76i

Table A.4—Power flows for simulation with 90% PV penetration

From Node	To Node	Real power flow (kW) without fault	Real power flow (kW) with fault
Main substation	Fdr_1	-3231.39	15,885.42
F1_Node006	SV01_Fdr1	-18.44358978	-106.6785733
F1_Node008	GV02_Fdr1	-104.8973132	-244.75598
F1_Node010	SV02_Fdr1	24.06725323	-162.082662
F1_Node012	GV03_Fdr1	-161.4335793	-263.1239065
F1_Node013	GV01_Fdr1	-548.2762286	-602.8893447
F1_Node017	GV04_Fdr1	-391.4825098	-407.3143925
F1_Node019	GV05_Fdr1	-60.03315505	-73.98539762
F1_Node022	GV06_Fdr1	-125.053579	-134.8040087
F1_Node027	GV07_Fdr1	-12.74666164	-13.54441857
F1_Node028	SV03_Fdr1	2.40080082	-2.922836599
F1_Node030	SV04_Fdr1	22.90622207	16.56187161
F1_Node033	GV08_Fdr1	-304.7559812	-311.7720982
F1_Node034	GV09_Fdr1	-591.7259908	-603.7323814
F1_Node035	GV10_Fdr1	-315.7347308	-317.2899393
F1_Node038	SV05_Fdr1	-27.03998735	-40.15489881
F1_Node041	SV06_Fdr1	40.92356279	31.95861702
F1_Node042	SV07_Fdr1	28.9986259	18.15615969
F1_Node045	GV11_Fdr1	-330.3909848	-332.971727
F1_Node046	GV20_Fdr1	-34.92413582	-39.47870339
F1_Node050	GV12_Fdr1	-48.19626102	-54.4752305
F1_Node053	GV49_Fdr1	-101.1725659	-112.9726132
F1_Node055	SV10_Fdr1	-63.54907375	-71.44639281
F1_Node057	SV11_Fdr1	-24.75098129	-32.64604433
F1_Node058	GV13_Fdr1	-88.69161373	-95.68433422
Power flow from vaults		-3234.002458	-1356.634476

APPENDIX B – CASE STUDIES FOR FEEDERS 2-7: 30% PV PENETRATION

B1. 30% PV Penetration with Fault in Feeder 2

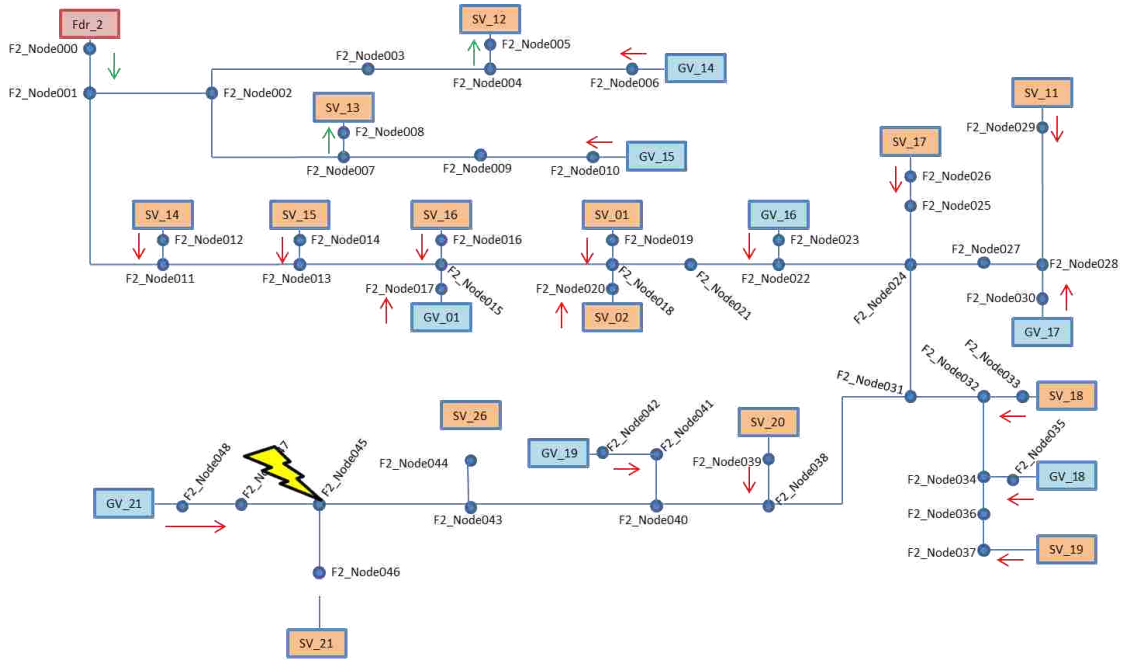

Figure B.1—Feeder network 2 with fault (30% PV)

Table B.1—Current calculations for Feeder network 2 simulation (30% PV)

From Node	To Node	Current (pu) without fault	Current (pu) with fault
Main substation	Fdr_2	-1.003-1.96i	13.874-0.099i
F2_Node005	SV12_Fdr2	0.047-0.094i	0.024-0.088i
F2_Node006	GV14_Fdr2	-0.238-0.066i	-0.252-0.064i
F2_Node008	SV13_Fdr2	0.069-0.158i	0.056-0.155i
F2_Node010	GV15_Fdr2	-0.055-0.164i	-0.062-0.169i
F2_Node012	SV14_Fdr2	0.004+0.002i	-0.042+0.023i
F2_Node014	SV15_Fdr2	0.027-0.053i	-0.009-0.035i
F2_Node016	SV16_Fdr2	0.004	-0.045+0.026i
F2_Node017	GV01_Fdr2	-0.148-0.089i	-0.205-0.062i
F2_Node019	SV01_Fdr2	0.006+0.003i	-0.071+0.038i
F2_Node020	SV02_Fdr2	0.075-0.17i	-0.07-0.11i
F2_Node023	GV16_Fdr2	-0.096-0.142i	-0.23-0.081i
F2_Node026	SV17_Fdr2	0.026-0.089i	-0.189+0.022i
F2_Node029	SV11_Fdr2	0.045-0.063i	-0.278+0.109i
F2_Node030	GV17_Fdr2	-0.062-0.187i	-0.506+0.021i
F2_Node033	SV19_Fdr2	0.052-0.14i	-0.314+0.053i
F2_Node035	GV18_Fdr2	-0.067-0.116i	-0.371+0.027i
F2_Node037	SV18_Fdr2	0.092-0.171i	-0.276+0.007i
F2_Node039	SV20_Fdr2	0.041-0.065i	-0.35+0.148i
F2_Node042	GV19_Fdr2	-0.135-0.091i	-0.76+0.232i
F2_Node044	SV26_Fdr2	0	0
F2_Node046	SV21_Fdr2	0.033-0.016i	-0.927+0.549i
F2_Node048	GV21_Fdr2	-0.722-0.092i	-0.87-0.055i
Current from vaults		-1.003-1.96i	-5.747+0.435i

Table B.2—Power flows for Feeder network 2 simulation (30% PV)

From Node	To Node	Real power flow (kW) without fault	Real power flow (kW) with fault
Main substation	Fdr_2	-1003.409	13873.59
F2_Node005	SV12_Fdr2	46.9915087369	24.5002347165
F2_Node006	GV14_Fdr2	-238.0572710302	-251.8279345384
F2_Node008	SV13_Fdr2	68.5507427217	55.8410135113
F2_Node010	GV15_Fdr2	-55.0810397057	-62.2265350356
F2_Node012	SV14_Fdr2	4.1136670377	-41.9734353496
F2_Node014	SV15_Fdr2	26.4841356374	-9.1543607712
F2_Node016	SV16_Fdr2	4.2391135137	-45.4513768846
F2_Node017	GV01_Fdr2	-148.3894727149	-203.9116061025
F2_Node019	SV01_Fdr2	6.2360840847	-71.2265415709
F2_Node020	SV02_Fdr2	74.4915790677	-69.0443289688
F2_Node023	GV16_Fdr2	-95.8090730692	-228.1056054424
F2_Node026	SV17_Fdr2	25.9494889951	-187.8836362632
F2_Node029	SV11_Fdr2	45.0737630907	-277.3420139980
F2_Node030	GV17_Fdr2	-62.3770168914	-501.1047166145
F2_Node033	SV19_Fdr2	51.5695568589	-310.8381726725
F2_Node035	GV18_Fdr2	-67.6141570735	-367.4535530262
F2_Node037	SV18_Fdr2	91.4689646289	-272.6111719492
F2_Node039	SV20_Fdr2	41.0751467594	-348.4072234609
F2_Node042	GV19_Fdr2	-135.4298266076	-752.9299271241
F2_Node044	SV26_Fdr2	0.0000000003	-0.0000000075
F2_Node046	SV21_Fdr2	32.5929868415	-923.9694899076
F2_Node048	GV21_Fdr2	-721.4822576823	-852.3367783405
Power flow from vaults		-1005.4033768003	-5697.45715980022

B2. 30% PV Penetration with Fault in Feeder 3

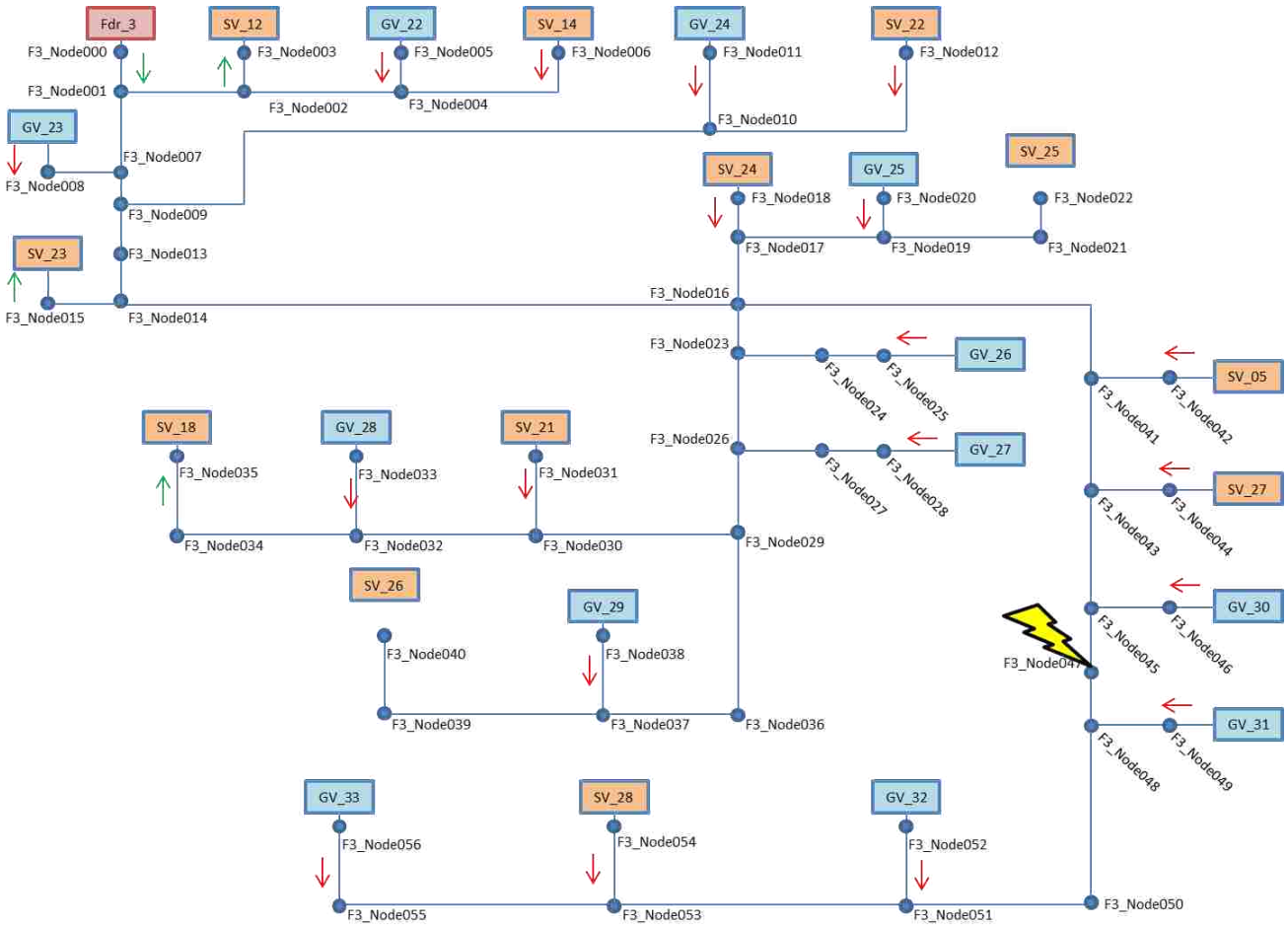

Figure B.2—Feeder network 3 with fault (30% PV)

Table B.3—Current calculations for Feeder network 3 simulation (30% PV)

From Node	To Node	Current (pu) without fault	Current (pu) with fault
Main substation	Fdr_3	-0.572-1.635i	14.934-0.448i
F3_Node003	SV12_Fdr3	0.042-0.095i	0.025-0.09i
F3_Node005	GV22_Fdr3	-0.082-0.109i	-0.095-0.105i
F3_Node006	SV14_Fdr3	-0.004-0.002i	-0.016+0.001i
F3_Node008	GV23_Fdr3	-0.159-0.038i	-0.172-0.034i
F3_Node011	GV24_Fdr3	0.009-0.053i	-0.038-0.04i
F3_Node012	SV22_Fdr3	0.044-0.097i	-0.005-0.083i
F3_Node015	SV23_Fdr3	0.024-0.053i	-0.088-0.017i
F3_Node018	SV24_Fdr3	0.029-0.062i	-0.106-0.019i
F3_Node020	GV25_Fdr3	-0.013-0.099i	-0.156-0.068i
F3_Node022	SV25_Fdr3	0	0
F3_Node025	GV26_Fdr3	0.008-0.049i	-0.133-0.012i
F3_Node028	GV27_Fdr3	-0.006-0.15i	-0.207-0.107i
F3_Node031	SV21_Fdr3	-0.031+0.005i	-0.322+0.066i
F3_Node033	GV28_Fdr3	-0.107-0.084i	-0.181-0.085i
F3_Node035	SV18_Fdr3	0.062-0.165i	-0.12-0.122i
F3_Node038	GV29_Fdr3	-0.178-0.051i	-0.302-0.03i
F3_Node040	SV26_Fdr3	0	0
F3_Node042	SV05_Fdr3	0.022-0.079i	-0.43+0.125i
F3_Node044	SV27_Fdr3	0.021-0.111i	-0.326+0.054i
F3_Node046	GV30_Fdr3	-0.079-0.105i	-0.373+0.028i
F3_Node049	GV31_Fdr3	-0.027-0.039i	-0.349+0.115i
F3_Node052	GV32_Fdr3	-0.076-0.033i	-0.386+0.104i
F3_Node054	SV28_Fdr3	0.035-0.102i	-0.468+0.137i
F3_Node056	GV33_Fdr3	-0.103-0.066i	-0.57+0.137i
Current from vaults		-0.572-1.635i	-4.816-0.043i

Table B.4—Power flows for Feeder network 3 simulation (30% PV)

From Node	To Node	Real power flow (kW) without fault	Real power flow (kW) with fault
Main substation	Fdr_3	-571.62	14933.56
F3_Node003	SV12_Fdr3	41.5036694689	25.1684049558
F3_Node005	GV22_Fdr3	-82.2240140727	-94.8017786993
F3_Node006	SV14_Fdr3	-4.1136686210	-15.9383872181
F3_Node008	GV23_Fdr3	-158.8394372013	-171.8052949481
F3_Node011	GV24_Fdr3	9.1620622564	-37.5135990756
F3_Node012	SV22_Fdr3	43.4790489461	-4.7688337820
F3_Node015	SV23_Fdr3	23.7213242858	-87.5775508753
F3_Node018	SV24_Fdr3	28.8549632394	-105.3353287216
F3_Node020	GV25_Fdr3	-12.8298078917	-154.3873390567
F3_Node022	SV25_Fdr3	0.0000002468	-0.0000033443
F3_Node025	GV26_Fdr3	7.8438623515	-132.7000285041
F3_Node028	GV27_Fdr3	-6.4092265820	-205.2705498625
F3_Node031	SV21_Fdr3	-30.6454688856	-321.2138634418
F3_Node033	GV28_Fdr3	-106.8552038129	-179.9847927300
F3_Node035	SV18_Fdr3	61.5647963415	-118.6459345977
F3_Node038	GV29_Fdr3	-177.9590855487	-300.2989326299
F3_Node040	SV26_Fdr3	0.0000025822	0.0000122458
F3_Node042	SV05_Fdr3	21.6562796441	-428.3485126891
F3_Node044	SV27_Fdr3	20.5037234662	-323.4436046910
F3_Node046	GV30_Fdr3	-79.4823365279	-369.2496629802
F3_Node049	GV31_Fdr3	-27.0388130535	-347.3216146090
F3_Node052	GV32_Fdr3	-76.0919029461	-383.2301472166
F3_Node054	SV28_Fdr3	35.0530260567	-464.9185622156
F3_Node056	GV33_Fdr3	-103.3203395017	-565.6188574061
Power flow from vaults		-572.466545759514	-4787.20476209283

B3. 30% PV Penetration with Fault in Feeder 4

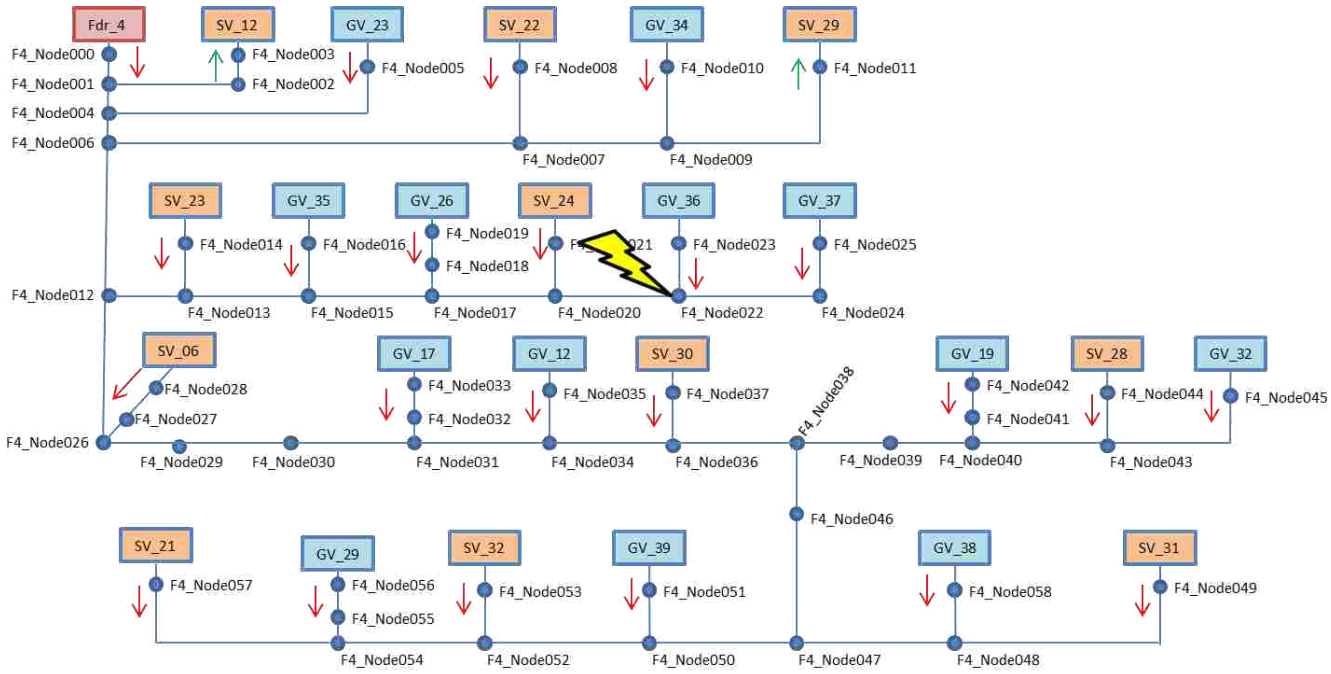

Figure B.3—Feeder network 4 with fault (30% PV)

Table B.5—Current calculations for Feeder network 4 simulation (30% PV)

From Node	To Node	Current (pu) without fault	Current (pu) with fault
Main substation	Fdr_4	-0.459-1.721i	16.227-1.088i
F4_Node003	SV12_Fdr4	0.041-0.095i	0.022-0.088i
F4_Node005	GV23_Fdr4	-0.159-0.037i	-0.174-0.032i
F4_Node008	SV22_Fdr4	0.044-0.095i	-0.009-0.076i
F4_Node010	GV34_Fdr4	0.016-0.064i	-0.051-0.042i
F4_Node011	SV29_Fdr4	0.05-0.112i	0.011-0.097i
F4_Node014	SV23_Fdr4	0.024-0.052i	-0.1
F4_Node016	GV35_Fdr4	-0.061-0.149i	-0.228-0.076i
F4_Node019	GV26_Fdr4	0.001-0.053i	-0.163+0.017i
F4_Node021	SV24_Fdr4	0.028-0.062i	-0.209+0.073i
F4_Node023	GV36_Fdr4	-0.001-0.092i	-0.115-0.068i
F4_Node025	GV37_Fdr4	0.003-0.095i	-0.282+0.057i
F4_Node028	SV06_Fdr4	0.053-0.111i	-0.101-0.056i
F4_Node033	GV17_Fdr4	-0.091-0.175i	-0.289-0.12i
F4_Node035	GV12_Fdr4	0.001-0.021i	-0.104+0.011i
F4_Node037	SV30_Fdr4	0.025-0.052i	-0.11-0.012i
F4_Node042	GV19_Fdr4	-0.163-0.072i	-0.316-0.045i
F4_Node044	SV28_Fdr4	0.056-0.098i	-0.097-0.067i
F4_Node045	GV32_Fdr4	-0.063-0.031i	-0.159-0.014i
F4_Node049	SV31_Fdr4	0.02-0.019i	-0.139+0.016i
F4_Node051	GV39_Fdr4	0.01-0.094i	-0.088-0.076i
F4_Node053	SV32_Fdr4	0.009-0.007i	-0.115+0.019i
F4_Node056	GV29_Fdr4	-0.162-0.047i	-0.249-0.033i
F4_Node057	SV21_Fdr4	-0.002+0.01i	-0.204+0.045i
F4_Node058	GV38_Fdr4	-0.139-0.102i	-0.275-0.077i
Current from vaults		-0.459-1.721i	-3.544-0.743i

Table B.6—Power flows for Feeder network 4 simulation (30% PV)

From Node	To Node	Real power flow (kW) without fault	Real power flow (kW) with fault
Main substation	Fdr_4	-458.76	16226.99
F4_Node003	SV12_Fdr4	41.1576145494	22.0672252064
F4_Node005	GV23_Fdr4	-158.7421797593	-174.1033722098
F4_Node008	SV22_Fdr4	43.8808044727	-9.0913574522
F4_Node010	GV34_Fdr4	16.0979391065	-50.6350260173
F4_Node011	SV29_Fdr4	50.3757840538	10.9508975858
F4_Node014	SV23_Fdr4	23.9167556600	-99.0855332589
F4_Node016	GV35_Fdr4	-61.5336911290	-225.7634048178
F4_Node019	GV26_Fdr4	0.7592072975	-162.6326551125
F4_Node021	SV24_Fdr4	27.8152756172	-207.5877918699
F4_Node023	GV36_Fdr4	-0.8418298080	-112.3665599298
F4_Node025	GV37_Fdr4	3.1903935237	-280.0205512709
F4_Node028	SV06_Fdr4	52.3971587514	-100.1330432467
F4_Node033	GV17_Fdr4	-90.9488338436	-286.8488121985
F4_Node035	GV12_Fdr4	1.2420263732	-103.5770159469
F4_Node037	SV30_Fdr4	25.0224966845	-109.8803464368
F4_Node042	GV19_Fdr4	-162.8197583321	-314.6475425957
F4_Node044	SV28_Fdr4	56.1901663589	-96.5749914285
F4_Node045	GV32_Fdr4	-63.4710825083	-158.6387712127
F4_Node049	SV31_Fdr4	20.0514029239	-138.2795282718
F4_Node051	GV39_Fdr4	9.7548928435	-87.8881410709
F4_Node053	SV32_Fdr4	8.9180630638	-115.1363887657
F4_Node056	GV29_Fdr4	-161.6893598582	-247.8725240128
F4_Node057	SV21_Fdr4	-1.9475141454	-203.7451387204
F4_Node058	GV38_Fdr4	-138.5412088465	-274.0900009976
Power flow from vaults		-459.765476950434	-3525.58037405193

B4. 30% PV Penetration with Fault in Feeder 5

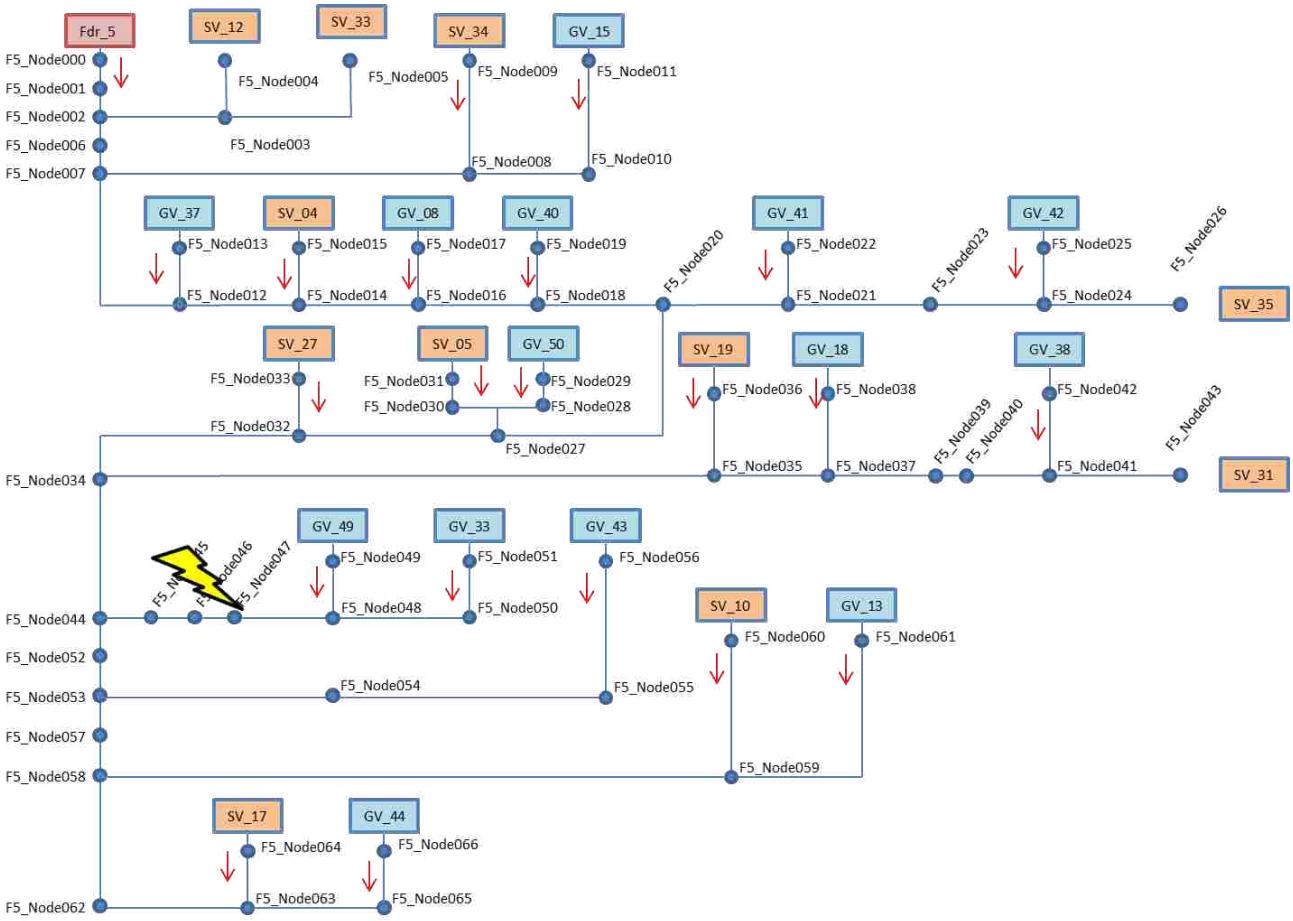

Figure B.4—Feeder network 5 with fault (30% PV)

Table B.7—Current calculations for Feeder network 5 simulation (30% PV)

From Node	To Node	Current (pu) without fault	Current (pu) with fault
Main substation	Fdr_5	-0.5-1.509i	10.881+0.13i
F5_Node004	SV12_Fdr5	0	0
F5_Node005	SV33_Fdr5	0	0
F5_Node009	SV34_Fdr5	0.027-0.019i	-0.135+0.024i
F5_Node011	GV15_Fdr5	-0.027-0.132i	-0.211-0.09i
F5_Node013	GV37_Fdr5	0.01-0.09i	-0.125-0.06i
F5_Node015	SV04_Fdr5	0.053-0.093i	-0.102-0.055i
F5_Node017	GV08_Fdr5	-0.084-0.012i	-0.258+0.027i
F5_Node019	GV40_Fdr5	-0.065-0.16i	-0.412-0.071i
F5_Node022	GV41_Fdr5	-0.071-0.041i	-0.472+0.061i
F5_Node025	GV42_Fdr5	-0.034-0.134i	-0.172-0.142i
F5_Node026	SV35_Fdr5	0	0
F5_Node029	GV50_Fdr5	-0.193-0.152i	-0.269-0.157i
F5_Node031	SV05_Fdr5	0.065-0.034i	-0.592+0.143i
F5_Node033	SV27_Fdr5	0.061-0.066i	-0.399+0.055i
F5_Node036	SV19_Fdr5	0.055-0.093i	-0.422+0.03i
F5_Node038	GV18_Fdr5	-0.065-0.083i	-0.444
F5_Node042	GV38_Fdr5	-0.121-0.062i	-0.649+0.063i
F5_Node043	SV31_Fdr5	0	0
F5_Node049	GV49_Fdr5	0.046-0.069i	-0.933+0.357i
F5_Node051	GV33_Fdr5	-0.067-0.022i	-0.827+0.27i
F5_Node056	GV43_Fdr5	-0.132-0.073i	-0.678+0.062i
F5_Node060	SV10_Fdr5	0.049-0.028i	-0.442+0.097i
F5_Node061	GV13_Fdr5	0.034-0.05i	-0.456+0.047i
F5_Node064	SV17_Fdr5	0.038-0.05i	-0.312+0.041i
F5_Node066	GV44_Fdr5	-0.078-0.047i	-0.459+0.048i
Current from vaults		-0.5-1.509i	-8.768+0.75i

Table B.8—Power flows for Feeder network 5 simulation (30% PV)

From Node	To Node	Real power flow (kW) without fault	Real power flow (kW) with fault
Main substation	Fdr_5	-499.62	10881.06
F5_Node004	SV12_Fdr5	0.0000000003	-0.0000000006
F5_Node005	SV33_Fdr5	0.0000000000	-0.0000000009
F5_Node009	SV34_Fdr5	26.5181324124	-134.7090505537
F5_Node011	GV15_Fdr5	-27.2588510153	-209.6500923437
F5_Node013	GV37_Fdr5	10.1949544022	-124.4854134158
F5_Node015	SV04_Fdr5	52.6842121325	-101.0766827905
F5_Node017	GV08_Fdr5	-84.1916104494	-256.6540233321
F5_Node019	GV40_Fdr5	-64.8246743228	-407.5744723133
F5_Node022	GV41_Fdr5	-70.8239257444	-469.2747381793
F5_Node025	GV42_Fdr5	-34.1278363521	-168.1818847510
F5_Node026	SV35_Fdr5	0.0000000005	-0.0000000048
F5_Node029	GV50_Fdr5	-193.2788434728	-263.1916866604
F5_Node031	SV05_Fdr5	64.6997775712	-589.8279137178
F5_Node033	SV27_Fdr5	60.4084341918	-396.8434214542
F5_Node036	SV19_Fdr5	54.7021313233	-418.6762461416
F5_Node038	GV18_Fdr5	-65.1862620036	-440.1891997334
F5_Node042	GV38_Fdr5	-120.5266627715	-644.2365207307
F5_Node043	SV31_Fdr5	0.0000000002	-0.0000000065
F5_Node049	GV49_Fdr5	45.6009186687	-928.3855645005
F5_Node051	GV33_Fdr5	-66.6197264715	-820.5163473702
F5_Node056	GV43_Fdr5	-131.3866201358	-672.6775910582
F5_Node060	SV10_Fdr5	48.8075983400	-439.5759515042
F5_Node061	GV13_Fdr5	33.9847313019	-452.5774221458
F5_Node064	SV17_Fdr5	37.4420370306	-310.1316316634
F5_Node066	GV44_Fdr5	-78.0212334445	-455.5930479608
Power flow from vaults		-501.203318808111	-8704.02890233268

B5. 30% PV Penetration with Fault in Feeder 6

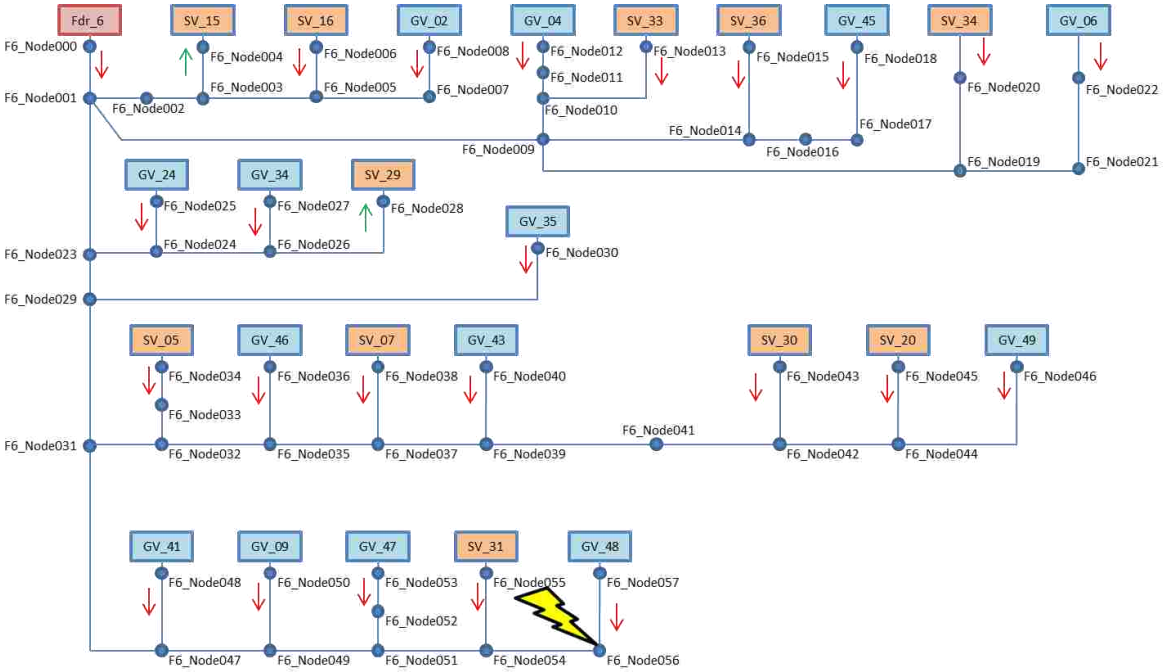

Figure B.5—Feeder network 6 with fault (30% PV)

Table B.9—Current calculations for Feeder network 6 simulation (30% PV)

From Node	To Node	Current (pu) without fault	Current (pu) with fault
Main substation	Fdr_6	-0.74-1.845i	14.279-0.776i
F6_Node004	SV15_Fdr6	0.022-0.053i	0.004-0.047i
F6_Node006	SV16_Fdr6	-0.003-0.002i	-0.022+0.004i
F6_Node008	GV02_Fdr6	-0.021-0.048i	-0.04-0.042i
F6_Node012	GV04_Fdr6	-0.099-0.094i	-0.139-0.082i
F6_Node013	SV33_Fdr6	0	0
F6_Node015	SV36_Fdr6	0.003-0.002i	-0.029+0.007i
F6_Node018	GV45_Fdr6	-0.136-0.075i	-0.161-0.069i
F6_Node020	SV34_Fdr6	0.004-0.048i	-0.015-0.045i
F6_Node022	GV06_Fdr6	-0.044-0.052i	-0.062-0.052i
F6_Node025	GV24_Fdr6	0.011-0.052i	-0.032-0.038i
F6_Node027	GV34_Fdr6	0.018-0.064i	-0.04-0.046i
F6_Node028	SV29_Fdr6	0.052-0.112i	0.013-0.1i
F6_Node030	GV35_Fdr6	-0.057-0.147i	-0.205-0.101i
F6_Node034	SV05_Fdr6	0.024-0.077i	-0.263+0.012i
F6_Node036	GV46_Fdr6	-0.014-0.101i	-0.167-0.064i
F6_Node038	SV07_Fdr6	0.065-0.118i	-0.175-0.049i
F6_Node040	GV43_Fdr6	-0.174-0.116i	-0.372-0.069i
F6_Node043	SV30_Fdr6	0.02-0.046i	-0.154-0.007i
F6_Node045	SV20_Fdr6	0.01-0.048i	-0.174-0.002i
F6_Node046	GV49_Fdr6	0.009-0.106i	-0.255-0.052i
F6_Node048	GV41_Fdr6	-0.103-0.08i	-0.424+0.027i
F6_Node050	GV09_Fdr6	-0.179-0.094i	-0.67+0.084i
F6_Node053	GV47_Fdr6	-0.08-0.14i	-0.597+0.068i
F6_Node055	SV31_Fdr6	-0.001-0.024i	-0.608+0.267i
F6_Node057	GV48_Fdr6	-0.069-0.143i	-0.78+0.192i
Current from vaults		-0.74-1.845i	-5.371-0.157i

Table B.10—Power flows for Feeder network 6 simulation (30% PV)

From Node	To Node	Real power flow (kW) without fault	Real power flow (kW) with fault
Main substation	Fdr_6	-739.99	14278.85
F6_Node004	SV15_Fdr6	22.0147462175	3.5964064463
F6_Node006	SV16_Fdr6	-3.4752751561	-21.6418904175
F6_Node008	GV02_Fdr6	-20.8673833336	-40.0673074749
F6_Node012	GV04_Fdr6	-98.9925665155	-138.8696735551
F6_Node013	SV33_Fdr6	0.0000000896	-0.0000003858
F6_Node015	SV36_Fdr6	3.2141336317	-28.6541470625
F6_Node018	GV45_Fdr6	-135.7652395062	-161.1574292782
F6_Node020	SV34_Fdr6	4.2034698857	-14.8818565569
F6_Node022	GV06_Fdr6	-44.0327696853	-62.3290326289
F6_Node025	GV24_Fdr6	11.0064005395	-31.7081262164
F6_Node027	GV34_Fdr6	18.3233687635	-40.0294668228
F6_Node028	SV29_Fdr6	51.9085419627	13.5811638134
F6_Node030	GV35_Fdr6	-56.6268569777	-202.8905917067
F6_Node034	SV05_Fdr6	24.2202112083	-262.3559840883
F6_Node036	GV46_Fdr6	-14.3938246112	-165.3214436206
F6_Node038	SV07_Fdr6	64.6014535397	-173.5474941626
F6_Node040	GV43_Fdr6	-173.4559638960	-369.5272181159
F6_Node043	SV30_Fdr6	19.6248638339	-153.7513370707
F6_Node045	SV20_Fdr6	10.1576575019	-172.9931572313
F6_Node046	GV49_Fdr6	8.4706645596	-253.9137828758
F6_Node048	GV41_Fdr6	-102.6058988702	-421.9165628224
F6_Node050	GV09_Fdr6	-178.4872612474	-665.4439025203
F6_Node053	GV47_Fdr6	-80.5536087790	-591.3606413972
F6_Node055	SV31_Fdr6	-0.5921792407	-606.4324528625
F6_Node057	GV48_Fdr6	-68.8297817243	-771.4942247476
Power flow from vaults		-740.933097809422	-5336.70655980752

B6. 30% PV Penetration with Fault in Feeder 7

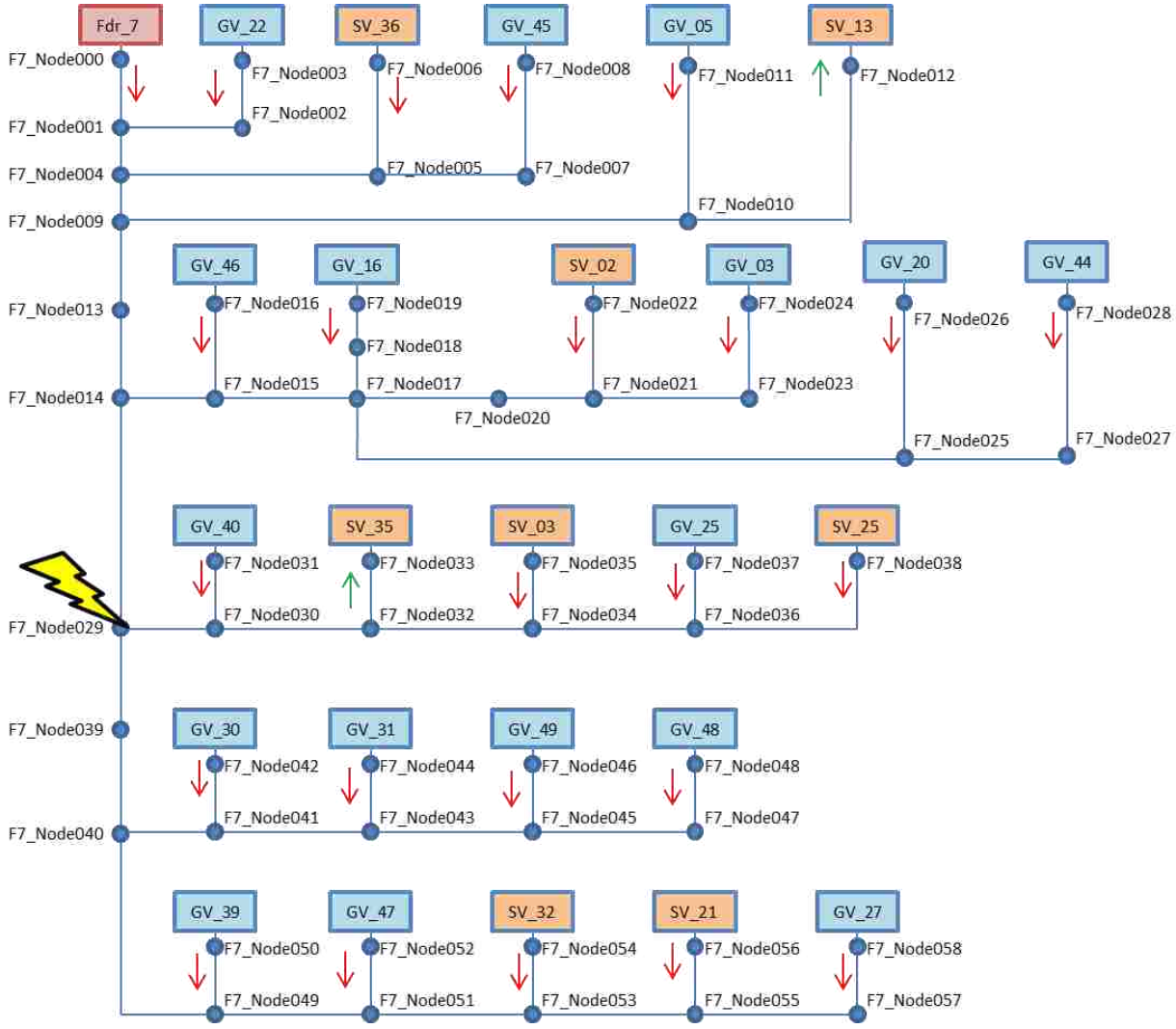

Figure B.6—Feeder network 7 with fault (30% PV)

Table B.11—Current calculations for Feeder network 7 simulation (30% PV)

From Node	To Node	Current (pu) without fault	Current (pu) with fault
Main substation	Fdr_7	-0.526-1.92i	15.159-0.783i
F7_Node003	GV22_Fdr7	-0.082-0.109i	-0.095-0.104i
F7_Node006	SV36_Fdr7	-0.001-0.003i	-0.034+0.007i
F7_Node008	GV45_Fdr7	-0.139-0.076i	-0.166-0.068i
F7_Node011	GV05_Fdr7	-0.01-0.024i	-0.086-0.001i
F7_Node012	SV13_Fdr7	0.072-0.151i	0.016-0.131i
F7_Node016	GV46_Fdr7	-0.018-0.098i	-0.188-0.047i
F7_Node019	GV16_Fdr7	-0.095-0.123i	-0.256-0.072i
F7_Node022	SV02_Fdr7	0.089-0.137i	-0.203-0.04i
F7_Node024	GV03_Fdr7	-0.016-0.038i	-0.177+0.012i
F7_Node026	GV20_Fdr7	-0.002-0.002i	-0.155+0.047i
F7_Node028	GV44_Fdr7	-0.109-0.074i	-0.263-0.03i
F7_Node031	GV40_Fdr7	-0.085-0.17i	-0.369-0.061i
F7_Node033	SV35_Fdr7	0.063-0.138i	0.061-0.139i
F7_Node035	SV03_Fdr7	0.032-0.041i	-0.162+0.038i
F7_Node037	GV25_Fdr7	0.008-0.066i	-0.188-0.009i
F7_Node038	SV15_Fdr7	0	0
F7_Node042	GV30_Fdr7	-0.074-0.093i	-0.285-0.018i
F7_Node044	GV31_Fdr7	-0.022-0.027i	-0.226+0.044i
F7_Node046	GV49_Fdr7	0.014-0.097i	-0.386+0.05i
F7_Node048	GV48_Fdr7	-0.067-0.125i	-0.379-0.03i
F7_Node050	GV39_Fdr7	-0.003-0.086i	-0.208-0.015i
F7_Node052	GV47_Fdr7	-0.079-0.123i	-0.388-0.019i
F7_Node054	SV32_Fdr7	-0.009+0.007i	-0.271+0.101i
F7_Node056	SV21_Fdr7	0	0
F7_Node058	GV27_Fdr7	0.006-0.127i	-0.284-0.032i
Current from vaults		-0.526-1.92i	-4.596-0.413i

Table B.12—Power flows for Feeder network 7 simulation (30% PV)

From Node	To Node	Real power flow (kW) without fault	Real power flow (kW) with fault
Main substation	Fdr_7	-526.32	15158.57
F7_Node003	GV22_Fdr7	-82.3724065921	-94.6956051689
F7_Node006	SV36_Fdr7	-0.8240722683	-33.5462843794
F7_Node008	GV45_Fdr7	-138.9624292609	-165.8179625283
F7_Node011	GV05_Fdr7	-9.7606930103	-86.0371442733
F7_Node012	SV13_Fdr7	72.0070133255	16.1075485099
F7_Node016	GV46_Fdr7	-17.6831284371	-186.6211390294
F7_Node019	GV16_Fdr7	-95.1374170917	-254.3296621785
F7_Node022	SV02_Fdr7	89.0526469249	-201.6715710494
F7_Node024	GV03_Fdr7	-16.2728438930	-175.8331147917
F7_Node026	GV20_Fdr7	-2.1597715371	-154.4510389362
F7_Node028	GV44_Fdr7	-108.4660032585	-260.9786118229
F7_Node031	GV40_Fdr7	-84.7187437375	-365.3018980944
F7_Node033	SV35_Fdr7	62.7571198163	62.7570254786
F7_Node035	SV03_Fdr7	31.4251247765	-161.7438276520
F7_Node037	GV25_Fdr7	8.2607731358	-187.1451829135
F7_Node038	SV15_Fdr7	0.0000000002	-0.0000000033
F7_Node042	GV30_Fdr7	-74.1980812190	-282.8151616231
F7_Node044	GV31_Fdr7	-22.1002356107	-224.9538343524
F7_Node046	GV49_Fdr7	14.0128853547	-384.1501199626
F7_Node048	GV48_Fdr7	-66.6749270560	-376.2521775972
F7_Node050	GV39_Fdr7	-3.3714805706	-206.5068309396
F7_Node052	GV47_Fdr7	-79.1987678862	-384.7101404376
F7_Node054	SV32_Fdr7	-8.9180439369	-270.0085060440
F7_Node056	SV21_Fdr7	-0.0000000001	-0.0000000039
F7_Node058	GV27_Fdr7	5.6333584141	-281.7235401924
Power flow from vaults		-527.670123618212	-4565.7331748166

APPENDIX C – VOLTAGE LIMITS

The steady state voltage is the voltage a Customer can expect to receive under normal operating conditions. Since the loads on a utility system are constantly changing, it is impossible to maintain a completely constant voltage. Thus the Company will provide voltage regulation to keep the steady state voltage within the ranges shown in Tables 3.1 and 3.2 as indicated by ANSI standard C84.1.

Table C.1—ANSI C84.1 Voltage Limits (Service Voltage)

Service Voltage (1)	*Range A (2)(4)*	*Range B (2)(6)*
Maximum	+5%	+5.83%
Minimum	-5%	-8.33%

1. Service voltage is measured at the point of common coupling between Customer and Company. Jurisdictional Public Service Commissions may specify other voltage limits.

Table C.2—ANSI C84.1 Voltage Limits (Utilization Voltage)

Utilization Voltage (6)	*Range A (2)(4)*	*Range B (2)(6)*
Maximum (equipment rated >600 V)	+5%	+5.83%
Maximum (equipment rated <600 V)	+4.17%	+5.83%
Minimum	-8.33%(-10% (3))	-11.67%(-13.33%(3))

2. Voltage limits in % deviation from nominal
3. For circuits with no lighting equipment
4. Range A applies to normal operations
5. Range B applies for short duration and/or abnormal conditions on the utility system (excluding fault conditions and transients).
6. Utilization Voltage is measured at the equipment using the electricity.

REFERENCES

[1] Coddington, M., Kroposki, B., Basso, T., Lynn, K., and Vaziri, M., "Photovoltaic systems interconnected onto secondary network distribution systems," *Photovoltaic Specialists Conference (PVSC), 2009 34th IEEE* , vol., no., pp.000405-000408, 7-12 June 2009.

[2] ETI MNPR® Specification version 9.00 with Communications September 2, 2010.

[3] Lopes, J.A. Pecas, Hatziargyriou, N., Mutale, J., Djapic, P., and Jenkins, N. Integrating distributed generation into electric power systems: A review of drivers, challenges and opportunities, "Electric Power Systems Research 77 (2007) 1189-1203". Oct. 2006.

[4] Passey, Robert, Spooner, Ted, MacGill, Iain, Watt, Muriel, and Syngellakis, Katerina. The potential impacts of grid-connected distributed generation and how to address them: A review of technical and non-technical factors. " Energy Policy 39 (2011) pp. 6280-6290".

[5] Coddington, M., Kroposki, B., Basso, T., Lynn, K., Sammon, Dan, and Vaziri, M., "Photovoltaic Systems Interconnected onto Secondary Network Distribution Systems—Success Stories," Technical Report NREL/TP-550-45061. Apr. 2009.

[6] IEEE 1547.6. Recommended Practice for Interconnecting Distributed Resources with Electric Power Systems Distribution Secondary Networks.

[7] Hernandez, J.C., De la Cruz, J., Ogayar, B. Electrical protection for the grid-interconnection of photovoltaic-distributed generation. Electric Power Systems Research 89 (2012) pp.85-99.

[8] Cipcigan, L.M., Taylor, P.C. Investigation of the reverse power flow requirements of high penetrations of small-scale embedded generation. IET Renew. Power Gener., Vol. 1, No. 3, September 2007.

[9] Buchanan, Susan. Developers Install Alternative Energy in Old and New Structures, The Louisiana Weekly. August 1, 2011.

[10] SEL-632 Network Protector Relay Instruction Manual

[11] Solanki, Sarika Khushalani. Ramachandran, Vaidyanath, Solanki, Jignesh.Steady State Analysis of High Penetration PV on Utility Distribution Feeder. 2012 IEEE.

[12] Eftekharnejad, Sara, Vittal, Vijay, Heydt, Gerald Thomas, Keel, Brian, Loehr, Jeffrey.Impact of Increased Penetration of Photovoltaic Generation on Power Systems. IEEE Transactions on Power Systems, Vol. 28, No. 2, May 2013.

[13] IEEE 399-1997, IEEE Recommended Practice for Industrial and Commercial Power Systems Analysis (IEEE Brown Book)

[14] Chapman, Stephen J. Electric Machinery and Power System Fundamentals. New York: McGraw-Hill, 2002.

[15] Ustun, Taha Selim, Ozansoy, Cagil, Zayegh, Aladin. Recent developments in microgrids and example cases around the world—A review. Renewable and Sustainable Energy Reviews 15 (2011) pp. 4030-4041.

[16] Liu, Y., Bebic, J., Kroposki, B., de Bedout, J., Ren, W. Distribution System Voltage Performance Analysis for High-Penetration PV. IEEE Energy2030, Atlanta, Georgia, USA. November 17-18, 2008.

VITA

Nigel Jordan was born in Biloxi, MS. He received his B.S. degree in Electrical Engineering from the University of Mississippi, Oxford, Mississippi in 2007. After graduation he worked as an electrical engineer with Southern Company in Birmingham, AL. During that period, he also attended the University of Alabama—Birmingham where he received his Masters of Business Administration (MBA) degree in December 2011. In 2012, Nigel moved to Baton Rouge, LA to pursue his graduate studies at Louisiana State University Agricultural and Mechanical College, while working as an electrical engineer with Dow Chemical in Plaquemine, LA. He is a candidate for the degree of Master of Science in Electrical Engineering for May 2014.